

الجمهورية الجزائرية الديمقراطية الشعبية
République Algérienne Démocratique et Populaire
وزارة التعليم العالي و البحث العلمي
Ministère de l'Enseignement Supérieur et de la
Recherche Scientifique

Université Mohamed Khider – Biskra
Faculté des Sciences et de la Technologie
Département :Génie Mécanique
Réf :



جامعة محمد خيضر بسكرة
كلية العلوم و التكنولوجيا
قسم الهندسة الميكانيكية
المرجع:

Thèse présentée en vue de
l'obtention Du Diplôme de
Doctorat en Génie Mécanique

Contribution au développement et à la caractérisation de bio-composites à base de déchets de palmier dattier; Application à l'isolation thermique

Spécialité: Energétique

Présentée par:

Maroua FERHAT

Soutenue publiquement le:09/04/2025

Devant le jury composé de:

Mr. Adel BENCHABANE	Professeur	Président	Université de Biskra
Mr. Adnane LABED	Professeur	Rapporteur	Université de Biskra
Mr. Hocine DJEMAI	Maître de Conférences 'A'	Co-rapporteur	Université de Biskra
Mr. Abdelhafid BRIMA	Professeur	Examineur	Université de Batna
Mr. Semcheddine DERFOUF	Professeur	Examineur	Université de Batna
Mr. Tarek DJOUDI	Maître de Conférences 'A'	Examineur	Université de Biskra

People's Democratic Republic of Algeria
Ministry of Higher Education and Scientific
Research
Mohamed Khider University of Biskra
Faculty of Sciences and Technology
Department of Mechanical Engineering

Mohamed Khider University – Biskra
Faculty of Science and Technology
Department: Mechanical Engineering
Réf :



جامعة محمد خيضر بسكرة
كلية العلوم و التكنولوجيا
قسم الهندسة الميكانيكية
المرجع:

Thesis presented for the
award of the Diploma of
Doctorat in Mechanical Engineering

**Contribution to the development and characterization of bio-composites based on
date palm waste; Application to thermal insulation**

Presented by: **Maroua FERHAT**

Defended on: 09/04/2025

In front of the jury composed of:

Mr. Adel BENCHABANE	Professor	President	University of Biskra
Mr. Adnane LABED	Professor	Supervisor	University of Biskra
Mr. Hocine DJEMAI	MCA	Co-Supervisor	University of Biskra
Mr. Abdelhafid BRIMA	Professor	Examiner	University of Batna
Mr. Semcheddine DERFOUF	Professor	Examiner	University of Batna
Mr. Tarek DJOUDI	MCA	Examiner	University of Biskra

Thanks

First and foremost, I extend my deepest gratitude to ALLAH for His blessings, which have enabled me to accomplish this work.

I want to express my sincere thanks to my thesis director, **Mr. Adnane LABED**, Professor at the University of Biskra, for his guidance and supervision throughout this thesis. His brilliant insights, kindness, constant availability, and numerous encouragements have been invaluable to me.

I am equally grateful to the thesis co-director, **Dr. Hocine DJEMAI**, a Lecturer at the University of Biskra, for the high-quality advice and many useful recommendations he provided during my research journey.

I also thank all the jury members for their time and effort in examining this work. I want to thank **Pr. Adel BENCHABANE** from the University of Biskra for agreeing to chair the defense jury and Professors **Abdelhafid BRIMA** and **Pr. Semcheddine DERFOUF** from the University of Batna and **Dr. Tarek DJOUDI** from the University of Biskra for their valuable input.

A special thank you to **Dr. Elhachemi GUETTAF TEMEM**, **Pr. Salim BITAM**, **Dr. Chawki MAHBOUB**, **Dr. Hamida BOUSSAHEL**, **Dr. Abdelhafid MOMMI**, **Dr. Mabrok HACINI**, **Pr. Nouredine BELGHAR**, and **Mrs. Nawel GRINE** for their help and availability. Finally, I would like to thank all the teachers in my Mechanical Engineering department and my colleagues, whose support has been greatly appreciated.

Dedication

With all respect and love, I dedicate this work to:

My dear parents whose unwavering support, encouragement, and sacrifices have been the foundation of my achievements. This work is a reflection of your love and belief in me.

My brothers and sisters have always been my strength and inspiration.

My friends, whose constant encouragement and companionship have made this journey more meaningful.

Maroua FERHAT

Resume

Cette étude vise à développer un matériau composite innovant biosourcé, avec de bonnes propriétés mécaniques et thermiques, par l'investigation des matériaux à base des déchets abandonnés dérivés de différentes parties de palmiers dattiers. Différentes combinaisons de ces matériaux ont été analysées pour évaluer leurs propriétés physiques, mécaniques et thermiques, en mettant l'accent sur la caractérisation des fibres du pétiole et du rachis, en particulier pour une utilisation dans des structures sandwich destinée à l'isolation thermique. Des analyses physiques et thermiques complètes, notamment des tests de densité, d'absorption d'eau, de conductivité thermique, d'ATG et de DSC, ont été menées sur ces fibres. Les fibres de rachis de palmier dattier ont été incorporées dans une matrice époxy comme couche de peau, avec des rapports pondéraux de fibres (0-15 % en poids). Les résultats ont indiqué que les fibres de rachis influençaient de manière significative l'absorption d'eau, la morphologie, la résistance mécanique et la résistivité thermique. La DRX a confirmé la nature amorphe du composite, tandis que l'analyse SEM a montré une hétérogénéité accrue avec une teneur en fibres plus élevée. Le composite Epoxy-Rachis ER10 % a démontré une forte isolation thermique (conductivité thermique de 0.21 W/(m•K), une diffusivité thermique de 0.17 mm²/s), un comportement de fracture ductile, atteignant un module de flexion de 3.21 GPa et une résistance à la flexion de 9.28 MPa. De plus, des fibres de pétiole de palmier dattier renforcées en acétate de polyvinyle (PVA) ont été utilisées pour former la couche centrale (le cœur) avec des rapports pondéraux de fibres compris entre 15 et 26 % en poids. Il s'avère que le composite Pt17 % présentait des propriétés d'isolation exceptionnelles (conductivité thermique de 0.11-0.12 W/(m•K) et diffusivité thermique de 0,096-0.109 mm²/s) et une faible densité de 0.3002 g/cm³, ce qui en fait le choix idéal pour les noyaux de panneaux sandwich légers. Les tests du cœur Pt17% avec des peaux ER10% ont révélé une rigidité substantielle et une forte adhérence intercouche en raison de la méthode de collage, ainsi qu'une excellente isolation thermique (0.2 W/m•K), soulignant le potentiel des déchets de palmier dattier pour le développement des matériaux composites durables et thermiquement efficaces pour les applications industrielles.

Mots clés :

Palmier dattier, déchet végétal, matériau composite, matériau naturel, conductivité thermique

Abstract

This study aims to develop an innovative bio-sourced composite material, with enhanced mechanical and thermal properties, by investigating sustainable composites derived from abandoned date palm waste. A range of combinations of these materials was analyzed to evaluate their physical, mechanical, and thermal properties, emphasizing the characterization of petiole and rachis fibers, particularly to be used in sandwich structures. Comprehensive physical and thermal analyses, including density, water absorption, thermal conductivity, TGA, and DSC tests, were conducted on these fibers. Date palm rachis fibers were incorporated into an epoxy matrix as the skin layer, with fiber weight ratios (0–15 wt.%). Results indicated that rachis fibers influenced significantly water absorption, morphology, mechanical strength, and thermal behavior. XRD confirmed the amorphous nature of the composite, while SEM analysis showed increased heterogeneity with higher fiber content. The Epoxy-Rachis ER10% composite demonstrated strong thermal insulation (thermal conductivity of 0.21 W/(m·K) and thermal diffusivity of 0.17 mm²/s) and ductile fracture behavior, achieving a flexural modulus of 3.21 GPa and bending strength of 9.28 MPa. Additionally, polyvinyl acetate (PVA) reinforced date palm petiole fibers were used to form the core layer with fiber weight ratios between 15–26 wt.%. It turns out that, the Pt17% composite exhibited exceptional insulation properties (thermal conductivity of 0.11–0.12 W/(m·K) and thermal diffusivity of 0.096–0.109 mm²/s) and a low density of 0.3002 g/cm³, making it ideal choice for lightweight sandwich panel cores. Testing the Pt17% core with ER10% skins revealed substantial stiffness and strong interlayer adhesion due to the bonding method, along with excellent thermal insulation (0.2 W/m·K), highlighting date palm waste potential to create durable, thermally efficient composite materials for industrial applications.

Keywords:

Date palm, plant waste, composite material, natural material, thermal conductivity

ملخص

تهدف هذه الدراسة إلى تطوير مادة مركبة مبتكرة حيوية المصدر، تتميز بخصائص ميكانيكية وحرارية جيدة، وذلك من خلال دراسة مواد مشتقة من نفايات مختلفة لأشجار النخيل. تم تحليل تركيبات مختلفة من هذه المواد لتقييم خصائصها الفيزيائية والميكانيكية والحرارية، مع التركيز على خصائص ألياف السعف والعراجين، خاصةً للاستخدام في الهياكل مختلفة الطبقات المصممة للعزل الحراري. أجريت تحليلات فيزيائية وحرارية شاملة، بما في ذلك اختبارات الكثافة، امتصاص الماء، التوصيلية الحرارية، التحليل الحراري الوزني (ATG) والتحليل الحراري التفاضلي (DSC) على هذه الألياف. تم دمج ألياف العراجين في مصفوفة إيبوكسية كطبقة خارجية، بنسب وزنية مختلفة من الألياف (0-15%). وأظهرت النتائج أن ألياف العراجين أثرت بشكل كبير على امتصاص الماء، والتشكل، وقوة التحمل الميكانيكي، والمقاومة الحرارية. وأكد تحليل حيود الأشعة السينية (DRX) الطبيعة غير البلورية للمركب، بينما أظهرت تحليلات المجهر الإلكتروني (SEM) زيادة في التباين مع زيادة نسبة الألياف. أظهر المركب إيبوكس-عراجين (ER10%) قدرة عالية على العزل الحراري (بموصلية حرارية قدرها 0.21 واط/م.ك) ونشرية حرارية قدرها 0.17 ملم²/ثانية)، وسلوك كسر مرن، مع بلوغ معامل مرونة في الانحناء قدره 3.21 غيغا باسكال وقوة انحناء قدرها 9.28 ميغاباسكال. بالإضافة إلى ذلك، استخدمت ألياف سعف النخيل المعززة بأسيتات البولي فينيل (PVA) لتشكيل الطبقة الوسطى (النواة) بنسب وزنية تتراوح بين 15 و26%. وأثبتت النتائج أن المركب Pt17% يتميز بخصائص عزل ممتازة (بموصلية حرارية تتراوح بين 0.11-0.12 واط/م.ك) ونشرية حرارية بين 0.096-0.109 ملم²/ثانية) وكثافة منخفضة تبلغ 0.3002 غ/سم³، مما يجعله الخيار المثالي لنواة الألواح الساندويتشية الخفيفة. وأظهرت الاختبارات على نواة Pt17% مع طبقات ER10% صلابة كبيرة وتماسكاً بين الطبقات بسبب طريقة الربط المستخدمة، بالإضافة إلى عزل حراري ممتاز (0.2 واط/م.ك)، مما يؤكد إمكانيات استخدام نفايات النخيل لإنتاج مواد مركبة مستدامة وفعالة حرارياً للتطبيقات الصناعية

الكلمات المفتاحية :

النخيل، المخلفات النباتية، المواد المركبة، المواد الطبيعية، التوصيل الحراري.

Figure List

Fig I. 1 Components of a composite material	6
Fig I. 2 Classification of different types of composite materials	6
Fig I. 3 Composite material with particles reinforced	7
Fig I. 4 Composite material with fibers reinforced.....	7
Fig I. 5 Composite material laminate.....	8
Fig I. 6 Sandwich structure	8
Fig I. 7 Sandwich with foam core.....	11
Fig I. 8 Sandwich with wood core	11
Fig I. 9 Sandwich with honeycomb core	12
Fig I. 10 Assembling of the sandwich	12
Fig I. 11 The most methods used to elaborate a sandwich	13
Fig I. 12 Manufacturing a sandwich structure by gluing	13
Fig I. 13 Application Field of Sandwich	14
Fig I. 14 Categories of bio-composite.....	15
Fig I. 15 Chemical composition of plant fibers	18
Fig I. 16 Date palm trees.....	20
Fig I. 17 Date palm Schema Components	20
Fig I. 18 Palm's components	21
Fig I. 19 Applications of the palm fiber waste.....	22
Fig I. 20 Boom made of bast fiber	22
Fig I. 21 Some applications of bio-composites in the industry.....	24
Fig II. 1 Comparative Analysis of the Chemical Composition of Date Palm Wood and Other Natural Fibers.....	28
Fig II. 2 Mechanical properties of date palm fibers	29
Fig II. 3 Thermal Conductivity and Relative Permittivity of Date Palm Materials: A Comparative Study of Petiole and Bunch Parts from Deglet-Noor, Mechdeglet, and Elghers Varieties	31
Fig II. 4 Comparison between experimental data for TS and E with their predicted results.....	32

Fig II. 5 Flexural modulus of date palm, date palm/bamboo and bamboo composite fibre	34
Fig II. 6 tensile properties of DPF/Epoxy	35
Fig II. 7 Tensile properties of DS-UPR composites; (a) Stress-strain curves (b) Tensile strain (%) , (c) Tensile strength, and (d) Tensile modulus	36
Fig II. 8 Erosion Efficiency of PVA/DPL Bio-Composites: Impact of Velocity on Wear Resistance	37
Fig II. 9 Comparative Analysis of Thermal Properties in Raw Wood and Wood-Plastic Composites (WPC)	38
Fig II. 10 Bar chart of average normal stresses in bending, in shear, and of average stiffness in bending and in shear	42
Fig III. 1 Rachis fiber with a size of 0.315 mm	46
Fig III. 2 Epoxy Resin (MEDAPOXY STR EA).....	47
Fig III. 3 Petiole granules with a size \leq 1mm.....	49
Fig III. 4 Molecular formula of polyvinyl acetate glue	50
Fig III. 5 Protocol to obtain the specimens bio-composite material (ER)	52
Fig III. 6 Preparation of Petiole agglomerate.....	53
Fig III. 7 Three points pending test of bio-composite (ER) (a): Geometric dimensions, (b): Three points bending.....	55
Fig III. 8 Three points pending test of bio-composite (Pt) (a): Universal machine TesT GMBH model 916713, (b): Three points bending test	56
Fig III. 9 Compression test of bio-composite (Pt) (a): Geometric dimensions, (b): Compression bending test.....	57
Fig III. 10 INNOVATEST VERZU 750 model of Brinell hardness test	58
Fig III. 11 INNOVATEST VERZU 750 model of Brinell hardness test	59
Fig III. 12 Kapton support	59
Fig III. 13 Operating Principle of the SETARAM LABSYS evo Thermogravimetric Analyzer. 60	
Fig III. 14 Protocol of gravimetric method.....	61
Fig III. 15 Principle of Thermo Scientific Quanta SEM Prisma E electron microscope.....	64
Fig III. 16 Principle of Malvern Panalytical X-ray diffractometer.....	65
Fig III. 17 Principle of PerkinElmer Spectrum Two with an ATR-FTIR.....	66

Fig IV. 1 SEM Analysis of : (a) a petiole particle Microstructure (b) a Rachis fibers Microstructure.....	70
Fig IV. 2 FTIR spectra analysis of a raw Petiole	71
Fig IV. 3 FTIR spectra analysis of rachis fibers	72
Fig IV. 4 XRD spectra analysis of Petiole particle.....	73
Fig IV. 5 XRD spectra of rachis fibers	74
Fig IV. 6 TGA and DSC analysis pattern of a petiole particle	75
Fig IV. 7 TGA and DSC analysis of rachis fibers	76
Fig IV. 8 Load-displacement curves of different bio-composites (ER) in three-point bending tests	77
Fig IV. 9 Flexural modulus of a different bio-composite ER.....	78
Fig IV. 10 Flexural strength of different bio-composite ER.....	78
Fig IV. 11 Hardness properties of different types of bio-composite ER	80
Fig IV. 12 Thermal behaviour of different types of bio-composite ER.....	81
Fig IV. 13 TGA and DSC of bio-composite ER.....	82
Fig IV. 14 Water absorption tendencies of bio-composite ER.....	83
Fig IV. 15 Enhancing Water-Molecule and Cellulose Interaction: A Schematic Diagram of Hydrogen Bonding.....	83
Fig IV. 16 Density values of different types of bio-composite ER	85
Fig IV. 17 SEM micrographs for the Rachis/Epoxy (ER) composites with 10 wt. % of the rachis	86
Fig IV. 18 DRX spectra of the bio-composite ER.....	87
Fig IV. 19 FTIR spectra of the bio-composite ER.....	88
Fig IV. 20 Load -. Displacement curve for different types of Pt in three points bending test.....	89
Fig IV. 21 Stress-strain curve of Pt17 by compression tests (a): in the transverse directions, (b): in the longitudinal directions	91
Fig IV. 22 TGA and DSC curve of bio-composite petiole agglomerate (PT17)	93
Fig IV. 23 Percentage of water absorption for different types of petiole agglomerate (Pt)	95
Fig IV. 24 Density of tested bio-composite materials	97
Fig IV. 25 SEM image of the Petiole agglomerate (Pt17).....	97

Fig IV. 26 XRD spectra of petiole agglomerate	99
Fig V. 1 Bio-composite ER10 used as a skin in the sandwich	104
Fig V. 2 Petiole agglomerate Pt17 used as cores in the sandwich	105
Fig V. 3 Sandwich preparation protocol (SP/R)	106
Fig V. 4 Sandwich specimen's types (a): SP/R to three points bending tests,	107
Fig V. 5 Geometric dimensions of a sandwich by three-point bending.....	107
Fig V. 6 Three-point bending test of Sandwich SP/R.....	108
Fig V. 7 Experimental Analysis of Thermal Properties Sandwich SP/R.....	109
Fig V. 8 Load-deflection curves of Sandwiches SP/R during three-point bending test	110
Fig V. 9 Thermal properties of sandwich structure beam specimens bio-composite	112
Fig V. 10 Equivalent Electrical Model of Thermal Resistance in Composite Walls	113
Fig V. 11 Comparison between the Thermal Resistance our new sandwich with different Sandwich materials	115
Fig V. 12 Schematic view of FPC models	116
Fig V. 13 Variation of the air outlet Températures Vs. FPCs length.....	119
Fig V. 14 Variation of the FPCs efficiencies Vs. the air flow rate, Q_v	119

Table List

Table II. 1 Results of tensile tests (Lif-Polypropylene)	32
Table II. 2 Results of tensile tests (Rachis/Epoxy)	33
Table II. 3 Overall stiffness (DG) values in different sandwiches	40
Table III. 1 Properties of Epoxy Resin (MEDAPOXY STR EA)	47
Table III. 2 Properties of vinyl glue PVA	50
Table III. 3 Five types of Bio-composite ER (Rachis fibers-resin epoxy)	51
Table III. 4 Five types of Bio-composite Pt (Petiole agglomerate)	52
Table IV. 1 Mechanical behavior for different types of bio-composite (ER).....	77
Table IV. 2 Thermal properties of different types of a bio-composite ER	80
Table IV. 3 Mechanical property values of different types of petiole agglomerate Pt.....	90
Table IV. 4 Elasticity modulus longitudinal and Transverse of petiole agglomerate (Pt17).....	91
Table IV. 5 Thermal properties of bio-composite material	92
Table IV. 6 Bulk density values of different types of petiole agglomerate	96
Table IV. 7 Chemical composition of petiole agglomerate (Pt17)	98
Table V. 1 Proprieties of bio-composite ER10	104
Table V. 2 Proprieties of bio-composite ER10	105
Table V. 3 Overall stiffness values of sandwich SP/R during by three-point bending test	110
Table V. 4 Thermal properties of new sandwich-structured composite	112
Table V. 5 Materials Composing the Sandwiches and Their Thermal Conductivity	114

Contents

<i>Thanks</i>	<i>III</i>
<i>Dedication</i>	<i>IV</i>
<i>Abstract</i>	<i>VI</i>
<i>Figure List</i>	<i>VIII</i>
<i>Table List</i>	<i>XII</i>
General Introduction.....	2
Chapter I: On composite materials and sandwich structures	
<i>I.1.Composites materials</i>	5
<i>I.2.1. Classification according to the nature of the components</i>	7
<i>I.2.1.1. Composite with particles reinforced</i>	7
<i>I.2.1.2.Composite with fibers reinforced</i>	7
<i>I.2.2.Classification according to the Shape of Components</i>	7
<i>I.2.2.1.Laminates</i>	8
<i>I.2.2.2.sandwich</i>	8
<i>I.3.Components of sandwich structures</i>	9
<i>I.3.1.Skins</i>	9
<i>I.3.2.Core</i>	10
<i>I.3.3.Adhesive</i>	12
<i>I.4.Manufacturing processes</i>	12
<i>I.5. Application Field of sandwich structures</i>	14
<i>I.6. Bio-sourced composite materials</i>	14
<i>I.6.1. Plant fiber reinforcement</i>	16

<i>I.6.1.1. Chemical composition of plant fibers</i>	16
<i>I.6.1.1.1. Cellulose</i>	16
<i>I.6.1.1.2.Hemicellulose</i>	17
<i>I.6.1.1.3.Lignin</i>	17
<i>I.6.1.1.4.Pectins</i>	17
<i>I.6.1.2.Properties and benefits of plant fibers</i>	18
<i>I.7.Date palm</i>	18
<i>I.7.1.Components of date palm</i>	20
<i>I.7.1.1.Palm</i>	21
<i>I.7.2.Date Palm By-Products and Their Applications</i>	21
<i>I.7.2.1.Date Palm Fiber</i>	21
<i>I.7.2.1.1.Palm Fibers</i>	21
<i>I.7.2.1.1.Bast Fibers</i>	22
<i>I.7.2.1.2.Wood Fibes</i>	22
<i>I.7.2.1.3.Surface Fibers</i>	23
<i>I.7.2.1.4.Fruit Fibers</i>	23
<i>I.8.Bio-composites (natural fiber composites)</i>	23
<i>I.8.1.Characteristics of bio-composites</i>	24
<i>I.8.2.Applications of bio-composites</i>	24

Chapter II: State of the art

<i>II.1. Search bibliographies on fibers</i>	27
<i>II.2. Search bibliographies on skin</i>	32
<i>II.3. Search bibliographies on core</i>	36
<i>II.4. Search bibliographies on sandwich</i>	39

Chapter III: Materials and Methods

<i>III.1. Material</i>	45
<i>III.1.1. Materials of the skins</i>	45
<i>III.1.1.1. Reinforcement (Rachis fibers)</i>	45
<i>III.1.1.2. Matrix (Epoxy resin)</i>	46
<i>III.1.2. Materials of the core</i>	48
<i>III.1.2.1. Reinforcement (petiole granules)</i>	48
<i>III.1.2.2. Matrix (Polyvinyl acetate glue (PVA))</i>	49
<i>III.2. Processes of preparing sandwich plates</i>	50
<i>III.2.1. Preparation of the skins</i>	51
<i>III.2. Preparation of the core</i>	52
<i>III.3. Experimental techniques</i>	54
<i>III.3.1.1. Three-point bending tests of bio-composite RE (Rachis fibers-resin epoxy)</i>	54
<i>III.3.1.2. Three point bending tests of bio-composite Pt (Petiole agglomerate)</i>	55
<i>III.3.1.3. Compression tests of bio-composite Pt (Petiole agglomerate)</i>	56
<i>III.3.1.3. Brinell hardness tests of a bio-composite RE (Rachis fibers-resin epoxy)</i>	57
<i>III.3.2. Thermo-physical properties</i>	58
<i>III.3.2.1. Thermal conductivity of Pt and RE</i>	58
<i>III.3.2.2. Thermogravimetric Analysis (TGA) and Differential Scanning Calorimetry (DSC)</i> 60	
<i>III.3.2.3. Water absorption test of Pt and RE</i>	61
<i>III.3.2.4. Density test Pt and ER</i>	62
<i>III.3.3. Microstructure properties</i>	63
<i>III.3.3.1. Scanning electron microscopy (SEM)</i>	63
<i>III.3.3.2. X-ray diffraction (XRD)</i>	64

<i>III.3.3.3. Fourier-transform infrared spectroscopy (FTIR).....</i>	<i>65</i>
---	-----------

Chapter IV: Results and discussion

<i>IV.1.Properties of a petiole particle and rachis fibers</i>	<i>69</i>
<i>IV.1.1. Scanning electron microscopy SEM results</i>	<i>69</i>
<i>IV.1.2. Fourier-transform infrared spectroscopy (FTIR) result.....</i>	<i>70</i>
<i>IV.1.2.1. FTIR analysis of a petiole particle</i>	<i>70</i>
<i>IV.1.2.2. FTIR analysis of Rachis fiber</i>	<i>71</i>
<i>IV.1.3. X-ray diffraction (XRD) analysis results</i>	<i>72</i>
<i>IV.1.3.1. XRD analysis of Petiole particle.....</i>	<i>72</i>
<i>IV.1.3.2. XRD analysis of Rachis fibers.....</i>	<i>73</i>
<i>IV.1.4. Thermogravimetry (TGA) and Differential Scanning Calorimetry (DSC) analysis</i>	<i>74</i>
<i>IV.1.4.1. TGA and DSC analysis of petiole particle</i>	<i>74</i>
<i>IV.1.4.2. TGA and DSC for Rachis fibers.....</i>	<i>75</i>
<i>V.2. Results and discussion of experimental techniques.....</i>	<i>76</i>
<i>IV.2.1. Mechanical characteristics of bio-composite ER (Rachis fibers-resin epoxy).....</i>	<i>76</i>
<i>IV.2.1.1. Load-displacement curves (Three-point bending tests) of bio-composite ER.....</i>	<i>76</i>
<i>IV.2.2.4. Bulk Density of bio- composite ER</i>	<i>84</i>
<i>IV.2.3.2. X-ray diffraction (DRX) of bio-composite ER.....</i>	<i>86</i>
<i>IV.2.6 Structural properties of petiole agglomerate (Pt)</i>	<i>97</i>
<i>IV.2.6.1. Scanning Electron Microscope (SEM) of petiole agglomerate (Pt)</i>	<i>97</i>
<i>IV.2.6.2. X-ray diffraction (XRD) of petiole agglomerate.....</i>	<i>99</i>

Chapter V: Experimental investigation of sandwich structure for thermal insulation purpose

<i>V.1. Sandwich components.....</i>	<i>104</i>
<i>V.1.1 Skin (Bio-composite ER10).....</i>	<i>104</i>

<i>V.1.2 Core (Petiole agglomerate Pt17)</i>	105
<i>V.1.3. Sandwich preparation [petiole agglomerate (Pt17)/Rachis fibers -epoxy resin (ER10)]</i>	106
<i>V.2. Experimental technique of sandwich structure (S_{P/R})</i>	107
<i>V.2.1. Mechanical properties of sandwich (S_{P/R})</i>	107
<i>V.2.2. Thermal properties of sandwich (S_{P/R})</i>	109
<i>V.3. Results and discussion</i>	109
<i>V.3.1. Results of Mechanical properties of sandwich (S_{P/R})</i>	109
<i>V.3.2. Thermal properties</i>	111
<i>V.4. Thermal Evaluation, Application in Solar Flat collector</i>	112
<i>V.4.1. Theoretical analysis</i>	112
<i>V.4.1.1. Thermal resistance of sandwiches</i>	112
<i>V.4.1.2. Comparison of Thermal Resistance of different Sandwiches</i>	113
<i>V.4.2. Application in Solar Flat plate collectors (FPCs)</i>	115
<i>V.4.2.1. Presentation of FPCs Models</i>	115
<i>V.4.4.2. Theoretical analysis</i>	116
<i>V.4.2.3.</i>	118
<i>Conclusion</i>	120

General Introduction

General Introduction

The rising energy consumption in residential buildings is largely due to the inadequate insulation properties of conventional construction materials. As insulation plays a key role in enhancing energy efficiency, there has been a growing interest in exploring sustainable, biodegradable, and bio-based alternatives, particularly natural fibers, for eco-friendly bio-composites. Vegetal fibers, either used alone or as additives, are becoming popular due to their abundance, low cost, biodegradability, renewability, and non-toxic properties [1]. Their low density also makes them suitable replacements for certain synthetic fibers like glass, carbon, and aramid fibers. However, incorporating natural fibers into polymer matrices can sometimes reduce the mechanical strength of composites, although exceptions exist [2]. The performance of these composites heavily depends on the bond between the fibers and the matrix, which significantly affects the material's mechanical and physical properties. In Algeria, date palm fibers (DPF) are an especially promising alternative, due to their wide availability and potential for use as renewable natural resources.

This doctoral thesis, aims to demonstrate the significant potential of date palm waste, particularly fibers from mature palms, as a renewable and sustainable resource for bio-composite materials, offering a compelling alternative to conventional wood-based products.

Following the research carried out in this area, and especially those carried out in our two Mechanics laboratories at the University of Biskra (LGM and LGEM laboratories). This investigation constitutes a continuation of the works carried out previously [3–5], with emphasis on one of the essential parts in the residues of the date palm, which is the petiole/rachis which proves to be more suitable for thermal insulation.

Within this environmental, economic, and innovative framework, the present study aims to develop and characterize new bio-composite materials that can serve as effective thermal insulation. This doctoral thesis investigates the mechanical behavior of bio-composite sandwich panels derived from date palm waste, aiming to develop and characterize a bio-sourced material for structural applications. The sandwich panels feature a core of petiole granules within a polyvinyl alcohol (PVA) matrix and a skin layer composed of rachis fibers embedded in an epoxy

resin matrix. To validate the selection of these materials, the thesis will conduct comprehensive tests to predict and evaluate the mechanical properties of each layer, supporting the effective use of date palm waste in sustainable composite insulator panel production. Various parameters, such as fiber ratio, are considered. Experimental analyses are conducted to evaluate the bio-composite's morphological, thermal, physical, and mechanical properties.

This study seeks to determine whether these new bio-composites meet the technical criteria for use as insulation material. To examine this issue in depth, this thesis is structured into five chapters as follows:

The first chapter introduces key concepts related to composite materials, including classifications, historical development, and applications, with a focus on natural fiber-reinforced composites.

In the second chapter, we review some existing research on composite materials utilizing date palm fibers as reinforcement within a matrix, which forms the basis of the materials used in this study.

The third chapter outlines the materials, experimental protocol, and manufacturing processes for different investigated bio-composites. The first composite consists of petiole fibers reinforced with polyvinyl alcohol (PVA) core, while the second is based on rachis fibers and expanded epoxy resin waste, forming the components of a sandwich structure. Additionally, this chapter presents the various morphological, mechanical, and thermophysical tests performed on the samples.

Analyzes and interpretations of the results from these tests are presented in the fourth chapter. A comparison with existing literature is also presented to assess the performance of the bio-composites developed in this study.

The fifth chapter is an application of the bio-composites developed in the previous sections as thermal insulation sandwich panels. We investigate the mechanical and thermal properties of a different combination of composite material based on the characterizations previously realized. The skin is made from an epoxy resin matrix reinforced with rachis fibers, and the core is composed of petiole particles embedded in PVA. Two different manufacturing methods are employed. The mechanical properties, such as three-point bending, and thermal conductivity are

General Introduction

analyzed for these sandwich panels. A comparison of thermal insulation performances with different sandwich is also presented for application in flat plate solar collectors.

At the end of the manuscript, we provide a general conclusion, which encompasses the results from this research as a comprehensive summary of the findings, highlighting the key contributions of this work and offering insights into future research prospects.

Chapter I: On composite materials and sandwich structures

Chapter I: On composite materials and sandwich structures

Introduction

Composite materials have garnered significant attention across various industries due to their lightweight nature, high strength and superior mechanical properties when compared to traditional materials. One particular area of interest within composite materials research involves utilizing natural fibers as reinforcement in sandwich structures. Historically, the utilization of plant fibers in composite materials can be traced back to ancient times when natural fibers like flax, hemp and sisal were commonly used for reinforcement. Recently, there has been a shift towards exploring the potential of palm tree fibers as a reinforcement in sandwich composite structures.

Palm tree fibers offer numerous advantages, including high strength, low density and biodegradability. Studies have indicated that incorporating palm tree fibers in sandwich composites can enhance mechanical properties such as increased flexural strength and impact resistance. Furthermore, palm tree fibers are readily available and sustainable making them an environmentally friendly option for composite materials.

The incorporation of palm tree fibers into sandwich composite materials holds great promise in transforming the industry through the provision of an environmentally friendly and economically viable substitute for synthetic fibers. As ongoing research in this domain progresses, it becomes imperative to delve into different processing methods and material blends to enhance the overall efficiency and effectiveness of palm tree fiber-reinforced sandwich composites.

I.1.Composites materials

Composite material is generally made up of one or more discontinuous phases distributed in a continuous phase (Fig I.1). In the case of several discontinuous phases of different natures, the composite is called a hybrid. The discontinuous phase is usually harder and has mechanical properties in traction superior to the continuous phase. The continuous phase is called matrix and the discontinuous phase is called reinforcement[6].

Natural materials like wood and bones exhibit composite structures combining fibers within a matrix to achieve specific mechanical properties [7]. Wood, for example, contains cellulose

fibers providing flexibility and strength against tension, embedded in a lignin matrix for structural support[8]. The fibrous nature of wood, evident in its grain, showcases the arrangement of these fibers within the matrix contributing to its overall mechanical behavior[9]. Similarly, bones possess a rigid yet lightweight structure due to the arrangement of collagen fibers within a mineral matrix, highlighting the diverse applications of composite materials in nature for achieving a balance between strength and flexibility.

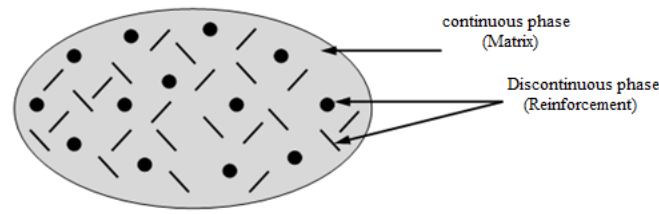


Fig I. 1 Components of a composite material [10]

I.2. Classification of composite material

There are a large number of composite materials that can be classified either according to the nature of the components or according to the shape of the components (Figure I.2) [11].

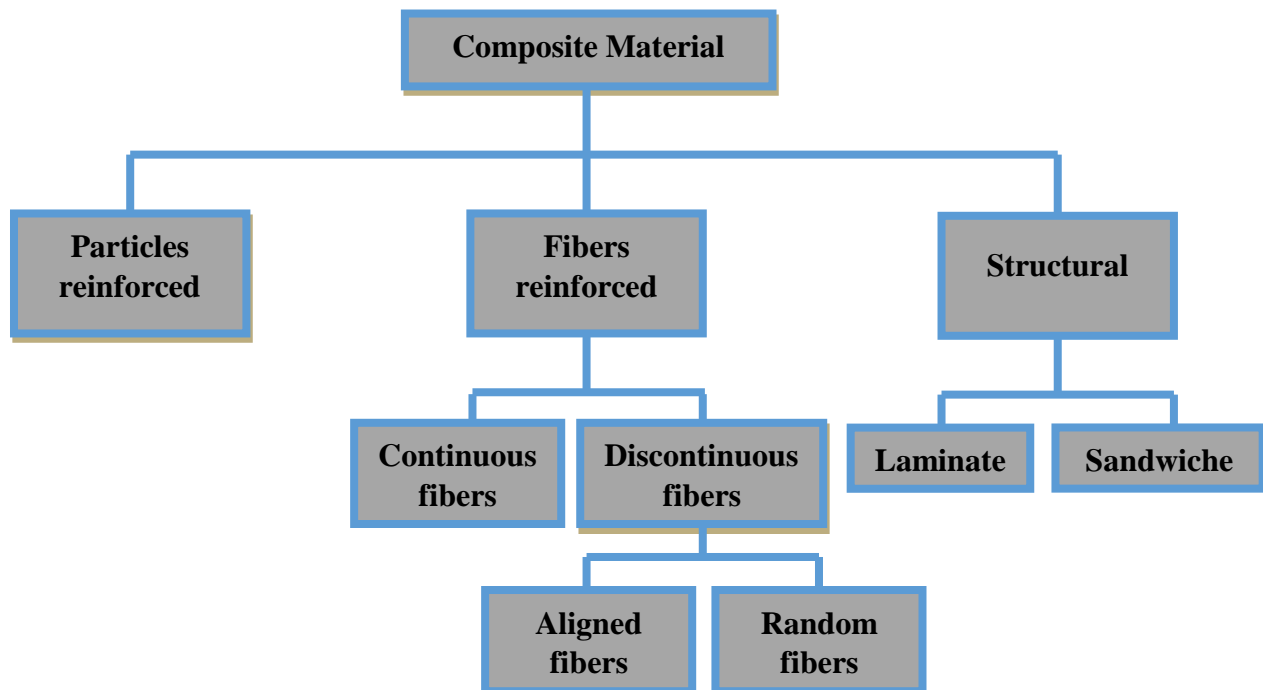


Fig I. 2 Classification of different types of composite materials [12]

I.2.1. Classification according to the nature of the components

There are two main classifications of composite materials according to the nature of the components (particles reinforced and fibers reinforced).

I.2.1.1. Composite with particles reinforced

When the reinforcement is in the form of particles, a composite material with reinforced particles is strong. These particles are generally used to improve certain properties of materials such as stiffness, temperature resistance, abrasion resistance and shrinkage reduction, etc. (Fig I.3) [13].

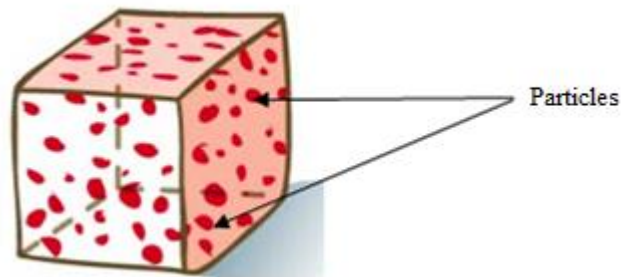


Fig I. 3 Composite material with particles reinforced

I.2.1.2. Composite with fibers reinforced

When the reinforcement is in the form of fibers, the composite with fibers is reinforced. They are either short fibers or long fibers [13]. (Fig I.4)

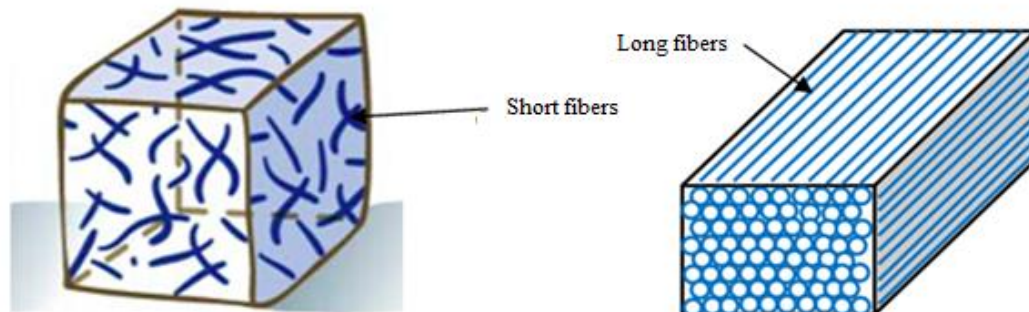


Fig I. 4 Composite material with fibers reinforced

I.2.2. Classification according to the Shape of Components

Composite materials can be classified according to shape:

I.2.2.1.Laminates

A laminate consists of a stack of monolayers and each one of them has an orientation specific to a reference frame common to the layers and designated as the laminate reference frame (Fig I.5). It is possible to finely adapt the mechanical properties of the laminate to external stresses. Therefore to achieve a high level of optimization by putting the material where it is most useful [13].

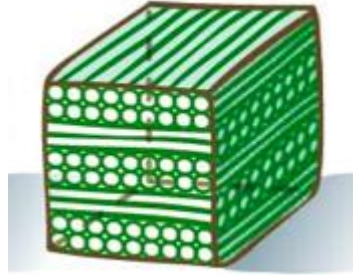


Fig I. 5 Composite material laminate

I.2.2.2.sandwich

Sandwich structures are crucial in composite part construction and are widely used across various application fields. These structures consist of two thin and rigid skins glued or welded to a lighter core with lower mechanical characteristics (Fig I.6) [5]. This core maintains the skin's spacing and transmits mechanical actions by shear from one skin to the other. Sandwich structures offer the unique ability to stiffen and lighten a structure while providing additional properties such as sound or thermal insulation depend on the chosen core material. This combination results in a construction that is strong, rigid and lightweight, demonstrating high efficiency and robustness



Fig I. 6 Sandwich structure

In sandwiches, the skins are often identical in material and thickness. These structures are called symmetrical sandwiches. However, in certain special cases, the two skins may have two

different thicknesses or two different materials. They are varied according to the loading conditions or the working environment. These structures are called asymmetrical sandwiches.

In general, sandwiches are symmetrical; the variety of sandwich construction depends on the structure of the core. It can be made of any material or any architectural form, but they are generally classified into several types: foam or solid core, honeycomb core, corrugated cardboard core and lattice.

The adhesion between the skins and the core is crucial for load transfer in sandwich structures where the skins bear bending loads while the core carries shear loads due to the skins' superior strength and stiffness in tension and compression compared to the core's low density [14]. Sandwich panels excel in bending offer resistance to buckling and shear and making them effective structural components. [15]

I.3.Components of sandwich structures

Sandwich structures are made of a wide variety of materials. These materials are characterized by great lightness and good flexural rigidity and high thermal insulation [16].

A sandwich is generally made of three components with different, but complementary properties: the skins, the core and the adhesive [17].

To successfully select the materials for a sandwich composite, it is important to understand how the structure functions as a whole. Therefore, it is also important to know the physical and mechanical properties of each of the materials used and how they contribute to the functioning of the composite material [18].

The skins should be made of materials with a high modulus of elasticity while the core should be made of materials with a low density [19].

I.3.1.Skins

In a sandwich structure, the skins can be made of several different materials, a metallic material or a composite material. The choice of the nature of the skin is mainly made according to the required mechanical performances [9].

Generally, high rigidity and excellent resistance to compression and traction are the main qualities sought [20]. The skins of sandwich materials are generally made of fibers coated with a resin-based matrix. There are several types of fibers among which we find [21] :

- **Metallic:** Skins in the form of sheets made of various metallic materials such as steel and aluminum alloys are most often used [22].

- **Synthetic or mineral:** Among the various synthetic fibers used we can cite:

Glass fibers which are obtained by spinning glass (silica + sodium and calcium carbonates) in fusion ($T > 1000^\circ \text{C}$), through platinum alloy spinnerets, Kevlar fibers (aramid) which are flavored polyamides obtained by synthesis at -10°C , then spun and stretched to obtain a high modulus of elasticity and have modulus ranging from 60 to 180 GPa and a density of approximately 1400 kg.m^{-3} . Carbon fibers which are acrylic filaments of tergal or rayon obtained from the distillation of coal or petroleum and have modulus that vary from 150 to 800 GPa and a density generally less than 2000 kg m^{-3} .

- **Plants:** Among the plant fibers used, we cite bamboo fibers, linen fibers, hemp fibers and date palm fibers. A plant fiber can be represented at different scales (Microscopic, macroscopic).

I.3.2.Core

In general, the core has a very low bending resistance. Its purpose is to absorb compression and shear forces. In addition, it must be able to support localized punching loads. Hollow cores, especially honeycombs, are generally used for structures with high mechanical performance. They have relatively high performance but have a relatively high manufacturing cost and are generally limited to flat structures. Solid cores, such as foams or balsa, allow the production of flat or curved sandwich structures with a relatively high performance-price ratio. Among the different types of cores that exist on the market, we find [23]:

- **Foams**

Foams (Fig. I.7) are the most frequently used, they are produced from polyvinyl chloride, polystyrene, polyurethane or other synthetic polymers. Their densities vary from 30 to 300 kg/m^3 and their thicknesses from 3 to 40 mm. The average sampling is 80 kg/m^3 of density and 15 mm of thickness. They are thermo-formable and therefore allow to production of parts of complex shapes. Their mechanical properties are good and adhere well to the resin and absorb little water. However, their weak point lies in a low impact resistance[24].

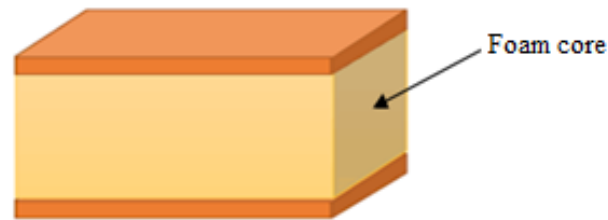


Fig I. 7 Sandwich with foam core

- **Wood**

Wood (Fig. I.8) is used for its very good compressive strength. Balsa is the most common variety because it is the lightest: with a density of 100 kg/m^3 . Wood is the least expensive material, but it is the most porous [23].



Fig I. 8 Sandwich with wood core [25]

- **Honeycomb**

It is a hexagonal structure (Fig. I.9) that can be made of various materials such as paper and aluminum. Its mechanical characteristics depend on the material and the size of the cells. Its density varies from 15 to 100 kg/m^3 and its thickness from 3 to 50 mm . It can be curved moderately, but the cells deform and then the mechanical properties change depending on the orientation. Gluing can also be a problem since it is done on the edge of the structure. Their properties are exceptional, but they are difficult to form and their prices are high. The most common varieties are Nomex and Korex which are made from Kevlar [24].

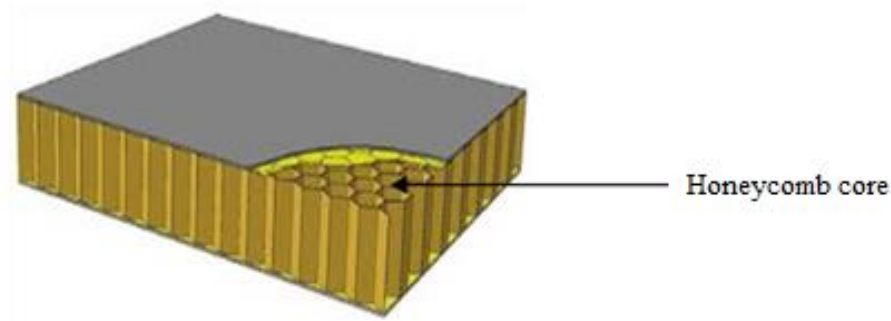


Fig I. 9 Sandwich with honeycomb core [26]

I.3.3. Adhesive

The assembly of the sandwich structure (Fig. I.10) can be carried out by gluing, welding or brazing. Whatever the method of assembly of the different layers, but the bond is perfect. The adhesive is an essential component involved in the manufacture of a sandwich. It allows a good assembly of the structure and a transmission of loads. Its main mechanical characteristic is the shear resistance. In the case of composite skins, the insertion of this third phase can be avoided by the use of a self-adhesive resin [27]

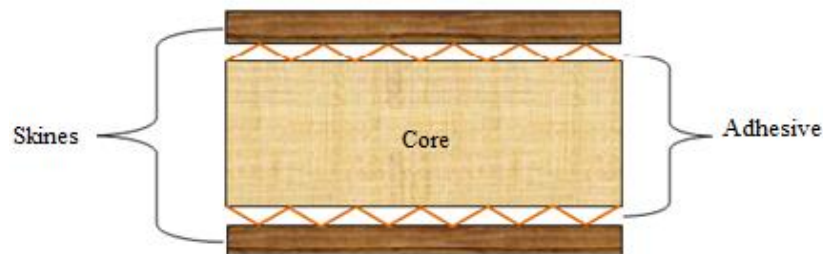


Fig I. 10 Assembling of the sandwich [27]

I.4. Manufacturing processes

Sandwich structures are manufactured by several methods with standard processing technologies (contact molding, vacuum bag molding, resin injection molding, press molding, filament winding molding or centrifugation,... etc.) which allow a core to be integrated into the thickness of the structure thus manufactured. Figure I.11 shows the most commonly used processes for the production of a sandwich.

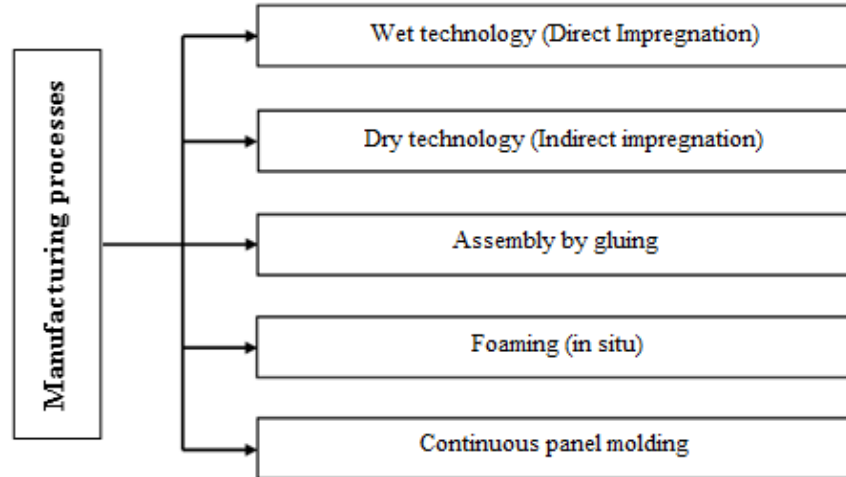


Fig I. 11 The most methods used to elaborate a sandwich [22]

The assembly of sandwiches by gluing remains a very widespread process which consists of associating the core and the skins with an adhesive. The shaping and assembly phases are then very distinct. The preparation of the surfaces is an important step which ensures quality adhesion[28] :

- Cleaning to remove grease or dust;
- Increasing the roughness;
- Priming by chemical attack of the metal skins...

The adhesive, the nature of which depends on the materials constituting the sandwich, must be applied uniformly. The stack (core + adhesive + skins) is put under pressure, (figure I.12) [22].

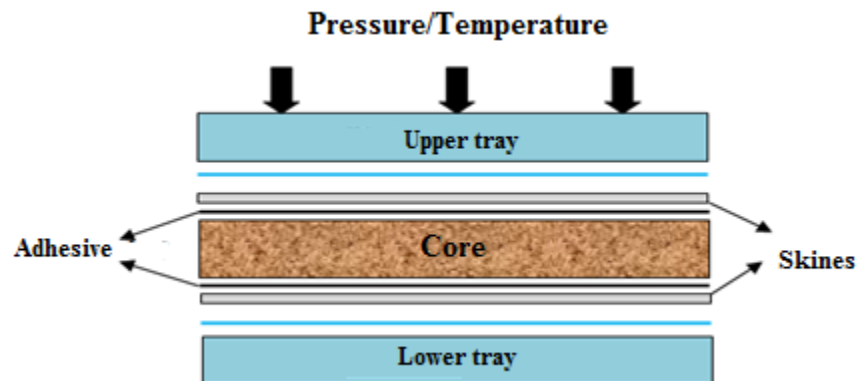


Fig I. 12 Manufacturing a sandwich structure by gluing [29]

I.5.Application Field of sandwich structures

Sandwich structures were invented in the early 19th century[30]. These structures provide great possibilities in several very different fields. The main goal is to increase the stiffness/weight ratio by using lightweight materials in the core of the sandwich structures. There are several fields of application. Therefore, we can cite some sectors of the use of sandwich structures as in the following figure (Fig I.13) [8].

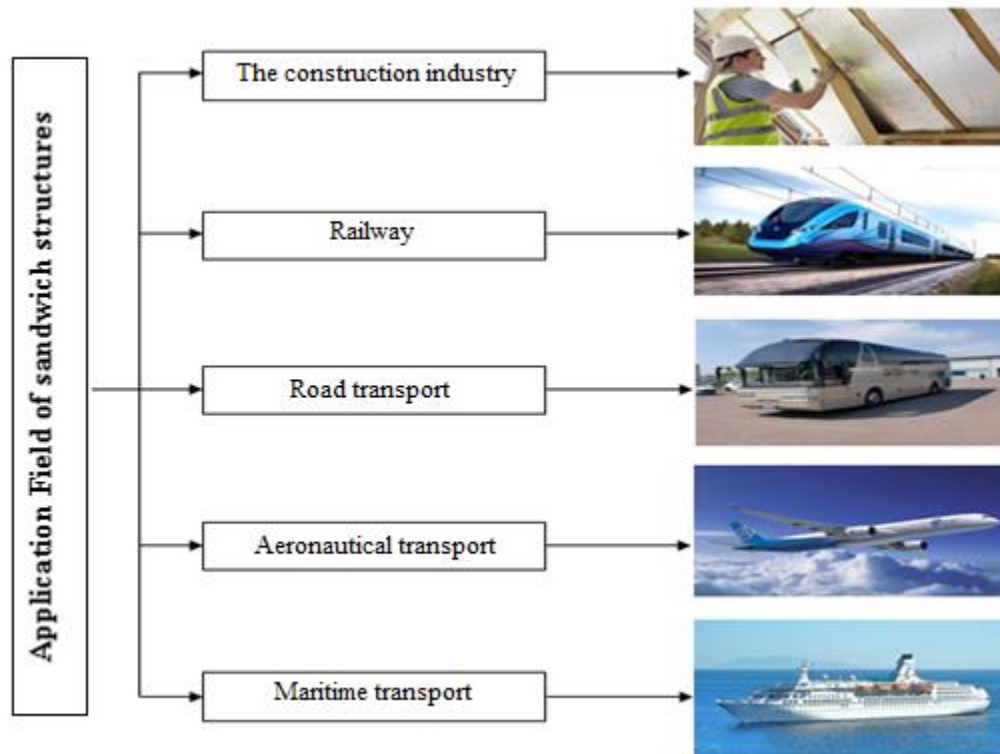


Fig I. 13 Application Field of Sandwich [8]

I.6.Bio-sourced composite materials

In today's world, the use of renewable resources in composite materials is gaining significant traction due to their economic, environmental and mechanical significance. Bio-composites, also known as biodegradable and biocompatible materials, involve at least one component derived from renewable sources like natural fibers or bio-polymers to showcase of the different levels of environmental friendliness and biodegradability based on their constituents [31]. These materials play a crucial role in various applications such as food packaging, agriculture, medical products, construction and more offer benefits like low cost, renewability and sustainability[32]. The

development of biopolymer-clay nanocomposites has further enhanced the properties of biopolymers lead to multifunctional applications with improved physicochemical and biological characteristics [28]. In addition to ,the use of bio-renewable and sustainable supplies in nanocomposites has shown exceptional advantages like rapid fabrication, better stability and diverse applications in sectors like food preservation, healthcare, energy storage and more[33]. Figure I.14 shows that bio-composite fall into two categories: Partially Eco-friendly and Eco-friendly (green).

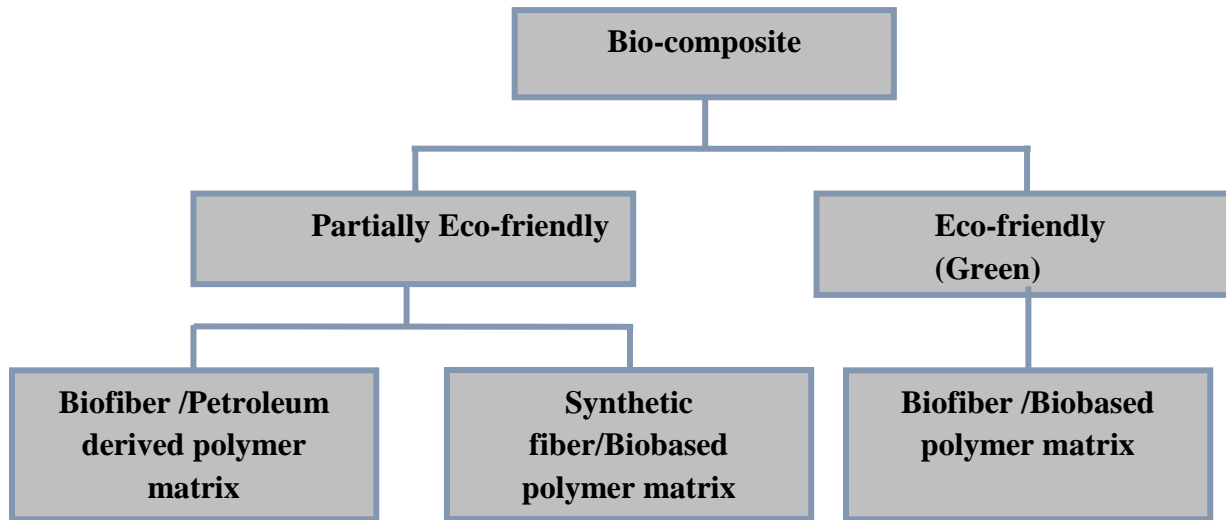


Fig I. 14 Categories of bio-composite

The development of bio-composites with high mechanical properties faces challenges due to the immature state of bio-polymers, variability in fiber properties and processing difficulties that limit their performance compared to traditional synthetic composites [34]. However, the environmental advantages of bio-composites have spurred new research efforts to enhance their properties and develop novel materials aim for a successful and sustainable bio-composite industry[32]. By exploring different extraction methods for natural fibers such as water treatment, alkaline chemical treatment ,burial in moist soil and utilizing innovative assembly techniques researchers have been able to improve the mechanical properties of bio-composites make them more competitive with synthetic materials while maintaining environmental benefits[35]. This continuous progress in characterizing and enhancing bio-composite properties holds the promise of achieving an environmentally friendly and economically stable bio-composite industry in the future.

I.6.1. Plant fiber reinforcement

Plant fibers are increasingly utilized as reinforcement in bio-sourced composite materials due to their exceptional mechanical properties and environmental benefits. These fibers, sourced from annual plants like *Cryptostegia Grandiflora*, offer advantages such as renewability, biodegradability and improved mechanical characteristics [36, 37]. Various extraction methods and assembly techniques impact the mechanical properties of these composites with chemical treatments significantly enhancing the tensile behavior of the materials [35]. Moreover, the hybridization of natural fibers with other biofibers or synthetic fibers can mitigate drawbacks like hygroscopic nature and lower mechanical performance result in composites with enhanced properties and improved sustainability [38]. Overall, the use of plant fibers in bio-sourced composites showcases a promising avenue for developing eco-friendly materials with diverse applications in various industries.

I.6.1.1. Chemical composition of plant fibers

Plant fibers are distinguished by their chemical composition, which greatly influences their durability, especially in alkaline environments. The chemical composition of plant fibers consists of various lignocellulosic and organic constituents (Fig.I.15).

I.6.1.1.1. Cellulose

Cellulose, a polysaccharide composed of $\beta(1\rightarrow4)$ linked D-glucose units, is the primary structural component of plant cell walls that provides them with rigidity and resilience [39]. Natural cellulosic fibers, extracted through various methods and treated with surface modifications, offer eco-friendly and sustainable alternatives to synthetic materials in industries like composites, textiles and packaging [40]. Cellulose-based materials, known for their high mechanical and thermal stabilities, have been extensively studied for their potential in developing green technologies and include composites with metal/semiconductor nanoparticles and polymers for energy conversion applications like solar cells and lithium-ion batteries[41]. By leveraging self-assembly techniques and additive manufacturing processes. Cellulose-based materials, particularly cellulose nanocrystals, exhibit promise in mimicking natural photonic structures for applications such as colorimetric sensors and optoelectronic devices, although further research is needed to optimize their optical properties and manufacturing processes [42].

I.6.1.1.2.Hemicellulose

Hemicellulose, the second most abundant organic substance after cellulose, contains 2.6 times more moisture than lignin [43]. It is a diverse group of non-cellulosic polysaccharides found alongside cellulose and lignin in plant cell walls. Unlike cellulose, hemicelluloses have a disordered and branched molecular structure and consist of various sugar monomers like glucose, mannose, galactose, xylose and arabinose [44]. Hemicelluloses play a crucial role in linking cellulose fibers and connecting them to lignin to enhance the flexibility and pliability of the plant cell wall[45]. Moreover, hemicelluloses exhibit higher susceptibility to hydrolysis compared to cellulose that contribute to their importance in various industrial processes and bioconversions [46].

I.6.1.1.3.Lignin

Lignin, a crucial biopolymer in plants, contributes significantly to structural support and stress tolerance. It is the second most abundant biopolymer after cellulose that forms ester linkages with hemicellulose and composed of coniferyl alcohol (G), p-coumaryl alcohol (H) and synapyl alcohol (S) precursors [47]. Lignin's aromatic structure and hydrophobic nature create a distinct network that reinforces and stiffens the plant's cellulose/hemicellulose matrix [48]. This complex polymer with its rich and versatile chemistry offers various applications and includes the production of biofuels, chemicals, resins, composites and functional coatings[49]. Efforts are ongoing to valorize lignin through techniques like producing lignin nanoparticles to enhance its potential applications across industries from pharmaceuticals to automobiles[50].

I.6.1.1.4.Pectins

Pectins, as acidic polysaccharides, found in plant cell walls possess high hydrophilicity attributed to the presence of carboxylic acid groups. These carboxylic acid groups enable pectins to interact with water molecules effectively, making them suitable for various applications such as water remediation and hydrogel formation[51]. Moreover, pectins, along with lignin and hemicellulose, play a crucial role in binding individual fibers in plant cell walls[52]. While pectins are known for their hydrophilic nature, they can also undergo hydrolysis under elevated temperatures, a process that can be significant in various industrial and biomedical applications[53]. This combination of properties makes pectins versatile compounds with potential uses in fields ranging from food and biomedical applications to environmental remediation[54].

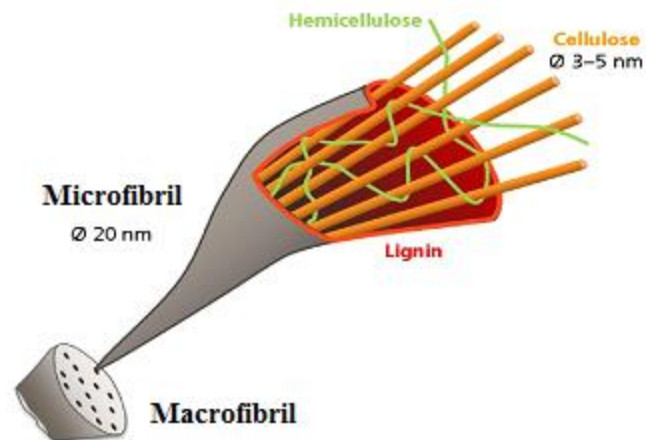


Fig I. 15 Chemical composition of plant fibers [49]

I.6.1.2. Properties and benefits of plant fibers

Plant fibers, particularly those derived from natural sources, are gaining recognition in the building industry as bio-based materials due to their commendable thermal insulating properties[1]. These fibers offer a promising alternative to conventional insulation materials, contributing to lower environmental impact and improved sustainability[55]. However, challenges such as hydrophilic properties and limited thermal stability hinder their widespread applicability, necessitating enhancements to overcome these drawbacks[56]. Recognizing the value of plant fibers in tropical climates is crucial due to their abundant availability to present a significant opportunity to address climate change concerns, especially in the building sector[57]. By leveraging the benefits of plant fibers and addressing their limitations through advancements, these materials hold great potential in mitigating environmental impacts and promoting sustainable practices in construction and insulation applications.

I.7. Date palm

The date palm is typically grown in Saharan oases. The one originating from North Africa is widely cultivated from Arabia to the Persian Gulf where it forms the characteristic vegetation of oases. It is also grown in the Canary Islands, in the northern Mediterranean, and the southern part of the United States. It is a cold-sensitive plant that grows on any type of soil and provided it with fertile and well-drained. In regions with a mild climate, it is grown outdoors, in a sunny position and mainly used as an ornamental plant for its slender appearance and foliage.

There are more than 2,600 species of palm trees. One might think that it is a tree with a trunk when it is actually a monocotyledon that does not contain wood or a trunk but has a stipe. Furthermore, it is a dioecious plant; it contains male and female palm trees. The palm tree has a very slender trunk that reaches up to 30 meters in height and visibly covered by the sheaths of dead leaves. The leaves gathered in a certain number of up to 20-30 maximum, form a sparse apical crown. They are pinnate; up to 6 meters long; the upper leaves are ascending, the basal ones curved downwards with tough, linear, rigid, spiky segments and green in color.

Date palms (*Phoenix dactylifera* L) are traditionally cultivated in South-West Asia and North Africa with increasing consumption worldwide and cultivation in regions like America, sub-Saharan Africa, Oceania and Southern Europe [58]. They are also grown in arid and semiarid regions of Iran to showcase a high degree of genetic diversity among different populations[59]. In Algeria, particularly in the southwest, date palms exhibit considerable genetic diversity with some cultivars facing the risk of extinction to emphasize the importance of conservation efforts [60]. Date palms are valued for their phytochemical-rich fruits, leaves and trunk contain compounds like polyphenols, flavonoids, carotenoids, tocopherols and triterpenoids which offer various health benefits such as antioxidant, anti-inflammatory and anti-tumor activities, along with effects against diabetes and cardiovascular issues[61].

The date palm (Fig.I.16), a significant agricultural resource in Algeria, generates a substantial amount of fibrous waste annually with Biskra alone producing up to 80,000 tons of waste per year. This waste includes various by-products such as Spadice, Grappe, Dry palms, Scrap dates and Lif, contributing to the estimated 382,200 tons of dried palms produced yearly in Algeria. With an average weight of 1.4 kg per palm and an annual production of 15 palms per tree, the approximately 18.4 million date palms in Algeria include 4.3 million in Biskra, significantly impact the total volume of dried palms in the region. The management and utilization of this substantial waste output from date palms present opportunities for sustainable resource utilization and environmental management in the Sahara Desert region[62].



Fig I. 16 Date palm trees

I.7.1.Components of date palm

Date palm tree (*Phoenix dactylifera* L.) is a versatile plant with various parts such as the trunk, crown, flowers and fruit. Each one of them plays a crucial role in its lifecycle and fruit production.

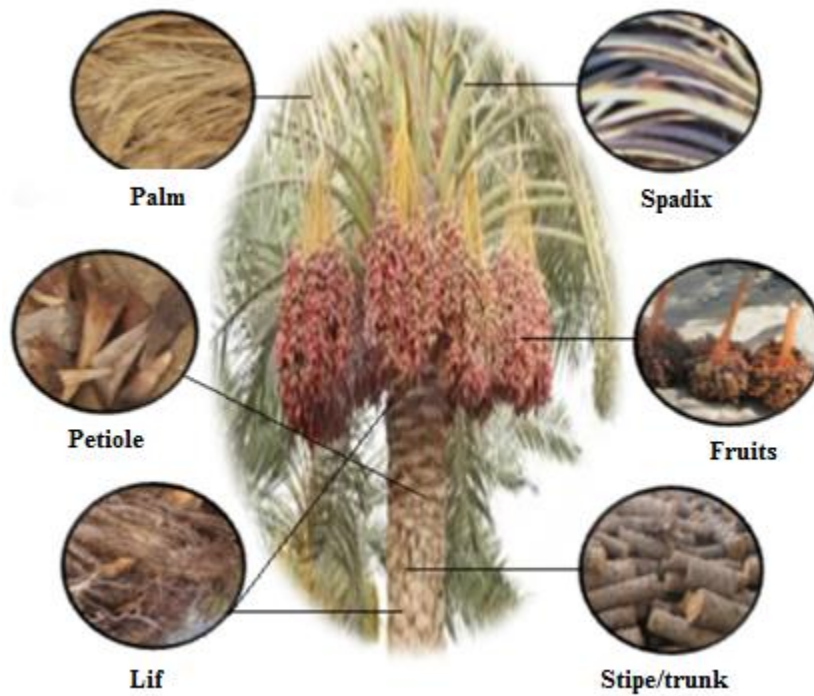


Fig I. 17 Date palm Schema Components

I.7.1.1.Palm

The palms (Fig.I.18) are one of the constituent elements of the date palm. They are made up of the petiole, the rachis, the spines and the leaflets which are arranged along the rachis. Palm can be 4 to 7 metres.

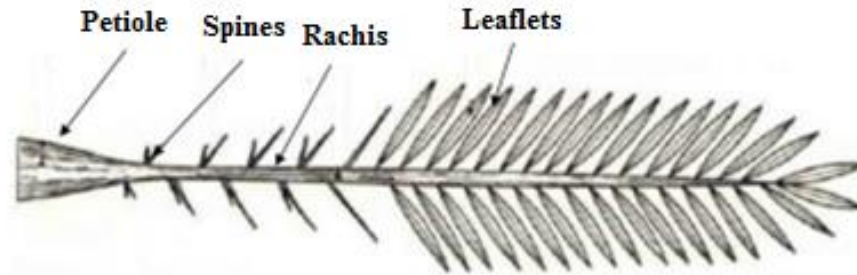


Fig I. 18 Palm's components

I.7.2.Date Palm By-Products and Their Applications

Date palm, beyond being a significant source of dates for human consumption, offers a plethora of valuable by-products that are extensively utilized. Date palm waste, including fibrous materials, dried fruits and seeds is rich in degradable biomass. It serves as a resource for natural fiber composites, active carbon precursors and nano-featured sheets [63].

These by-products are the result of palm waste that is destroyed throughout the year.

I.7.2.1.Date Palm Fiber

The date palm has a fibrous structure and possesses five types of fibers:

I.7.2.1.1.Palm Fibers

Palm fibers are found in the petiole of the leaf. These fibers are long, flexible and have high tensile strength and make them ideal for several applications:

- Ropes: Due to their strength and flexibility, leaf fibers are twisted together to create ropes that are durable and can withstand heavy loads.
- Mats: The fibers are woven into mats used for various purposes and include floor coverings, wall hangings and even temporary roofing.
- Baskets: Palm fibers are also woven into baskets which are lightweight yet strong and make them suitable for carrying goods and agricultural produce.(Fig.I.19)



Fig I. 19 Applications of the palm fiber waste

I.7.2.1.1. Bast Fibers

Bast fibers are located in the trunk of the fruit. These fibers are shorter and stiffer than palm fibers :

- Brooms (Fig.I.20): The bast fibers make them suitable for making brooms that are effective for sweeping.
- Brushes: bast fibers are used in the manufacture of brushes for cleaning purposes.
- Other Tools: The fibers' durability lends them to being used in various other tools that require a combination of strength and rigidity.



Fig I. 20 Boom made of bast fiber

I.7.2.1.2. Wood Fibres

Wood fibers are found in the trunk of the tree. These fibers are short and stiff and though not as strong as leaf or bast fibers. They have their own set of uses:

- Paper: Wood fibers are processed to make paper, a common and essential product.
- Particleboard: The fibers are combined with adhesives to create particleboard are used in construction and furniture making.

- Wood Products: Other products, such as MDF (Medium Density Fiberboard) are also made using wood fibers.

I.7.2.1.3.Surface Fibers

Surface fibers are present on the surface of the trunk. These fibers are short and soft and do not possess the strength of other fiber types:

- Stuffing for Mattresses: The softness of surface fibers makes them suitable for stuffing mattresses to provide cushioning and comfort.

- Pillows: Similarly, they are used to stuff pillows to offer a soft and comfortable filling.

I.7.2.1.4.Fruit Fibers

Fruit fibers are found in the date fruit. These fibers are short and soft with lower strength compared to other fiber types:

- Animal Feed: The fibers are mixed into animal feed to provide a source of roughage that aids in digestion.

- Fertilizer: Fruit fibers are also used as organic fertilizer to enrich the soil with nutrients and to improve its structure for better plant growth.

I.8.Bio-composites (natural fiber composites)

Bio-composites, which are natural fiber composites, are gaining traction as a sustainable alternative to traditional materials in various industries. These composites, made by combining natural fibers like hemp, linen and kenaf with biopolymer matrices, offer advantages such as low cost, renewability, biodegradability and reduced environmental impact [32]. Research highlights the potential of bio-composites in applications like packaging, construction, vehicle parts, biofuels and medical uses to showcase their versatility and wide-ranging benefits [64]. Studies emphasize the importance of optimizing fiber surface modifications to enhance the interfacial bonding with the polymer matrix leads to improved mechanical properties and biodegradability of the resulting bio-composites[65]. In addition to, the development of novel bio-composites using natural fibers and bio-resins demonstrates comparable mechanical performance to conventional composites to indicate their potential for semi-structural applications [66]. Overall, bio-composites represent a promising avenue for sustainable material development, offering durability, lightness and recyclability for various industrial applications [64].

Fig I.21 present some application for bio-composite in the industry.



Fig I. 21 Some applications of bio-composites in the industry

I.8.1.Characteristics of bio-composites

Bio-composites, which combine natural fibers with polymer matrices, exhibit unique characteristics that set them apart from traditional composites. The mechanical properties of bio-composites are influenced by factors like the type of fiber used, the characteristics of the polymer matrix and the manufacturing techniques employed [67]. Natural fibers provide adequate mechanical strength and excellent vibration absorption capabilities while the polymer matrix offers chemical resistance and ease of use[68]. Studies have highlighted the favorable mechanical and thermal properties of bio-composites to showcase their potential for various industrial applications such as in vehicles, aerospace structures, buildings and soundproofing applications[69]. The use of lignocellulosic fibers in polymer matrices has gained traction due to their biodegradability, renewability and cost-effectiveness to make bio-composites a promising material for sustainable and environmentally friendly solutions in different industries.

I.8.2.Applications of bio-composites

Bio-composites are increasingly utilized across various industries due to their sustainable attributes and superior performance characteristics. In the automotive sector, they play a crucial role in manufacturing lightweight interior components such as dashboards and door panels which

significantly enhance fuel efficiency and reduce emissions. In construction, bio-composites are employed for structural elements, insulation materials and sustainable cladding solutions to offer excellent thermal and acoustic properties that contribute to energy-efficient buildings. Moreover, in the packaging industry, bio-composites provide eco-friendly alternatives to traditional plastics, particularly in food packaging to help to reduce plastic waste and promote sustainability. The aerospace industry also benefits from bio-composites use them for lightweight components that improve fuel efficiency and overall aircraft performance. Beyond these sectors, bio-composites find applications in consumer goods include furniture and sporting equipment like bicycles and skis where durability and reduced environmental impact are essential. In electronics, they are increasingly used for device casings and housings to support the push for greener technology. Furthermore, bio-composites are making strides in the medical field with applications in biodegradable implants and sustainable medical device housings. This wide range of applications underscores the versatility and growing importance of bio-composites in fostering sustainability and innovation across multiple industries.

Conclusion

In this chapter, we provided an overview of composite materials and their classifications, focusing on bio-sourced composites reinforced with natural fibers from date palms specifically fibers and wood. We discussed the extraction methods and manufacturing processes of these composites, highlighting their good mechanical and physical properties. We noted that the properties vary depending on the extraction part and treatment methods. Date palm wood and fibers show promise for use in particle boards and sandwich structures due to their low density and good thermal insulation. This research aims to further explore these materials for use in bio-composites, utilizing mechanical and biological extraction techniques and various matrix types.

Chapter II state of the art

Chapter II: State of the art

Introduction

Numerous studies in the literature explore composite materials reinforced with plant fibers. In this chapter, we focus on research that closely aligns with our work. We provide a detailed summary of these studies, highlighting the objectives and significant findings of each. By presenting the key results, we aim to offer insight into the advancements made in this field and how they contribute to the development of bio-composite materials. Our goal is to establish a clear connection between existing research and our work, showing how date palm fibers and different matrices have been utilized to achieve improved mechanical, thermal, and physical properties in composite materials.

II.1. Search bibliographies on fibers

Almi et al. [70] presented an experimental investigation of the physical, chemical, mechanical, and thermal properties of eight different types of date palm residues from Biskra, Algeria. The study aims to evaluate the potential of these residues, individually or in combination, for producing composite materials. The results show that the rachis variety exhibits high tensile strength and Young's modulus, at 213 MPa and 8.5 GPa, respectively. The petiole variety stands out for its mechanical properties due to its low bulk density of 0.160 g/cm³, high porosity of 81.52%, and significant water absorption rate of 140%. Furthermore, thermal analysis reveals that the leaflets variety has the highest resistance to heat degradation, with primary degradation occurring at 360°C. Figure II.1. shows the result of A comparative study of the chemical composition of date palm wood and other natural fibers.

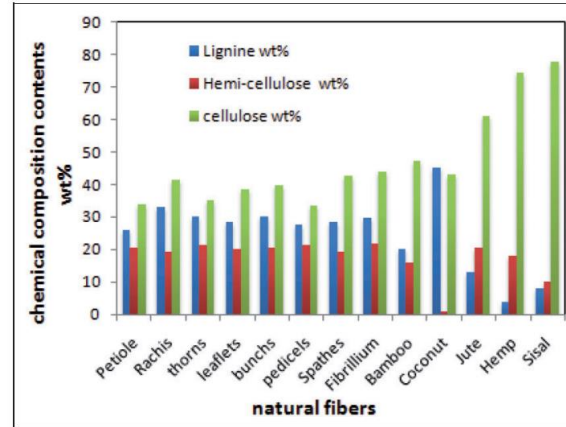


Fig II. 1 Comparative Analysis of the Chemical Composition of Date Palm Wood and Other Natural Fibers[70]

Abdalla Abdal-hay et al. [71] conducted a detailed study on date palm fibers (DPFs) with different diameters classified into three distinct ranges: 800-600 μm , 600-400 μm , and 400-200 μm , they investigated the impact of alkali treatment on these fibers. They employed a range of analytical techniques, including scanning electron microscopy for morphological observations, energy-dispersive X-ray spectroscopy density mapping for quantitative elemental analysis, X-ray diffraction, and Fourier-transform infrared spectroscopy, to examine both treated and untreated fibers. In addition to these analyses, the tensile properties of individual fibers and fiber/epoxy composites were evaluated with comparisons between chemically treated and untreated fibers. The DPFs in the composites were randomly aligned and discontinuous. The results revealed a strong dependency of mechanical properties on both alkali modification and fiber diameter. For instance, the tensile strengths of untreated and treated fiber composites with diameters of 400-200 μm were 18.5 MPa and 40.6 MPa, respectively shown in Figure II.2. FT-IR analysis further confirmed the significant effect of 6% alkali treatment on the surface properties of the DPFs, indicating the enhancement in bonding characteristics after treatment.

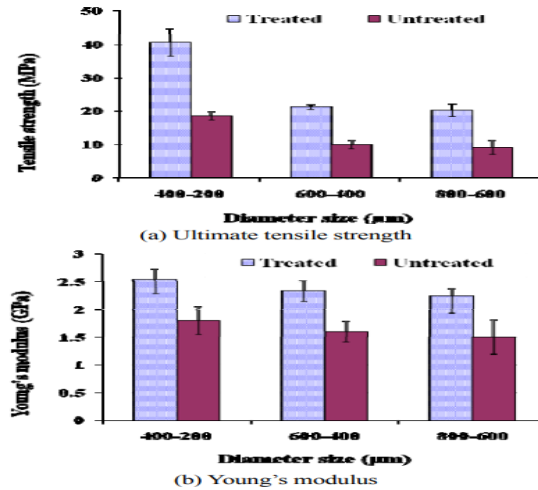


Fig II. 2 Mechanical properties of date palm fibers [71]

Elseify et al. [72] conducted an extensive study on date palm fibers (DPFs), focusing on extracting cellulosic fibers from four distinct parts of the palm: the midrib, peduncle, leaflets, and reticulum. The research revealed that DPFs possess excellent physical, mechanical, chemical, morphological, and thermal properties, which are comparable to or even superior to other well-known natural fibers such as flax, hemp, and sisal. A key aspect of the study was the comparative analysis between date palm fibers and other natural fibers, showcasing DPFs' potential for various applications. The results indicated that the density of date palm fibers reached a maximum of 1.32 g/cm³. Additionally, the thermal conductivity of date palm mesh fibers was found to range between 0.475 and 0.0697 W/mK.

Mahdavi et al. [73] present new insights into date palm fibers (DPF), focusing on their morphological and chemical characteristics, bulk density, and the morphological and mechanical properties of DPF/HDPE wood plastic composites. The study utilized fibers derived from three parts of the date palm: the trunk, rachis, and petiole. The findings revealed a significant difference in fiber length between the trunk and petiole, while the rachis showed no significant variation compared to the other parts. Aspect ratios varied notably among the three parts, where the petiole exhibited the highest values and the trunk the presented the lowest one. The chemical composition also varied significantly across different parts of the date palm, with the rachis containing the highest levels of cellulose and lignin. Bulk density measurements showed the lowest value at 0.082 g/cm³ for the trunk. The highest mechanical strengths in the composites were observed with 30% and 40% fiber content, depending on the specific part of the tree used.

Agoudjil et al. [74] conducted a detailed analysis of the thermophysical, chemical, and dielectric properties of three varieties of date palm wood from Biskra, Algeria. The study utilized Scanning Electron Microscopy (SEM) and Energy Dispersive Spectroscopy (EDS) to examine the microstructure and chemical composition of the wood. The micrographs revealed that date palm wood exhibits irregular surfaces with numerous filaments and pores, characteristics that likely contribute to its insulating properties. Key findings from the study indicate that the orientation of the fibers within the wood has a more significant impact on its relative permittivity (dielectric properties) than on thermal conductivity. Despite this, date palm wood showed promising insulating performance under both vacuum and atmospheric pressure, making it a viable material for energy-efficient and safe insulation applications. Regarding Figure II.3, which compares the thermal conductivity and relative permittivity of date palm materials, the study focused on two distinct parts: the petiole and the bunch. These parts were taken from three varieties: Deglet-Noor, Mechdeglet, and Elghers. This comparative analysis highlighted how the different parts and varieties influence the thermal and dielectric properties, with certain combinations demonstrating superior performance in terms of insulation.

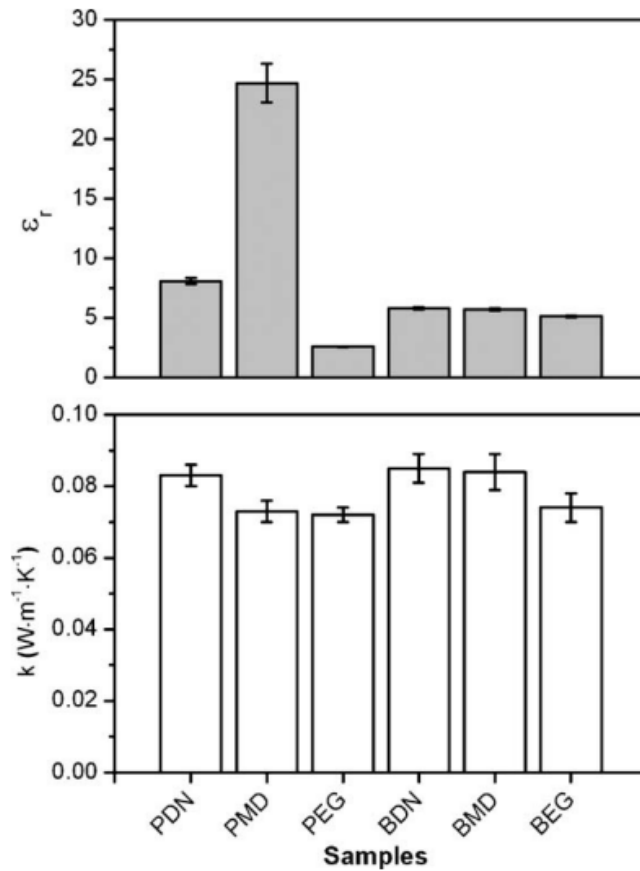


Fig II. 3 Thermal Conductivity and Relative Permittivity of Date Palm Materials: A Comparative Study of Petiole and Bunch Parts from Deglet-Noor, Mechdeget, and Elghers Varieties[74]

Bezazi et al. [75] improved the physical, chemical, and tensile properties of vascular fibers extracted from Algerian date palm trunks. The study used the Taguchi L16 orthogonal array to optimize experiments, comparing boiling and soaking methods for fiber extraction, followed by NaOH treatments at varying concentrations and durations. Characterization techniques like SEM-EDX, ATR-FTIR, XRD, and TGA were employed to analyze the fibers. Statistical analysis, including signal-to-noise ratio and ANOVA, identified key factors affecting tensile strength and Young's modulus, with a desirability function developed to optimize these properties in figure II.4.

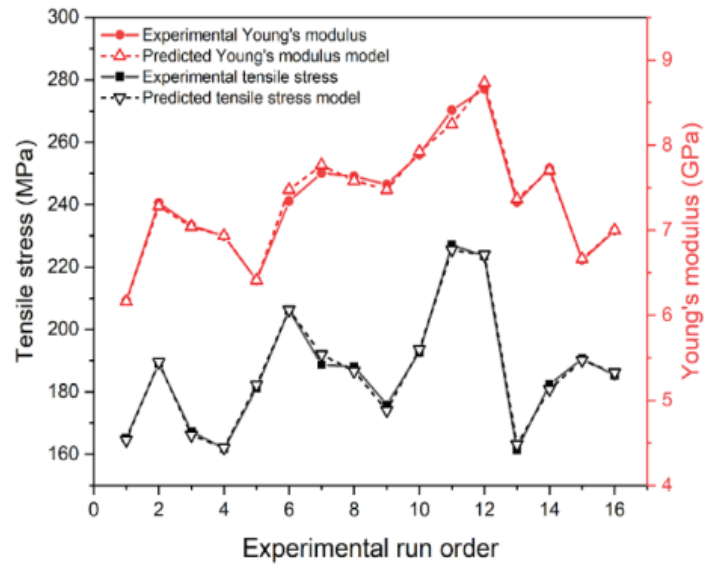


Fig II. 4 Comparison between experimental data for TS and E with their predicted results[75]

II.2. Search bibliographies on skin

In a study conducted by R, Benzidane [76], mechanical characterization of composites was carried out using Rachis/epoxy without chemical treatment. The investigation explored various mass fractions, including 5%, 10%, and 15%. This finding underscores the significance of considering different mass fractions in composite fabrication to achieve desired mechanical properties, offering valuable insights for developing composite materials with enhanced performance characteristics. The results show that the rachis variety exhibits high Young's modulus, at 3.57 GPa a rachis/epoxy 15 % untreated and 3.24 GPa a rachis/epoxy 10 % treated.

Y. Djebloun [77] conducted a study on the mechanical characteristics of thermoplastic matrix composites, specifically polypropylene, reinforced with fibers extracted from date palm trees (Lif). Utilizing a single-screw extrusion machine. He fabricated blends comprising polypropylenes and Lif fibers across a range of mass fractions, including 3%, 4%, and 5%. This investigation aimed to assess how different concentrations of Lif fibers impacted the mechanical properties of the resulting composites. By varying systematically the mass fractions of fibers, this study sought to gain insights into the relationship between fiber content and the mechanical performance of composite materials. The results of all tested specimens are presented in the following table II.1.

Table II. 1 Results of tensile tests (Lif-Polypropylene) [77]

samples	Mass fractions (%)	Mechanical properties		
		E(MPa)	σ (MPa)	ε (%)
PPL0	0	622.043±17.70	10.62	28.363±9.739
PPL3	3	642.70±23.78	19.19±2.008	9.057±3.241
PPL4	4	682.83±8	13.381±0.957	6.520±3.239
PPL5	5	686.30	/	5.25

The investigation conducted by Djoudi [4] delved into the mechanical properties of composite materials featuring a polypropylene matrix reinforced with fibers extracted from date palm rachises. These composites were meticulously crafted with different mass fractions, namely 4%, 7%, 10%, and 15%. This study aimed to evaluate the effect of concentrations of date palm rachis fibers on the mechanical behavior and performance of the resulting composites. Through systematic experimentation and analysis, a meticulous examination of the impact of these different fiber concentrations on crucial mechanical properties such as tensile strength, flexural strength, impact resistance, and modulus of elasticity is carried out by evaluating the performance across this range of mass fractions. The investigation sought to provide valuable insights into the optimal fiber concentration for enhancing polypropylene-based composites' mechanical integrity and durability, thereby contributing to advancements in sustainable and resilient materials engineering. The results of all tested specimens are presented in the following table II.2.

Table II. 2 Results of tensile tests (Rachis/Epoxy)[4]

Specimen	Mass fractions (%)	Mechanical properties		
		σ (MPa)	ε (%)	E (MPa)
PFR04	4	23.06±0.65	0.064±0.02	0.66±0.02
PFR07	7	18.81±0.59	0.064±0.08	0.79±0.08
PFR10	10	18.14±0.06	0.062±0.08	0.90±0.12
PFR15	15	10.79±3.71	0.019±0.05	0.99±0.13

The investigation conducted by A.B.M. Supian [78] investigated the physical and mechanical properties of date palm fiber-reinforced epoxy composites, including various components such as leaf stalk, tree trunk, fruit stalk, and leaf sheath. Additionally, the study investigated date palm/bamboo hybrid composites suitable for non-structural and semi-structural applications. Fabrication of these composites was achieved through a hand lay-up technique combined with compression molding. Mechanical testing, including tensile, flexural, and low-

velocity impact testing, was conducted to characterize both the date palm fiber/bamboo hybrid composite and pure composites. The study also examined the effects of exposure to liquid water and environmental conditions on the durability of these biobased composites, water absorption behavior, thickness swelling, changes in density, and physical performance. Results indicated that the date palm fiber/bamboo hybrid composite exhibited superior mechanical properties compared to date palm fiber composite without hybridization, with tensile strength, flexural strength, and impact toughness values recorded at 39.16 MPa, 61.10 MPa, and 12.70 J/m, respectively shown in figure II.5. Notably, the physical tests revealed that the date palm fiber/bamboo hybrid composite displayed reduced thickness swelling and water absorption compared to the single date palm fiber composite, suggesting its potential for application in non-structural and semi-structural components.

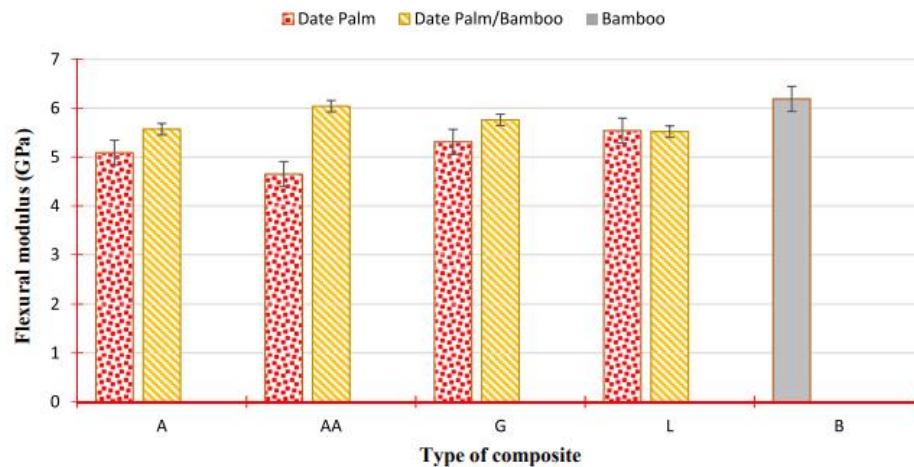


Fig II. 5 Flexural modulus of date palm, date palm/bamboo and bamboo composite fibre [78]

The research conducted by B.Alshammari [79] focuses on the production of epoxy composites reinforced with 50 wt% of date palm leaf sheath (G), palm tree trunk (L), fruit bunch stalk (AA), and leaf stalk (A) as fillers using the hand lay-up technique. The fabricated composites underwent comprehensive characterization and comparison in terms of mechanical, physical, and morphological properties. Mechanical analysis demonstrated that the incorporation of AA significantly enhances tensile (figure II.6) (20.60–40.12 MPa), impact strength (45.71–99.45 J/m), flexural strength (32.11–110.16 MPa), and density (1.13–1.90 g/cm³) properties. The recorded

higher water absorption and thickness swelling values in the AA/epoxy composite are attributed to its elevated cellulosic content compared to other composite materials. Microscopic examination of fiber pull-out, matrix cracks, and fiber dislocations on the fractured surface morphology confirmed the observed trends in mechanical properties. Overall, the findings suggest that reinforcing the epoxy matrix with AA filler significantly enhances the properties of the developed composite materials. Consequently, date palm fruit bunch stalk filler emerges as a sustainable and environmentally friendly reinforcement material akin to other natural fibers, suitable for various commercial, structural, and non-structural applications requiring high mechanical strength.

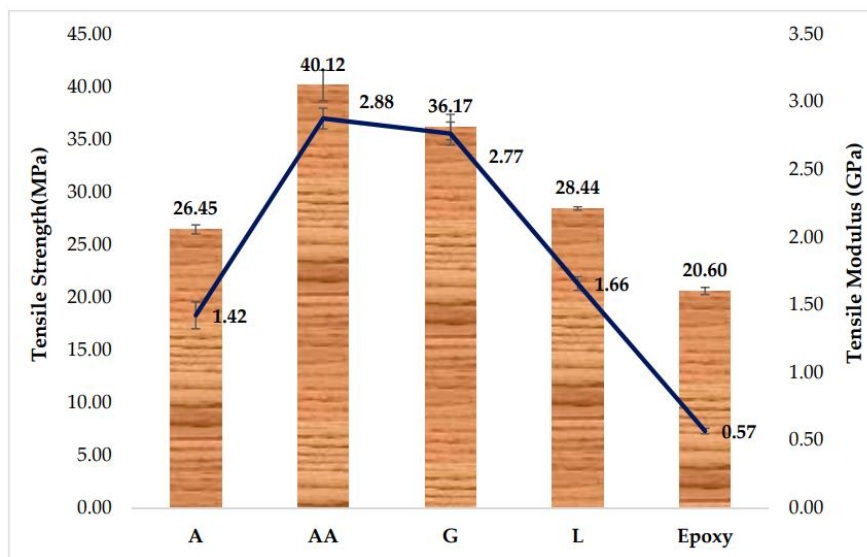


Fig II. 6 tensile properties of DPF/Epoxy [79]

Abu-Jdayil [80] conducted an investigation on the potential of date palm seeds (DS), the predominant waste in the dating industry, as a filler in unsaturated polyester (UPR) matrix for the development of thermal insulation material. Homogeneous DS-UPR composites with a natural filler content of up to 70 vol% were successfully prepared at room temperature via a thermoset curing process. The developed composites underwent comprehensive physical, thermal, and mechanical testing. Furthermore, various characterization techniques, including scanning electron microscopy (SEM), differential scanning calorimetry (DSC), thermogravimetric analysis (TGA), and Fourier-transform infrared spectroscopy (FTIR), were employed to analyze the properties of the composites. Density and water retention measurements were validated using different theoretical models. FTIR analysis indicated the presence of hydrogen bonding between DS fibers

and UPR, particularly notable at higher filler loadings. Substituting up to 50 vol% of UPR with DS resulted in composites demonstrating promising thermal insulation and construction properties, exhibiting low thermal conductivity (0.126 – 0.138 W/(m·K)), low thermal diffusivity (0.109 – 0.096 mm²/s), low water retention (0.47–3.44%), and high compressive (38.4–88.0 MPa) and tensile strengths (figure II.7)(9.4 – 35.1 MPa). Additionally, the incorporation of date seeds into the unsaturated polyester matrix marginally increased its glass transition temperature and enhanced its thermal stability. The novel DS-UPR composite presents itself as a viable alternative insulation material due to its superior properties compared to traditional thermal insulators.

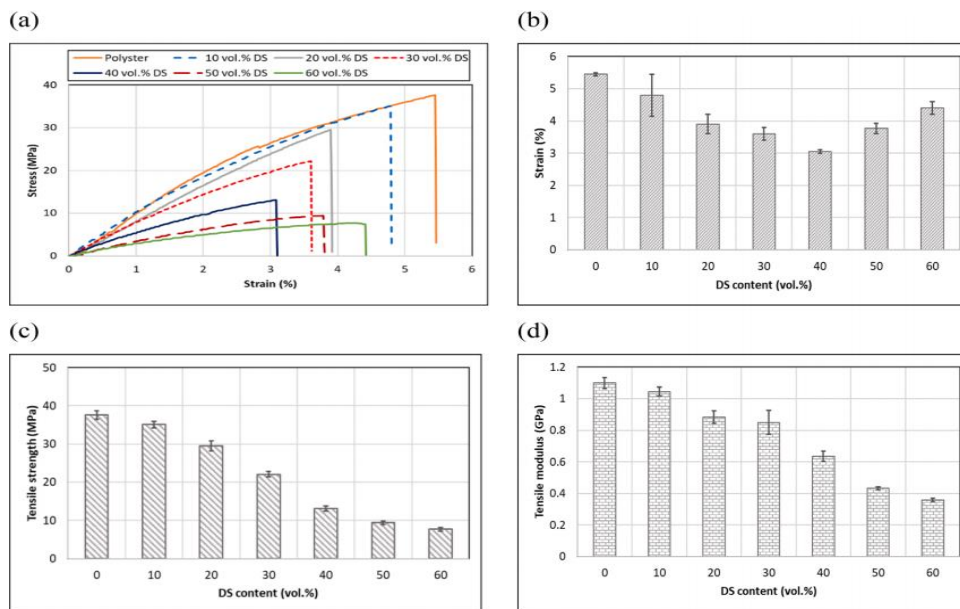


Fig II. 7 Tensile properties of DS-UPR composites; (a) Stress-strain curves (b) Tensile strain (%), (c) Tensile strength, and (d) Tensile modulus [80]

II.3. Search bibliographies on core

K. Almi[81] developed and studied composite materials based on various date palm wood particles using two matrices (unsaturated polyester resin, and vinyl poly acetate adhesive). All date palm wood particle boards were produced under a constant pressing pressure of 0.1 MPa over a temperature range of 28°C to 200°C for 10 minutes. The results obtained from various physical-thermal and mechanical tests demonstrate the influence of binder content (matrix), particle size and molding conditions (temperature, pressing duration) on the physical and mechanical properties of the produced boards. The mechanical properties, elasticity modulus and rupture stress of the date palm wood particle become higher when using smaller particles ($d \leq 0.5\text{mm}$ and $d \leq 1\text{mm}$) with

PVA adhesive at a molding temperature of 80°C. The elasticity modulus and bending rupture stress reach values of 1.73 GPa and 22.25 MPa, respectively.

Mohanty et al. [82] conducted a study on the solid particle erosion behavior of short date palm leaf (DPL) fiber-reinforced polyvinyl alcohol (PVA) composite. The investigation utilized silica sand particles ($200 \pm 50 \mu\text{m}$) as an erodent at various impingement angles ($15\text{--}90^\circ$) and impact velocities (48–109 m/s). The influence of fiber content (wt. % of DPL fiber) on the erosion rate of PVA/DPL composite was also explored. The results revealed that neat PVA exhibited the maximum erosion rate at a 30° impingement angle, while PVA/DPL composites displayed the maximum erosion rate at a 45° impingement angle, regardless of fiber loading, indicating semiductile behavior. The erosion efficiency of PVA and its composites varied from 0.735% to 16.289% for different impact velocities studied. The eroded surfaces were examined under a scanning electron microscope (SEM) to gain insights into the erosion mechanism.

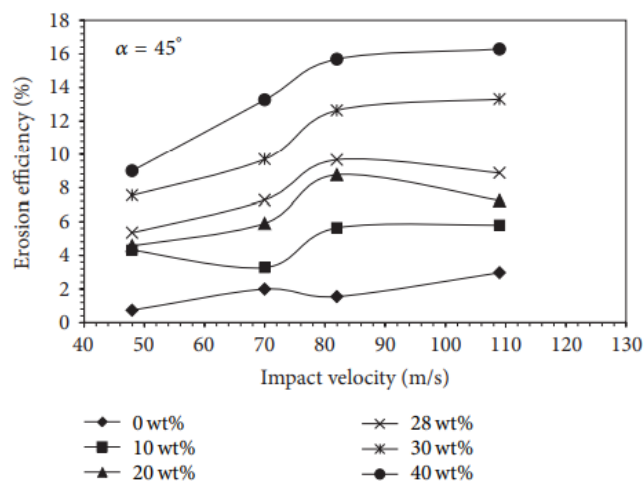


Fig II. 8 Erosion Efficiency of PVA/DPL Bio-Composites: Impact of Velocity on Wear Resistance [82]

Djoudi et al. [83] study focuses on valorizing waste from date palm trees that are often left abandoned in palm groves to produce new composite material as an alternative to conventional insulators. This approach involves creating a composite material from petiole wood (WPC) with varying particle sizes (ranging from 0 to 1, 1 to 3, and 3 to 5 mm) and characterizing its physical, thermal, and mechanical properties. The results demonstrated that the material's relative anisotropy and particle size distribution's impact on these properties. The WPC composites exhibited low

density within the 0.16-0.56 g/cm³ range and low thermal conductivity between 0.109-0.122 W/mK, indicating their insulator efficacy shown in figure II.9. These properties were comparable to other thermal insulation materials such as cork agglomerate and traditional wood. In addition to, tensile and three-point flexural tests highlighted the promising mechanical properties of the new composite, suggesting potential industrial applications for WPC materials.

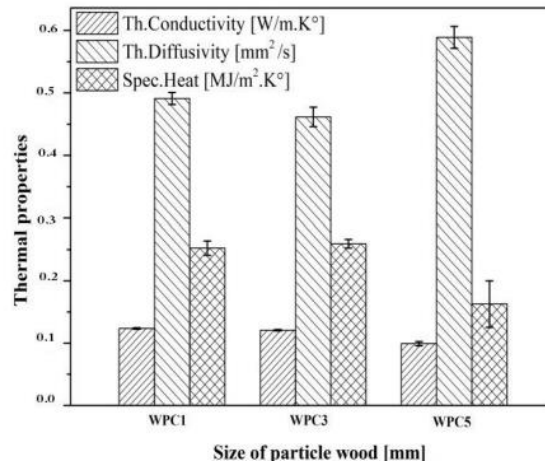


Fig II. 9 Comparative Analysis of Thermal Properties in Raw Wood and Wood-Plastic Composites (WPC) [83]

Masri et al. [84] presented an experimental study on the characterization of innovative wood-plastic composites using waste materials (date palm fronds and expanded polystyrene). Date palm frond waste is utilized as reinforcement particles while dissolved expanded polystyrene waste in a solvent serves as the matrix. The results obtained from mechanical, thermal and morphological tests on composite materials prepared in various particle sizes and mass fractions demonstrate excellent adhesion at the wood/matrix interface. Mechanical properties are satisfactory with a flexural modulus and maximum stress reaching up to 0.78 GPa and 2.84 MPa, respectively and a density ranging from 542 to 824 kg/m³, comparable to conventional materials such as hardwood, softwood and MDF. The average thermal conductivity ranges between 0.11 and 0.16 W/m•K.

Boukhattem [85] conducted an experimental study on the water absorption and humidity effects on thermal conductivity and density of binderless date palm fiber (DPF) mesh boards and mortar-DPF composites. The results showed that both thermal conductivity and density increased significantly with water content. Incorporating DPF mesh in the mortar reduced density and

thermal conductivity due to increased porosity. In addition to, DPF's addition lowered water retention capacity and benefits the thermal insulation. The experimental data were compared with theoretical models to determine the intrinsic thermal conductivities of DPF and mortar.

Benmansour [86] investigated the utilization of a novel material composed of natural cement, sand and date palm fibers (DPF), aiming to assess its potential as an insulating building material. Various composites were prepared with varying weight concentrations (ranging from 0% to 30%) and utilizing three sizes of fibers. Experimental analyses were carried out on water absorption, thermal conductivity and compressive strength. Findings indicate that integrating DPF reduces both the thermal conductivity and compressive strength of the composite while also decreasing its weight. With a DPF loading below 15%, the composite meets the thermal and mechanical requirements of construction materials and suggesting its suitability for use in wall structures. Thus, the incorporation of DPF as filler in mortar presents a promising option for application as thermal insulation material in buildings.

Ouchabi et al. [87] investigated the preparation of rigid polyurethane (PU) with an apparent density of about 40 kg/m³ using commercial polyols and polyisocyanate. This reference petrochemical formulation was modified by incorporating natural and renewable components such as date palm particles (DPP). The aim was to mitigate environmental impacts and reduce costs associated with petroleum-based polyurethane (PU) by developing polyurethane/date palm particles (PU-DPP) composites with comparable or superior heat insulating and mechanical properties to those of the reference material (PU). Composites were fabricated with varying DPP loadings: 5%, 10%, and 20% by weight. The results indicated that the heat-insulating and mechanical properties of the PU-DPP composites were on par with those of the reference petrochemical formulation (PU). Moreover, these mechanical and thermal performances were competitive with existing insulating materials in the market. Consequently, PU-DPP emerges as a promising candidate for the development of efficient, cost-effective and safe insulating materials.

II.4. Search bibliographies on sandwich

Djemai et al. [88] presented an experimental study on the mechanical behavior of four bio-sourced sandwich materials differentiated by their core types. The skins of these sandwiches are made of a composite material composed of rachis fibers and epoxy resin, while the cores are made of: 1) raw petiole and petiole agglomerate in two sizes (0-1 mm and 1-3 mm), and 2) cork

agglomerate for comparison. The comparison between these sandwiches is based on their overall stiffness, determined by three-point bending tests. The results show that the overall stiffness of the petiole agglomerate with a size of 0-1 mm, combined with rachis fibers and epoxy resin, is higher than that of the other sandwiches in table II.3 represented a result properties mecanique of sandwiches.

Table II. 3 Overall stiffness (D_G) values in different sandwiches[88]

Sandwich	$D_G(Mpa)$	$CV(\%)$
<i>SP01</i>	<i>818.90±32.77</i>	<i>4.00</i>
<i>SP03</i>	<i>485.99±17.06</i>	<i>3.51</i>
<i>SRP</i>	<i>569.11±46.06</i>	<i>8.09</i>
<i>SCA</i>	<i>106.73±13.94</i>	<i>13.06</i>

The investigation of Djoudi et al. [89] aims to study the feasibility of implementing a new bio-composite with a sandwich structure made from date palm tree waste. This work developed several sandwich-structured composite plates based on this waste. The skins are composite materials composed of an epoxy matrix and palm tree fibers (Epoxy/Rachis fibers), while the core is made of raw wood or a composite with petiole wood particles. After conducting three-point mechanical bending tests, macroscopic analysis and SEM micrographs were used to determine the damage the specimens sustained. Characterization tests on the new bio-composites showed good thermal properties, with thermal conductivity below 1 W/m.K, ranging from 0.0148 W/m.K to 0.0178 W/m.K. Additionally, the composites are characterized by their low volumetric mass, less than 1.2 g/cm³."

Khalili et al.[90] prepared composites from virgin and recycled polypropylene (PP and rPP) reinforced with 15 wt% sisal fibers, using compression molding to create a three-layer sandwich structure. The composites were assessed for their physical and mechanical properties. A factorial experimental design was employed to statistically evaluate the mechanical properties. The densities of the composites varied between 0.892 and 0.927 g/cm³. FTIR and XRD analyses indicated a partial removal of amorphous materials from the sisal surface after alkali treatment.

Djemai et al.[91] Presented an experimental investigation of damage in sandwich structures. These sandwich panels result from the combination of glass-polyester as skins and cork agglomerate as the core. For this purpose, a delamination test (mode I) is carried out on double cantilever beams (DCB) in sandwich beams. The initiation crack is characterized by toughness obtained from the determination of energy release rate (GIC) using the modified beam theory method. The skins of these sandwiches are considered orthotropic materials, while the core is considered an isotropic transverse material. The results show that the energy release rate at the initiation of the crack in (DCB) specimens remains almost constant despite the variation of the initial crack and good adhesion between the skins and core is also noticed.

Benzidane et al. [92] utilized date palm wood to develop sandwich panels and demonstrate through tensile tests that rachis fibers are more efficient than petiole fibers. Subsequently, petiole wood is used as the sandwich core, while short rachis fibers (5%, 10%, 15%) reinforce the epoxy skins. The skins undergo tensile and bending tests, identifying 15% Mf untreated short fibers as the optimal choice for skin stiffness. Three parameters are analyzed to optimize the core design: orientation (longitudinal, transverse, radial), length of the wood pieces (30 mm, 100 mm), and thickness (10 mm, 15 mm, 20 mm). The sandwich efficiency is evaluated through three-point bending tests, linear elastic beam theory, and failure mode analysis. The dominant failure modes are bottom skin failure and core shear, with core shear not occurring in the transverse orientation of the core.

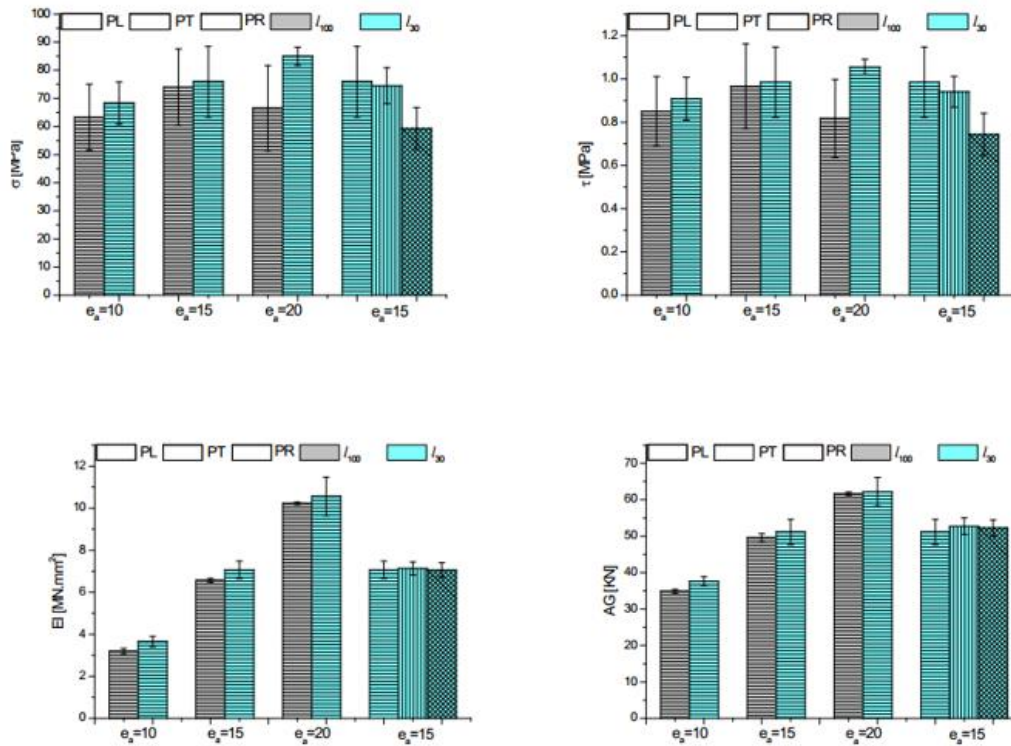


Fig II. 10 Bar chart of average normal stresses in bending, in shear, and of average stiffness[92]

Conclusion

Based on the literature review, there is strong potential for natural fibers and matrices in improving composite materials' mechanical and thermal properties. While past research shows promising results, further exploration is needed. Our work builds on these findings, focusing on novel approaches to enhance mechanical strength and thermal insulation. By addressing key challenges, we aim to advance the field toward more sustainable and efficient material solutions.

Chapter III Materials and Methods

Chapter III: Materials and Methods

Introduction

In this chapter, we examine the mechanical, physical and thermal properties of sandwich structures made from petiole and rachis fibers. The petiole used in the core and the rachis fibers used in the skin. Sandwich structures are valued for their lightweight yet strong characteristics where the choice of core and skin materials plays a critical role in performance. With their unique hierarchical structure, petioles and rachis fibers offer excellent reinforcement and present promising bio-based options. Through systematic analysis, we explore their mechanical behavior, thermal conductivity and insulation properties to highlight the potential of these materials in sustainable engineering applications.

III.1. Material

The sandwich structures that are proposed in this work consist of bio-composite (Rachis fibers - epoxy resin) in the skins and petiole agglomerate in the core

III.1.1. Materials of the skins

The bio-composite material of the skins of this study is elaborated of the date palm wastes (Rachis fibers) as reinforcement while the epoxy resin is used as a matrix

III.1.1.1. Reinforcement (Rachis fibers)

The rachis fibers used in this study were meticulously prepared at the Technical Institute for the Development of Saharan Agriculture (ITDAS) in Biskra which is located in southeastern Algeria. The preparation process began with the harvesting of the palms, from which the rachises were carefully separated from other components such as spines and leaflets. The separated rachis were then thoroughly cleaned using a damp cloth to ensure all dust and impurities were removed. Following the cleaning, the rachis was left to dry for three days, a critical step aimed at significantly reducing its moisture content. Once dried, the rachises were cut into manageable pieces, ranging from 5 to 20 cm in length which facilitated the subsequent grinding process. These pieces were then subjected to grinding to produce fibers of various sizes. The ground fibers were further refined by sieving them through a series of metal sieves with different diameters (0.1 mm, 0.315 mm, 0.5 mm,

and 0.8 mm) for 20 minutes result in four distinct fiber size categories. Among these, fibers with a diameter of 0.315 mm were selected for further processing. These chosen fibers underwent steam washing using a coffee press and ensuring thorough cleaning and were then dried in an electric oven set at 60°C for 48 hours to achieve the desired consistency and quality. The detailed steps of this preparation protocol are illustrated in Figure III.1, providing a comprehensive overview of the meticulous process undertaken to produce high-quality rachis fibers for this study.



Fig III. 1 Rachis fiber with a size of 0.315 mm

III.1.1.2. Matrix (Epoxy resin)

The matrix used in this study is an epoxy resin which falls under the category of thermosetting polymers. Epoxy resins are known for their excellent mechanical and thermal properties and their resistance to chemicals and moisture.

In my specific case, the epoxy matrix is created by mixing two components: a primary resin referred to as MEDAPOXY STR EA and a hardener referenced as MEDAPOXY STREB Figure III. 2. This is a common practice in epoxy resin applications. Epoxy resins are typically supplied as two separate components that must be mixed in a specific ratio. The primary resin contains the epoxy groups while the hardener contains compounds that can react with the epoxy groups to initiate cross-linking which is essential for curing and hardening the epoxy (For 2/3 g of resin, add 1/3 g of hardener). The epoxy resin used in this study was sourced from **Granitex-Algeria**[93]. Construction Produces and has specific properties. It had a density of 1.1 g/cm³, which indicates the mass per unit volume of the resin. Additionally, the viscosity of the epoxy resin was measured to be 11000 Mpa.s, representing its resistance to flow. These properties are crucial considerations for the handling, applying, and performing the epoxy resin in the research study. Table III.1 shows the properties of epoxy resin (MEDAPOXY STR EA).

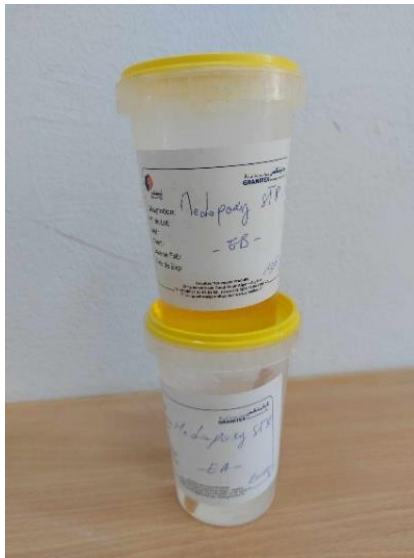


Fig III. 2 Epoxy Resin (MEDAPOXY STR EA)

Table III. 1 Properties of Epoxy Resin (MEDAPOXY STR EA)[93]

Properties	Epoxy MEDAPOXY STR EA
Density (ISO 758)(g/cm ³)	1.12 ± 0.05
Viscosity (NF T76-102) (MPa)	11000 Mpa. sa 25 °C
DPU(NFP18810)	1h 15min at 20°C and 65% HR
Curing time	at 20 °C and 65% HR

Overweight	6 h
Dur	16 h
Rc (NA427)	>70 MPA
Rf (NA 234)	>25 MPA
Adhesion to concrete (NFP18 858))	>3 MPA
Duration of commissioning	10 j 20°C
Thermal conductivity (w/m°C)	0.17

III.1.2. Materials of the core

The bio-composite material of the core in this study is elaborated of the date palm wastes (Petiole granules) as reinforcement while polyvinyl acetate glue (**PVA**) is used as a matrix

III.1.2.1. Reinforcement (petiole granules)

Our study will focus on utilizing the waste from the renewable section of palm trees specifically targeting the Daglet Noor variety. This particular variety represents a significant portion accounting for 61.45% of Algeria's total palm tree population [74, 94].

In our endeavor to conduct this research, we undertook a meticulous approach to specimen collection to focus specifically on the Daglet Noor palm variety. Recognizing the paramount importance of acquiring a substantial quantity of specimens for comprehensive characterization, we embarked on the collection of petiole cuttings which were then left to undergo a natural drying process outdoors allowing for an extended period of over a year. This deliberate choice aimed to ensure that the specimens were adequately prepared for subsequent analyses. To facilitate a thorough and systematic characterization, we meticulously segregated each type of petiole diligently separating them from other botanical components such as leaves, thorns, stems and panicles. This rigorous separation process was essential to ensure the integrity and purity of each specimen, thereby enabling us to collect a diverse array of specimens from various parts of the palm tree. Following this meticulous separation, the surfaces of the wood underwent a meticulous cleaning regimen, meticulously wiped down with a damp cloth to eliminate any extraneous dust or impurities that could potentially compromise the accuracy of our analyses. Subsequently, the petioles underwent a further period of air-drying lasting 24 hours, a crucial step to ensure the optimal condition of the specimens before further processing. Once dried, the petioles were meticulously ground into a finely powdered form with varying particle sizes meticulously controlled. This grinding process was essential to facilitate subsequent analyses by providing homogenous and representative specimens for characterization. Following the grinding process, the powdered material was meticulously sieved using a series of multiple-diameter sieves with each sieve

possessing a diameter of less than 1 mm, as meticulously illustrated in Figure III.3. This intricate sieving process was instrumental in ensuring that the resulting specimens were of consistent particle size to enhance the accuracy and reliability of our subsequent analyses. Through these meticulous steps, we were able to procure a comprehensive collection of high-quality specimens meticulously characterized and prepared for in-depth analysis and investigation.

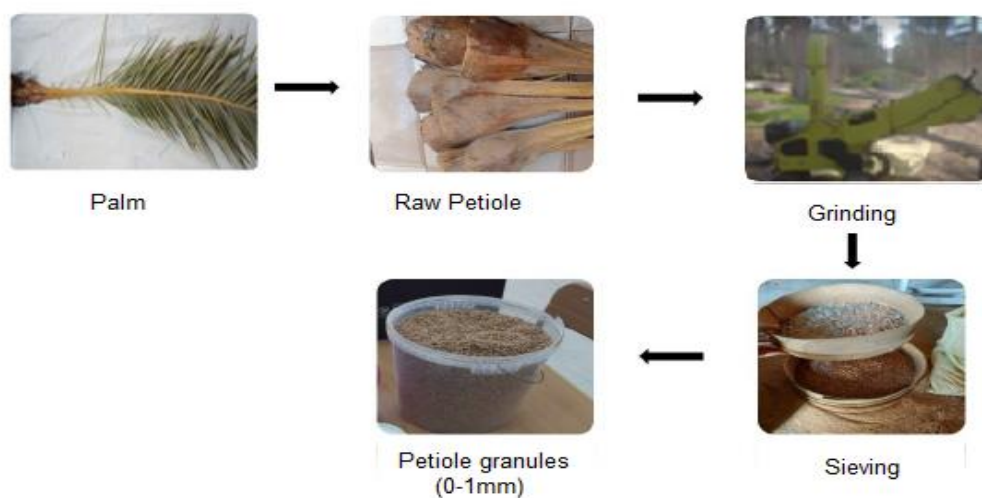


Fig III. 3 Petiole granules with a size $\leq 1\text{mm}$

III.1.2.2. Matrix (Polyvinyl acetate glue (PVA))

Polyvinyl acetate glue (PVA) (Figure III.4) commonly called white glue is an aqueous solution of polyvinyl acetate widely used to bond hydrophilic materials such as wood, paper, cardboard and fabric. These adhesives are particularly valued in interior carpentry and repair projects where aesthetic considerations are of utmost importance and materials are not exposed to high humidity conditions [95]. The versatility of PVA glues makes them suitable for various applications including bonding paper, cardboard and fabric which are commonly used in various craft and construction projects. One important advantage of PVA glues is their ability to form a transparent adhesive layer upon drying. This property ensures that the bonds remain virtually invisible which is highly desirable for applications where the appearance of the bonded materials is important [96]. Furthermore, the strong adhesion provided by PVA glues enhances the durability of the bonded materials to make them a reliable choice for long-term repairs and assemblies. The summary features of polyvinyl acetate glue presented in table (III.2) provide an overview of its key properties for various bonding applications [81, 97]. These properties highlight the effectiveness

of the glue in creating strong and aesthetically pleasing bonds to make it a staple in both professional and domestic settings. The transparent nature of the dried adhesive film not only maintains the visual integrity of the bonded materials but also adds to the versatility and appeal of PVA glues in many practical applications.

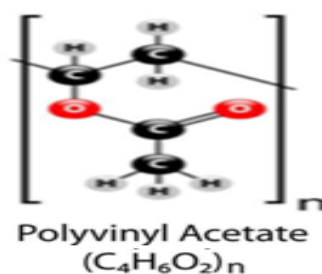


Fig III. 4 Molecular formula of polyvinyl acetate glue

Table III. 2 Properties of vinyl glue PVA

Properties	PVA
Density (g/cm ³)	1.19 ± 0.03
Viscosity (Poiseuille)	160 ± 40
pH	3.0 ± 1.0
Glass transition temperature	at 22°C (°C) 30
Operating temperature (°C)	10 – 35
Solubility parameter δ	(J ^{1/2} cm ^{-3/2}) 19.1-22.6
Dielectric constant (Farad m ⁻¹)	3.5
Refractive index	1.46–1.47
Boiling point (°C)	112
Ef (MPa)	at 22°C 1300-2300
Thermal conductivity (w/m°C)	0.16

These properties collectively make polyvinyl acetate glue a popular choice for a wide range of bonding applications and offer a reliable adhesion and an ease of use for various materials in interior settings.

III.2. Processes of preparing sandwich plates

In this study, we were preparing sandwich plates by gluing. It is done by three steps:

The first step: consists of the elaboration of the skins. The second step: consists of the elaboration of the core and finally the assembly between them.

III.2.1. Preparation of the skins

The bio-composite that is used in this part is composed by the rachis fibers as reinforcement and the epoxy resin (MEDAPOXY STR EA) as the matrix. So, the bio-composite is named ER (Rachis fibers-resin epoxy).

Five types of ER were prepared to study and choose the best among them. They are differentiated by their fiber content, which is detailed in Table (III.3).

Table III. 3 Five types of Bio-composite ER (Rachis fibers-resin epoxy)

Bio-composite material	Matrix%	Reinforcement:
ER0	100	0
ER5	95	5
ER7	93	7
ER10	90	10
ER13	87	13
ER15	85	15

To prepare the bio-composite (ER) of its five types, we follow the following steps:

- Mix the reinforcements (Rachis fibers) and the matrix (epoxy resin) according to the fiber ratios given in each type of ER.
- This mixed compound is poured into a pre-prepared mold to create panels with dimensions of $(140 \times 100 \times 3) \text{ mm}^3$
- These panels are left to dry in air under ambient conditions for 10 hours, allowing the resin to harden, thus forming a cohesive composite structure.
- After the drying stage, the panels are cut to obtain samples with final dimensions of $100 \times 10 \times 3 \text{ mm}^3$. According to ASTM D790 [98] and EN ISO 14125 [99].

This process is summarized in the protocol shown in Figure III.5.

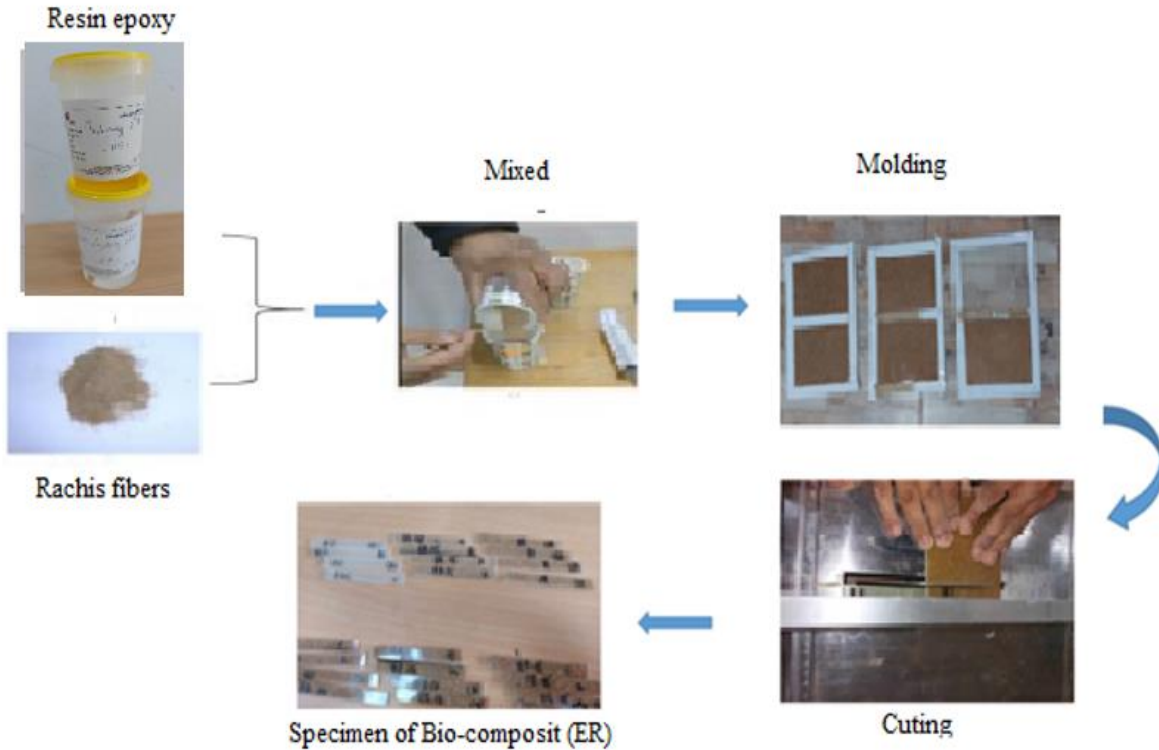


Fig III. 5 Protocol to obtain the specimens bio-composite material (ER)

III.2. Preparation of the core

The bio-composite that is used in this part is composed of the petiole particles as reinforcement and the polyvinyl acetate glue (PVA) as the matrix. So the bio-composite is named Pt (petiole agglomerate).

Five types of Pt were prepared to study and choose the best among them. They are differentiated by their percentage of petiole particles, which are detailed in Table (III.4).

Table III. 4 Five types of Bio-composite Pt (Petiole agglomerate)

Petiole agglomerate (Pt)	Petiole particles (%)	Polyvinyl acetate glue (%)
Pt15	15	85
Pt17	17	83
Pt20	20	80
Pt23	23	77
Pt26	26	74

To prepare the bio-composite (ER) of its five types, we follow the following steps:

- Mix the reinforcements (petiole particles) and the matrix (Polyvinyl acetate glue) according to the petiole particles ratios given in each type of Pt
- Fill this mixture into a mold (250x250x20)mm to obtain the bio-composite (**Pt**)
- Compact and press by hand, then place in an oven at 50°C for 24 hours just to dry.
- Demould the resulting plate (petiole agglomerate plate)
- Dry the resulting plate for more than 20 days, then adjust the plate with a planer to obtain the required dimensions (250x250x15) mm³.

Finally, we can summarize these stages of development of the heart (petiole agglomerate) by this protocol (Fig III.6)

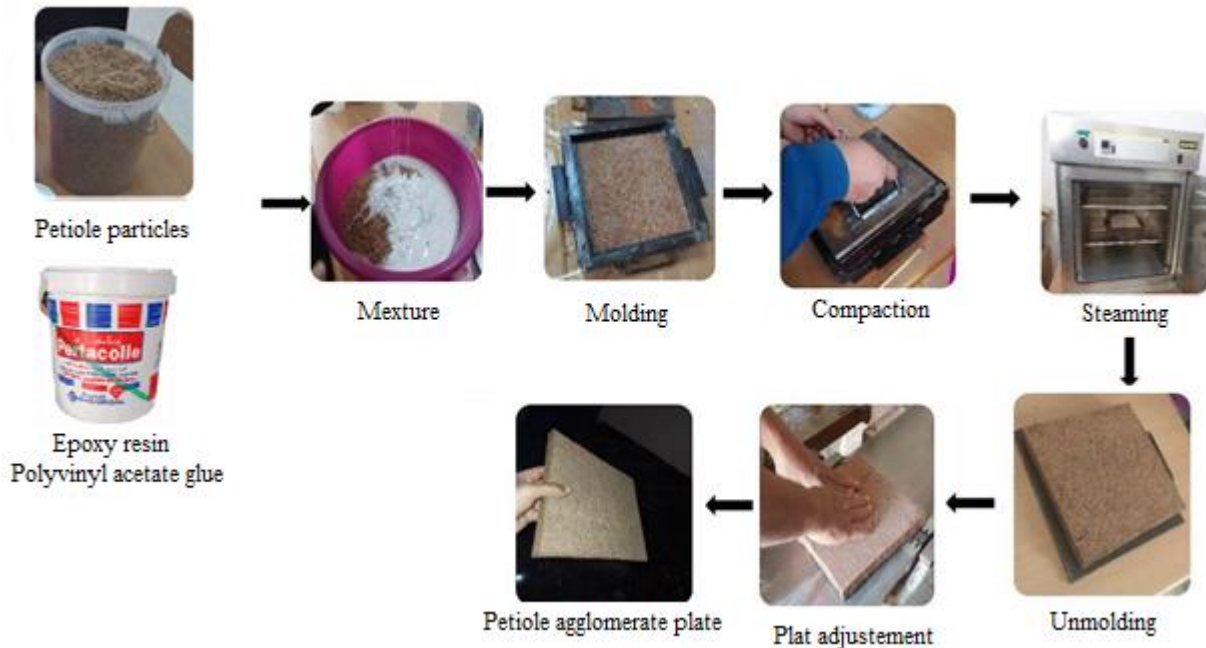


Fig III. 6 Preparation of Petiole agglomerate

These plates (Pt) are obtained to study several experimental techniques, mechanical (three-point bending and compression), physical (water absorption) and thermal (thermal conductivity).

For the three-point bending specimens, the plates are cut according to ASTM D790 standards [9], with the dimensions of (160 × 15 × 10) mm³. Simultaneously, thermal conduction specimens were molded according to ASTM standards such as ASTM E1952 [10] and ASTM E1954 [11],

with dimensions of $(40 \times 40 \times 20)$ mm³. In addition to, compression specimens were cut in uniform dimensions of $(20 \times 20 \times 20)$ mm³. The rigorous adherence to recognized standards underlines the commitment to maintain the quality and reliability of the materials and data resulting from these comprehensive tests.

III.3. Experimental techniques

Several tests were carried out in this study, to characterize these new bio-materials (**ER** and **Pt**) in mechanical, physical, morphological and thermal fields.

III.3.1. Mechanical properties

Three-point bending and compression tests are performed to obtain the mechanical behavior on the agglomerated petiole biomaterial (Pt) and on the biomaterial (ER) (Rachis fibers-epoxy resin).

III.3.1.1. Three-point bending tests of bio-composite RE (Rachis fibers-resin epoxy)

Three-point bending tests in the biomaterial RE (Rachis fibers-resin epoxy) are obtained to determine the elasticity modulus of (E_f) and ultimate stress (σ_{max}).

These tests are carried out in the technology hall of the Department of Mechanical Engineering of the University of Biskra.

These tests were conducted on “INSTRON” universal machine type 5969, with computer-controlled acquisition Bluehill3 with 5 KN force sensors and 2[mm /min] constant crosshead speed.

The specimens used in these tests are according to ASTM 790-81.2005 standard [100] of dimension $(100 \times 10 \times 3)$ mm³.

We consider a bio-composite (RE) with (b) in width, (L) in length and (h) in thickness (Figure III.7 (a)). They were performed by applying the load (P) in a perpendicular direction in the middle of the upper face of the specimen. It was placed on two supports with 60 mm of distance (Figure III.7 (b)). Elasticity modulus (E_f) (Flexural modulus) and Flexural strength (σ_{max}), are calculated from the linear part of a curve load (P) – deflection (f). We can calculate by this formula:

$$E_f = \frac{\Delta P}{\Delta f} \cdot \frac{L^3}{4bh^3} \quad (III.1)$$

$$\sigma_{max} = \frac{P.L}{b.h} \quad (III.2)$$

with:

$\frac{\Delta P}{\Delta f}$: is the slope of the linear part of curve $P=f(\text{deflection}(f))$.

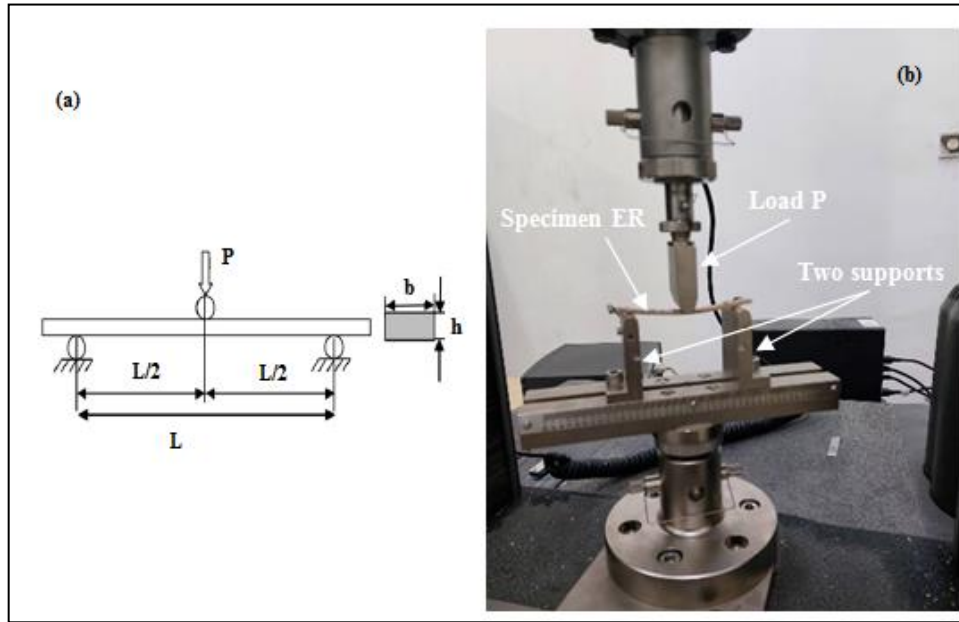


Fig III. 7 Three points pending test of bio-composite (ER) (a): Geometric dimensions, (b): Three points bending

III.3.1.2. Three point bending tests of bio-composite Pt (Petiole agglomerate)

Three-point bending tests in the biomaterial Pt (Petiole agglomerate) are obtained to determine the elasticity modulus of (E_f) and ultimate stress (σ_{\max}).

These tests were carried out in the educational laboratories of the mechanical engineering department at Mohamed Khider University in Biskra on a universal machine type TesT GMBH model 916713 (Fig.III.7 (a)) with a 05 KN force sensor with a test speed of 2 mm/min and control and data acquisition by the testwine software.

The specimens used in these tests according ASTM 790-10 standard [101] of dimension $(200 \times 15 \times 10) \text{ mm}^3$.

We consider a bio-composite (Pt) with (b) in width, (L) in length and with (h) in thickness They were performed by applying the load (P) in perpendicular direction in the middle of the upper face of the specimen. It was placed on two supports with 160 mm of distance (Figure III.8 (b)).

Elasticity modulus (E_f) (Flexural modulus) and Flexural strength (σ_{max}), are calculated from the linear part of a curve load (P) – deflection (f), We can calculate by the same equations (III.1 and III.2).

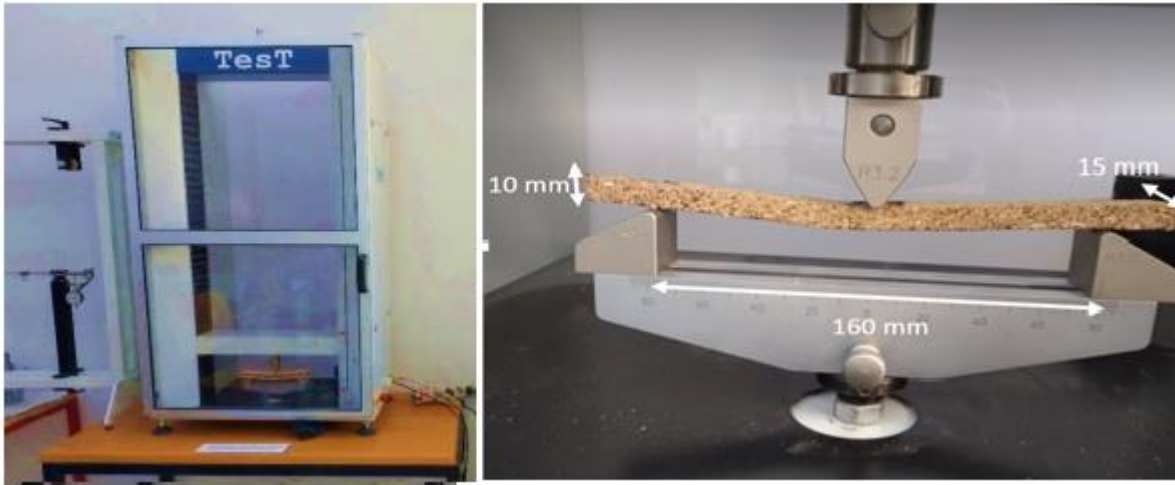


Fig III. 8 Three points pending test of bio-composite (Pt) (a): Universal machine TesT GMBH model 916713, (b): Three points bending test

III.3.1.3. Compression tests of bio-composite Pt (Petiole agglomerate)

Compression test was performed on specimens (Pt) in both longitudinal (PCL) and transverse (PCT) directions according to the standard ASTM D198-22 [102], ASTM D3501 [103] with specimen dimensions set at $(20 \times 20 \times 20) \text{ mm}^3$ represented in Figure (III.9).

These tests were carried out in the educational laboratories of the mechanical engineering department at Mohamed Khider University in Biskra on a universal machine type TesT GMBH model 916713, with a 05 KN force sensor, with a test speed of 2 mm/min and control and data acquisition by the testwine software.

Elasticity modulus (E_C) (elasticity modulus) is calculated from the linear part of a curve stress (σ) – strain (ϵ), We can calculate by formula:

$$E_C = \frac{\Delta\sigma}{\Delta\epsilon} \quad (\text{III.3})$$

With:

$\frac{\Delta\sigma}{\Delta\varepsilon}$: is the slope of the linear part of curve $\sigma = f(\varepsilon)$.

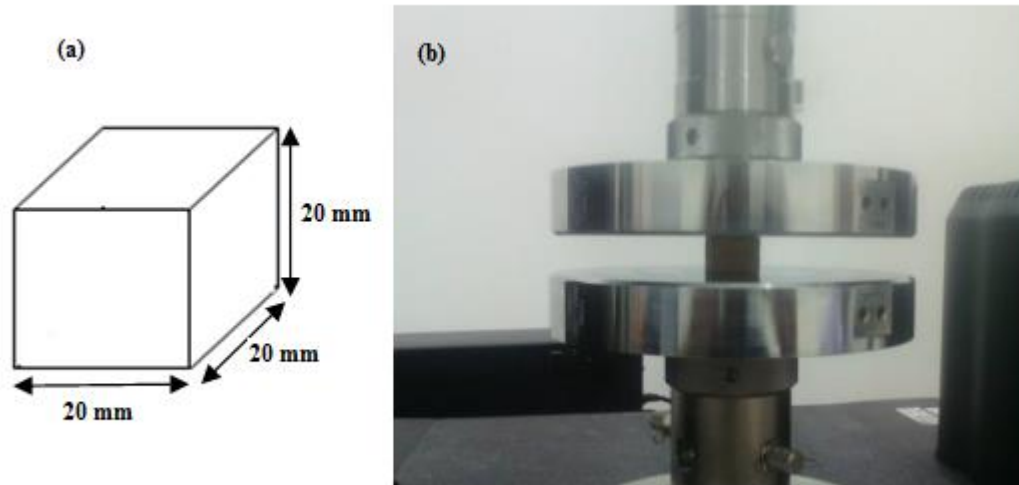


Fig III. 9 Compression test of bio-composite (Pt) (a): Geometric dimensions, (b): Compression bending test

III.3.1.3. Brinell hardness tests of a bio-composite RE (Rachis fibers-resin epoxy)

The assessment of Brinell hardness on the Rachis/epoxy composite specimen was meticulously conducted using the INNOVATEST VERZU 750 model Figure III.10, a state-of-the-art Brinell hardness tester machine renowned for its precision and reliability in material characterization. Applying a standardized testing procedure, a precisely calibrated 6.25 kg load was uniformly exerted onto the specimen's surface for a duration of precisely 10 seconds. A robust hard metal ball indenter, featuring a diameter meticulously set at 2.5 millimeters to ensure consistent and accurate indentation, facilitated this load application. Following the application of the load, the resulting indentations were meticulously examined and measured at ten distinct random locations across the specimen's surface using an advanced microscope which enabled precise measurements of the indentation diameters. These measurements were then meticulously averaged, with the accompanying standard deviation meticulously computed to ascertain the consistency and reliability of the obtained results. The computation of the Brinell hardness number (BHN) was conducted in strict adherence to the prescribed Equation (III.4) where the BHN value is calculated based on the applied force (P), the diameter of the indenter (D), and the diameter of the resulting indentation (d). This comprehensive approach ensured the acquisition of accurate and reliable data pertaining to the

Brinell hardness of the Rachis/epoxy composite specimen, thereby facilitating a thorough understanding of its mechanical properties and performance characteristics.

$$\text{BHN} = \frac{2P}{\pi D(D - \sqrt{D^2 - d^2})} \quad (\text{III.4})$$



Fig III. 10 INNOVATEST VERZU 750 model of Brinell hardness test

III.3.2. Thermo-physical properties

To optimize the use of natural fibers in composite materials, understanding their thermo-physical properties is essential. Petiole particles and rachis fibers, as reinforcements offer unique characteristics that influence the performance of composites under various conditions. To explore these properties, a series of physical tests were conducted on composites with different ratios of petiole particles and rachis fibers. These tests, which included thermal conductivity measurement, thermo-gravimetric analysis (TGA), water absorption and Bulk density analysis, provided valuable data on the chemical composition, thermal stability and water interaction. By analyzing these factors, we gain critical insights into the composites' behavior to contribute to the development of more efficient and sustainable bio-composite materials.

III.3.2.1. Thermal conductivity of Pt and RE

The thermal conductivity (λ) of a material is a physical quantity that characterizes its ability to conduct heat and is expressed in $\text{Wm}^{-1}\text{K}^{-1}$. The heat transfer mode associated with this quantity is thermal conduction. There are other properties related to heat transfer thermal diffusivity (α), expressed in m^2/s , characterizes the material's ability to transmit a temperature signal from one point to another within the material. There is also the volumetric heat capacity or specific heat (C_p),

expressed in $\text{J/m}^3 \text{K}$ which characterizes the material's ability to store heat. The measurement of the thermal properties of our bio-composite plates (ER and Pt) was carried, out using the Hot Disk-Thermoconcept thermal analyzer (figureIII.11). Measurements were conducted under controlled conditions at 23°C and 29% humidity. This thermal characterization device utilizes the transient plane source technique, governed by the international standard ASTM E1952 – 20 [104]. A probe consisting of a double nickel spiral on an insulating Kapton support (Figure III.12) is placed between two flat specimens of the material to be characterized. This probe is available in various diameters, allowing the characterization of specimens of any size with thicknesses ranging from a few millimeters for insulators to a few centimeters for conductors. The Hot Disk apparatus allows direct measurement of thermal conductivity and diffusivity and indirect measurement of volumetric heat capacity of the material through the following relationship.



Fig III. 11The Hot Disk-Thermoconcept thermal characterization device.



Fig III. 12 Kapton support

III.3.2.2. Thermogravimetric Analysis (TGA) and Differential Scanning Calorimetry (DSC)

Thermogravimetric Analysis (TGA) measures a sample's mass change with temperature, providing insights into phase transitions, decomposition, and degradation [105]. Differential Scanning Calorimetry (DSC) detects exothermic and endothermic changes in polymers [106]. Combined with Principal Component Analysis (PCA) methods, TGA and DSC offer a comprehensive approach to material design and analysis [107].

We utilized a coupled Thermogravimetric analyzer (TGA/DSC) device, specifically the SETARAM Instrumentation LABSYS evo (Figure III.13). The sample size ranged between 15 and 30 mg with a heating rate of 10°C/min under a standard atmosphere. TGA results are typically displayed as a curve showing mass or mass percentage variation with temperature or time. Additionally, the first derivative of the TGA curve, known as the differential Thermogravimetric (DTG) curve, provides information about the rate of mass change. Mass changes occur due to material loss or reactions with the surrounding atmosphere, which can result from various phenomena. The glass transition temperature (T_g) is determined at the "ONSET" point from the DSC thermogram, and the exothermic heat (ΔH) of the polymerization reaction is calculated from the exothermic peak relative to the baseline.

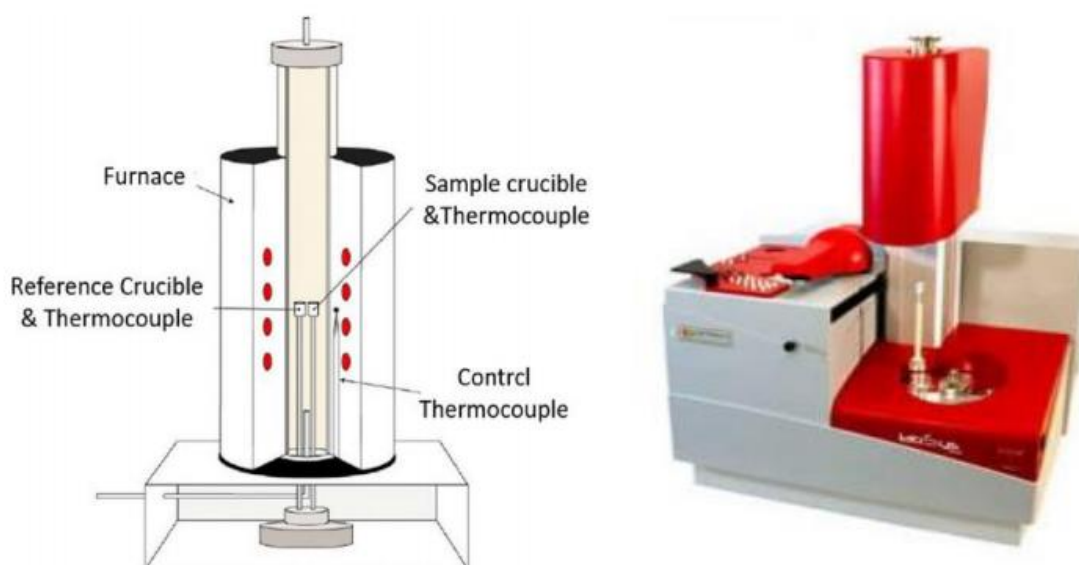


Fig III. 13 Operating Principle of the SETARAM LABSYS evo Thermogravimetric Analyzer

III.3.2.3. Water absorption test of Pt and RE

To determine the water absorption properties of the bio- material Pt (petiole agglomerate), we used the gravimetric method conducted following the guidelines outlined in ASTM D 570-98 (2010) [18–23]. Samples were cut to dimensions of $(30 \times 15 \times 10) \text{ mm}^3$, and their initial weights were recorded. These specimens were then immersed in distilled water, and their weights were measured at 2-hour intervals for ten hours, after which the material was decomposed. The water absorption percentage (H %) was calculated using a standard formula (equation III.5). In addition, another set of tests was performed using of bio-composite ER specimens of dimensions $20 \times 10 \times 3 \text{ mm}^3$, with initial weights recorded before immersion in distilled water, followed by weight measurements at 24-hour intervals over one week to evaluate the long-term water. The water absorption values for the composites were calculated using the formula:

$$H(\%) = \frac{W_n - W_d}{W_d} \times 100 \quad (\text{III.5})$$

Where (W_n) represents the weight of the composite material after immersion and (W_d) is the weight of the composite before immersion in distilled water. This test provides valuable insights into the material's water absorption behavior because it is essential to evaluate its suitability for various applications. The simplified protocol is illustrated in Figure III.14.

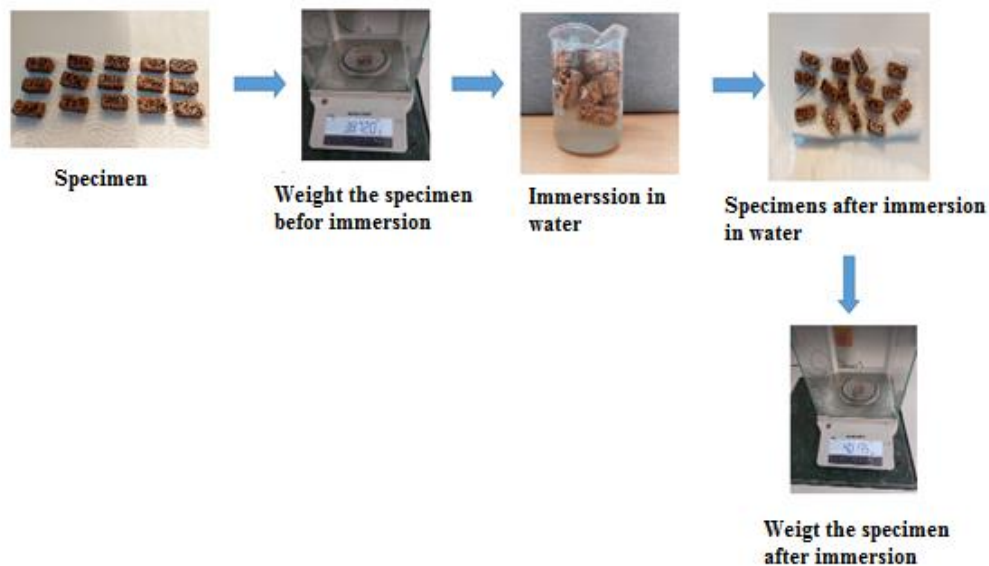


Fig III. 14 Protocol of gravimetric method

III.3.2.4. Density test Pt and ER

The determination of density for various types of petiole agglomerate (Pt) is achieved through precise measurement of their volume and mass. This procedure involves meticulous steps: Initially, specimens of the different petiole agglomerate types are weighed using a high-precision electronic balance (Kern V3.1) with an accuracy of 10^{-4} g. This weighing process occurs within a controlled environment to maintain at a constant temperature of 25°C to ensure consistent measurement conditions. Subsequently, the volume of these specimens is determined through hydrostatic weighing. Each specimen is immersed in a container filled with paraffin to prevent water absorption to allow the measurement of the increase in liquid volume which corresponds to the volume of the specimens. Finally, the apparent density (ρ) is calculated using the following formula [6]:

$$\rho = \frac{m'}{(v-v') - \frac{m-m'}{\rho^*}} \quad (\text{III.6})$$

With

m' : The dry mass of the specimens,

m : Specimens mass after packaging of paraffin,

ρ^* : The density of paraffin (0.88g/cm^3),

v : specimens and water volume and

v' : A volume of water.

For the bio-composite ER study, bulk density measurements were conducted following the ASTM D 1895-17[108] standard, as detailed in the studies of [109, 110], for determining the density of solid materials. This standard ensures consistency and comparability of results across different studies. To enhance accuracy, five replicates were performed for each specimen, minimizing potential errors and increasing the reliability of the obtained data. The density (d) of each sample was calculated using the fundamental formula:

$$d = \frac{m}{V} \quad (\text{III.7})$$

Where \mathbf{d} is the density of the samples (g/cm^3), \mathbf{m} is the mass (g), and \mathbf{V} is the volume (cm^3).

By measuring the mass of the specimens and accurately determining their volume, the density value can be obtained. This analysis provides valuable information about the compactness and packing of molecules within the material which is essential for understanding its physical properties and behavior.

III.3.3. Microstructure properties

To optimize the use of natural fibers in composite materials, understanding their Microstructure properties is essential. This study utilizes a combination of techniques and include a scanning electron microscopy (SEM), X-ray diffraction (XRD) and Fourier-transform infrared spectroscopy (FTIR), to characterize a novel biomaterial. By integrating these advanced analytical methods, we aim to deliver a comprehensive assessment of the biomaterial's thermal stability, moisture affinity, crystal structure, and molecular composition. This multi-faceted approach allows for a deeper understanding of the material's properties to contribute to its potential use in various applications.

III.3.3.1. Scanning electron microscopy (SEM)

Scanning electron microscopy (SEM) is a technique that uses electron-matter interactions to create high-resolution surface images. The electron beam scans the specimen surface, causing it to emit particles that detectors analyze to form a virtual 3D image. Advances in SEM include using generative adversarial networks (GANs) for training convolutional neural networks (CNNs) in nanoparticle classification, backscattered-electron SEM (BSE-SEM) for quantitative material characterization, and cryogenic plasma FIB/SEM for improved imaging of biological samples. Electron mirrors in SEMs now allow simultaneous imaging of top and bottom surfaces, enhancing in-situ observations and potential future corrections for spherical aberration.

The images were taken by a Thermo Scientific Quanta SEM Prisma E electron microscope made in the USA (Fig III.15) Image resolution can be up to 3 nm at 30 kV to 7 nm at 3 kV. The image obtained gives a topographic view of the surface with a much greater depth of field than in optical microscopy. An accelerating voltage of 10-15 kV was used to avoid the degradation of the sample which would take place if the speed of impact of the incident electrons on the object was too great.

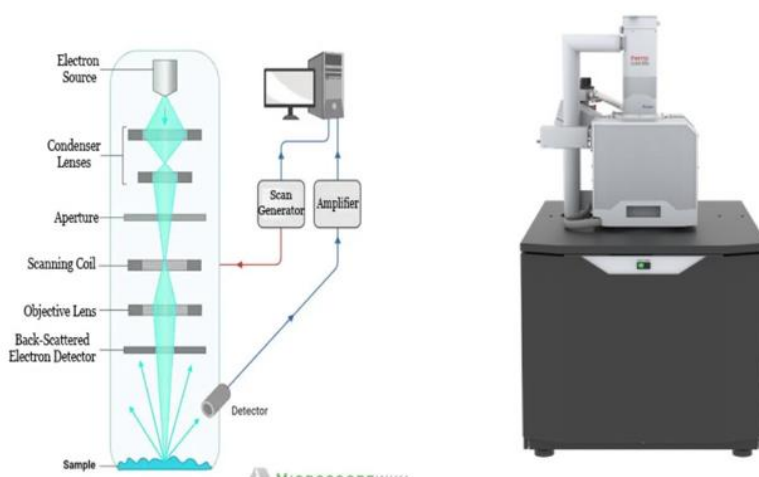


Fig III. 15 Principle of Thermo Scientific Quanta SEM Prisma E electron microscope

III.3.3.2. X-ray diffraction (XRD)

X-ray diffraction (XRD) is a crucial technique in mineralogical research for identifying various minerals and includes radioactive and atomic minerals like uranium and associated ores [111]. The technique is based on kinematical and dynamical diffraction theories, which can have limitations due to instrument and user constraints, affecting the structural models derived [112]. In situ, synchrotron high-energy X-ray powder diffraction is widely used for analyzing crystallographic structures in functional devices and complex environments and enables precise identification through techniques like Rietveld refinement and machine learning [113]. In our study, XRD analysis was conducted to evaluate the crystallinity of powdered specimens using a Malvern Analytical X-ray diffractometer (Fig III.16). Scans were performed over a 2θ range of $5-90^\circ$ at a speed of 0.04° per step with a wavelength (λ) of 1.54060 \AA . The degree of crystallinity (X_c) was determined by analyzing the intensity data from the XRD scans. To calculate crystallite size from XRD data, the Scherrer equation uses ASTM E1122-02 standard [114].

$$D = \frac{K\lambda}{\beta \cos\theta} \quad (\text{III.8})$$

While

D : is the crystallite size, K : is the shape factor (typically 0.9), λ : is the X-ray wavelength (1.5406 \AA for $\text{CuK}\alpha$), β : is the FWHM in radians, θ : is the Bragg angle.

This method provides a detailed understanding of the crystalline structure which is critical for interpreting the material's properties.

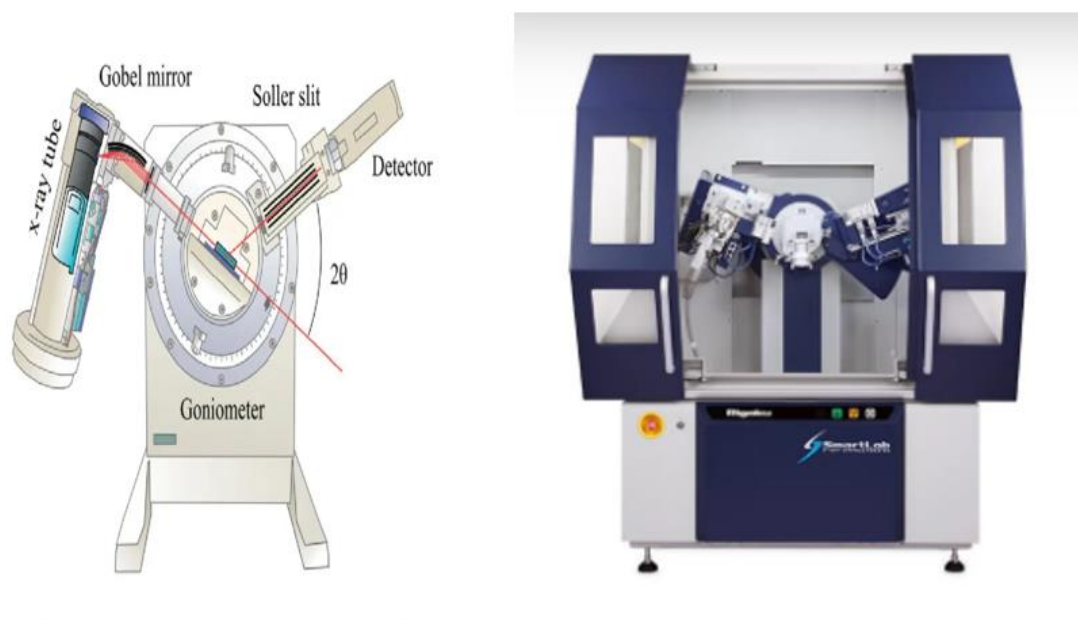


Fig III. 16 Principle of Malvern Panalytical X-ray diffractometer

III.3.3.3. Fourier-transform infrared spectroscopy (FTIR)

Infrared spectroscopy is a powerful analytical technique that determines the chemical composition of a substance by identifying specific absorption bands on the spectrum each corresponding to the vibration pattern of chemical bonds between atoms [115]. This method, widely used in various industries including food, aids in both qualitative and quantitative analyses by identifying functional groups within molecules [116]. Recent advancements have introduced machine learning models that predict molecular structures directly from IR spectra with high accuracy, outperforming traditional methods [117]. Additionally, convolutional neural networks now autonomously identify functional groups in organic molecules based on their IR spectra, eliminating the need for manual interpretation and database searching [118]. Furthermore,

integrating infrared ion spectroscopy with mass spectrometry has enabled the creation of silicon spectral libraries for small-molecule identification, highlighting the potential for de novo identification of unknown compounds based on their IR spectra [119].

We acquired the infrared spectra using PerkinElmer Spectrum Two with an ATR-FTIR unit (Fig III.17). Although various IR spectrometers are available, those with synthetic diamond components are most common due to the diamond's chemical inertness, IR transparency, and ability to withstand high pressures. At the diamond sample interface, the IR light penetrates only a few micrometers, analyzing the characteristic peaks of palm petiole and rachis fibers. The fiber was placed on a diamond crystal with a resolution of 2 cm^{-1} and analyzed within a spectral range of $400\text{--}4000\text{ cm}^{-1}$.

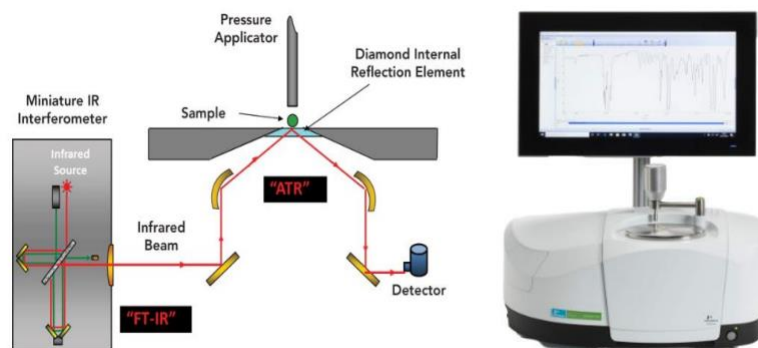


Fig III. 17 Principle of PerkinElmer Spectrum Two with an ATR-FTIR

Chapter IV Results and discussion

Chapter IV: Results and discussion

Introduction

The implementation of composite materials and sandwich panels is a well-established technique that has been utilized across various industries for a significant period. These structures are renowned for their lightweight nature and advantageous properties, such as thermal and acoustic insulation, impact resistance, and fatigue resistance. These properties are closely linked to the selection of materials for the skins and core, as well as the quality of their interfaces. Incorporating Bio-sourced composite materials plant materials in the production of these sandwich panels presents considerable environmental benefits. In Algeria, there is a growing interest in palm fibers as agricultural residues due to their high availability and mechanical properties[120].

This chapter presents the analysis and study of the results obtained in the previous Chapter. Before that, we focus on investigating the properties of a petiole particle and rachis fibers. The chemical composition and functional groups of fibers are identified using FTIR spectroscopy, while their thermal and morphological characteristics were analyzed through thermo gravimetric analysis (TGA), differential scanning calorimetric (DSC), and scanning electron microscopy (SEM). Additionally, we examined the mechanical and thermo physical properties of bio-composite materials made from various combinations of raw petiole and rachis fibers (ER and Pt).

IV.1.Properties of a petiole particle and rachis fibers

IV.1.1. Scanning electron microscopy SEM results

The longitudinal surface morphology of a petiole particle and rachis fibers of the Deglet Noor variety was analyzed using scanning electron microscopy (SEM) at various magnifications, as shown in Fig IV.1 (a) and Fig IV.1. (b)

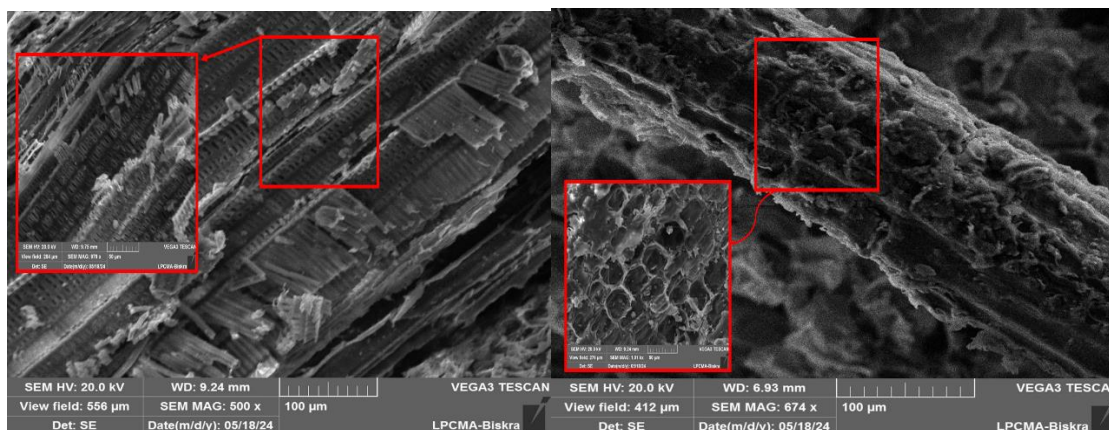


Fig IV. 1 SEM Analysis of : (a) a petiole particle Microstructure (b) a Rachis fibers Microstructure

The SEM micrographs reveal thick lines on a rough surface with regularly arranged rectangular and square-shaped boxes and some randomly distributed lignin. Numerous circular or irregularly shaped holes are also observed on the surface, and the fibers exhibit inconsistent shapes and non-uniform dimensions. These micrographs highlight significant irregularities and surface roughness, reflective of the fibers' natural texture. This rough surface can enhance mechanical interlocking in composite materials, affecting overall adhesion and performance. The variations in shape and dimension among the fibers suggest inherent variability in the raw material, potentially impacting the uniformity and consistency of the final composite product.

IV.1.2. Fourier-transform infrared spectroscopy (FTIR) result

IV.1.2.1. FTIR analysis of a petiole particle

The infrared spectra results of petiole particles are shown in Figure IV.2. The peak at 3500 cm^{-1} corresponds to the stretching of OH hydrogen bonds. The decrease in peak intensity at 3500 cm^{-1} is due to lignin, hemicellulose, and other components on the fiber surface, resulting in a large number of exposed OH groups. As a result, the fibers become more hydrophilic. The peaks at 1730 cm^{-1} are attributed to C=O stretching vibration in the carboxylic acid in lignin or ester groups of hemicellulose and pectin for untreated fibers. The peak at 1228 cm^{-1} is responsible for the C–O stretching of acetyl lignin. The C–H bending deformation of hemicellulose is attributed to 1367 cm^{-1} . The peak intensity at 1020 cm^{-1} also notes the decrease, which is attributed to the elongation of the C-O-C ether groups of lignin [121].

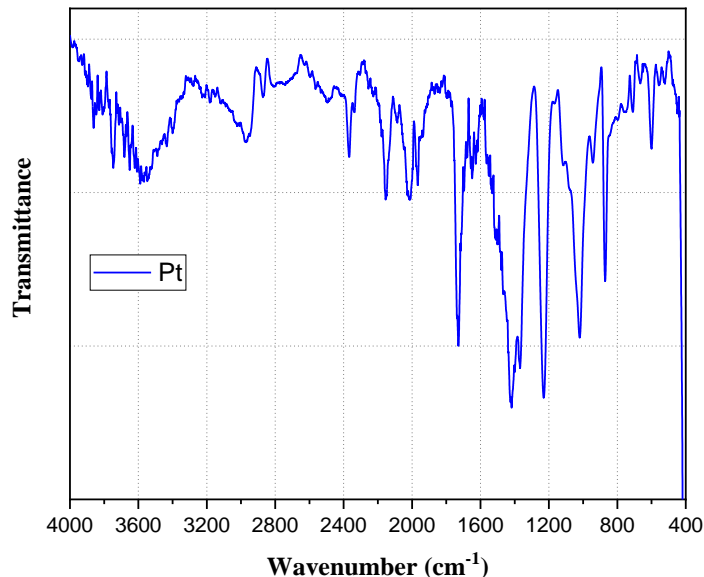


Fig IV. 2 FTIR spectra analysis of a raw Petiole

IV.1.2.2. FTIR analysis of Rachis fiber

The FTIR analysis conducted on rachis fibers revealed their chemical and molecular structures, as shown in Figure IV.3. The prominent absorbance peak at 3360 cm^{-1} corresponds to O–H stretching vibration and hydrogen bonding in hydroxyl groups [122]. Additionally, the 2850 cm^{-1} and 2923 cm^{-1} peaks indicate CH symmetric and asymmetric stretching groups, respectively, in cellulose and hemicellulose. The peak at 1730 cm^{-1} is attributed to the C=O stretching vibration in the acetyl groups of hemicellulose [123]. The wave number at 1228 cm^{-1} is associated with C=O stretching groups in hemicellulose [122]. Peaks at 1490 cm^{-1} suggest the presence of C=O stretching in carboxylic acids and esters, both of which are components of lignin [124]. The peak at 1020 cm^{-1} indicates C–O stretching within the polysaccharide rings of cellulose. A minor band observed at 898 cm^{-1} signifies the C–O–C stretching of the β -glycosidic linkage in cellulose [125].

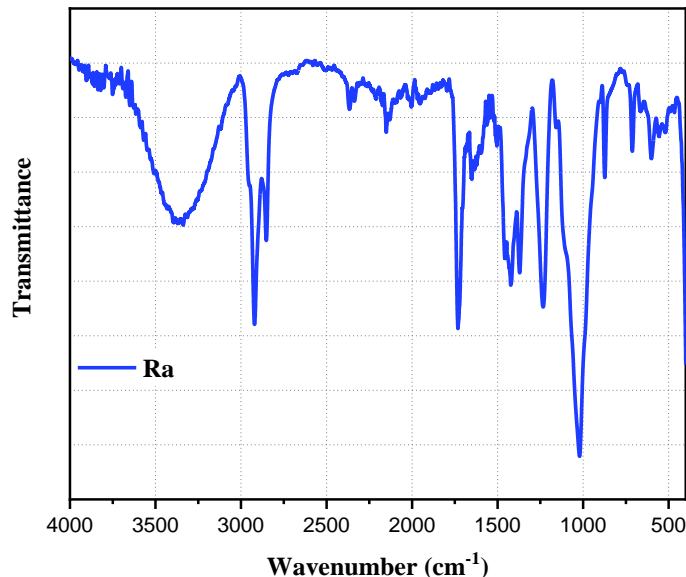


Fig IV. 3 FTIR spectra analysis of rachis fibers

IV.1.3. X-ray diffraction (XRD) analysis results

IV.1.3.1. XRD analysis of Petiole particle

Figure IV.4 Present X-ray diffraction (XRD) analysis patterns of petiole particles, highlighting key crystalline characteristics. The spectrum exhibits a sharp peak at $2\theta = 11.54^\circ$, a broad peak at 20.72° , and a less defined peak at 29.08° , corresponding to the (110), (101), and (113) crystallographic planes, respectively. The presence of these peaks indicates the existence of crystalline regions within the fibers, with the broad peak at 20.72° suggesting a significant level of crystalline order. The calculated crystallinity index of 67.07% reveals that a substantial portion of the fiber material is crystalline, which is consistent with values reported in the literature for similar untreated natural fibers. The broadness of the peak at 11.54° and the less defined nature of the peak at 29.08° may indicate some degree of amorphous regions within the fiber structure T.Djoudi [4] and H.Benchouia [126].

These results suggest that the natural structure of petiole fibers includes both crystalline and amorphous regions, contributing to their overall mechanical properties and suitability for various applications. This structural information is crucial for understanding the inherent properties of untreated petiole fibers and can serve as a baseline for future studies on their potential enhancements and applications

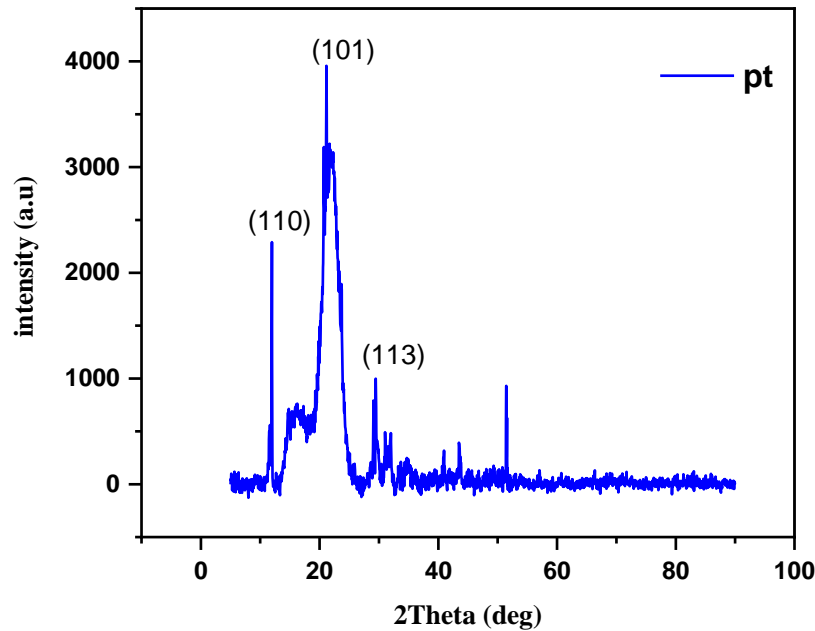


Fig IV. 4 XRD spectra analysis of Petiole particle

IV.1.3.2. XRD analysis of Rachis fibers

Figure IV.5 presents a rachis fibers' X-ray diffraction (XRD) profiles, highlighting significant crystalline features. The spectrum shows a broad peak at $2\theta = 16.54^\circ$ and a sharp peak at $2\theta = 21.82^\circ$, corresponding to the (111) and (110) crystallographic planes, respectively. These peaks indicate crystalline regions within the fibers, reflecting a notable level of crystalline order. The calculated crystallinity index of 54.66% demonstrates that a substantial portion of the fiber material is crystalline, aligning with the values reported in the literature for similar untreated natural fibers. Studies presented by Dallel [127] and Amroune [128] have shown that date palm fibers, extracted from rachis and leaves, exhibit similar spectra, with crystallinity rates of 50% and 55%, respectively, which is consistent with the findings in this work.

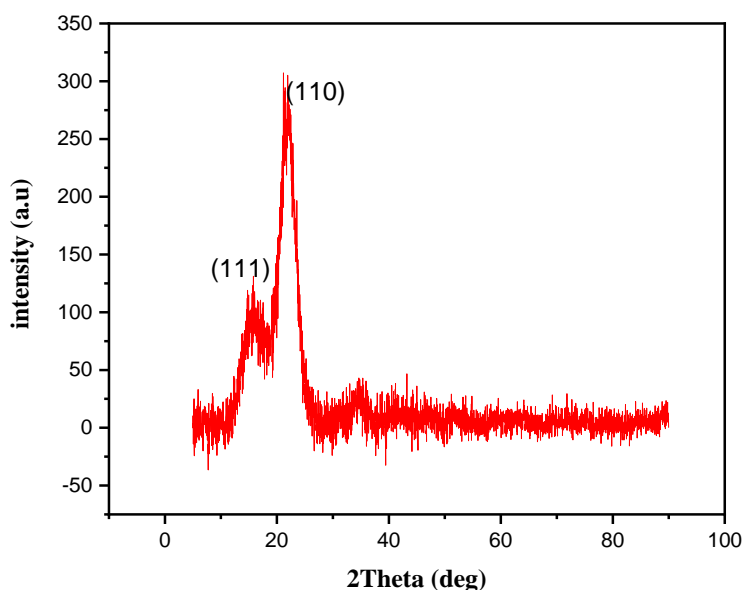


Fig IV. 5 XRD spectra of rachis fibers

IV.1.4. Thermogravimetry (TGA) and Differential Scanning Calorimetry (DSC) analysis

IV.1.4.1. TGA and DSC analysis of petiole particle

Thermal stability is commonly evaluated by determining the onset temperature of thermal decomposition and was used to measure the weight loss of composites as a function of rising temperature. Higher decomposition temperatures give greater thermal stability. Fig IV.6 shows the fibers' thermal degradation curves as a function of palm petiole fibers. The fiber presented two stages: a first stage with a slight weight loss in the range of (30-190 °C), due to the release of humidity retained in the fiber component, and a second stage where hemicellulose and lignin degradation happened (200-300 °C), while another loss of mass at (300-450 °C), is related to the degradation of the cellulose. The release of noncombustible gases, such as carbon dioxide can explain it, and carbon monoxide is present in the samples containing high cellulose content [121][10]. The final process is around (450-700 °C), which produces a reactive coal residue. As for DSC analysis, all samples showed broad exotherms extending from 70 to 140 °C, which correlated to water vaporization. The heat flow from untreated fibers is remarkably more significant than the other samples. This showcased that the untreated fibers required higher heat

energy for evaporating more extensive water content, in line with the weight loss shown in the TGA curve.

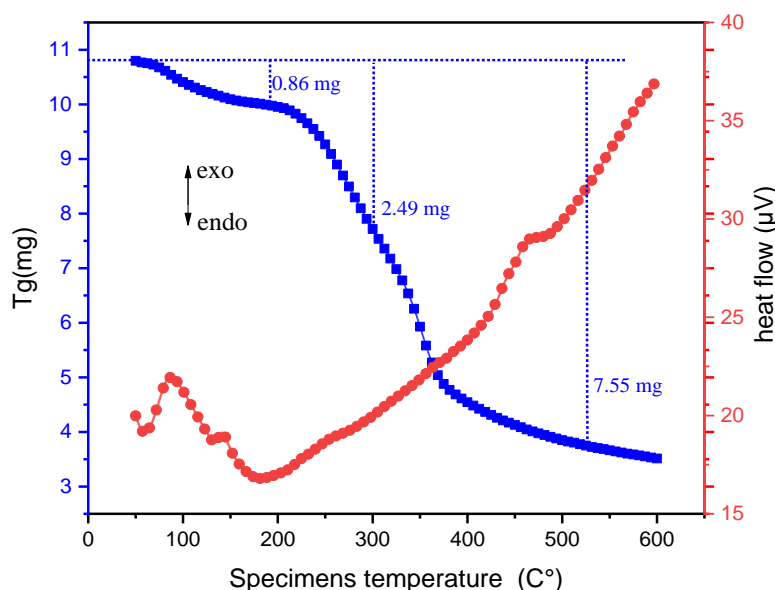


Fig IV. 6 TGA and DSC analysis pattern of a petiole particle

IV.1.4.2. TGA and DSC for Rachis fibers

The TGA and DSC analysis of petiole fiber reveals a distinct thermal decomposition profile shown in Figure IV.7. Initially, a slight weight loss occurs below 150°C due to moisture evaporation, which is common in natural fibers. The main decomposition stage takes place between 200°C and 400°C, where a significant mass loss is observed, likely due to the degradation of hemicellulose, cellulose, and lignin, as evidenced by the sharp decline in the TGA curve. This process corresponds to the exothermic activity seen in the DSC curve, indicating energy release during the breakdown of these organic components. A slower degradation phase follows from 450°C to 600°C, with a small ash residue (1.55 mg) remaining, reflecting the inorganic content. The DSC also highlights an exothermic peak in the range of 70°C to 140°C, related to moisture vaporization. Overall, this thermal profile demonstrates the fiber's moisture content, thermal stability, and decomposition stages, crucial for determining its suitability for applications in bio-composites.

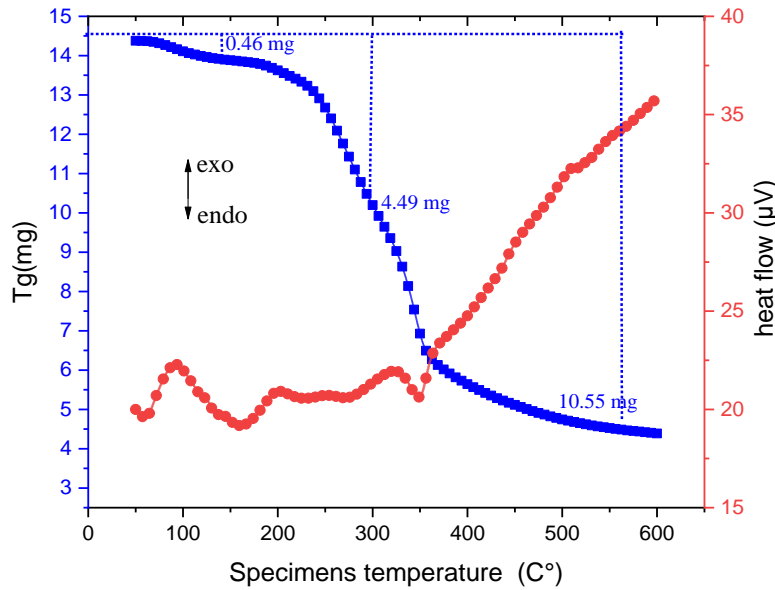


Fig IV. 7 TGA and DSC analysis of rachis fibers

V.2. Results and discussion of experimental techniques

IV.2.1. Mechanical characteristics of bio-composite ER (Rachis fibers-resin epoxy)

IV.2.1.1. Load-displacement curves (Three-point bending tests) of bio-composite ER

The load-displacement curves for the bio-composite ER (Rachis fiber/epoxy resin) are shown in Figure IV.8, categorized by varying percentages of fibers (0%, 5%, 7%, 10%, 13%, and 15%). These curves serve as representations of the material's mechanical properties, offering insights into its behavior under different loads. The data was directly obtained using an INSTRON machine, a reliable tool for assessing material properties. This information is crucial for comprehending the mechanical performance of bio-composite materials across diverse load conditions.

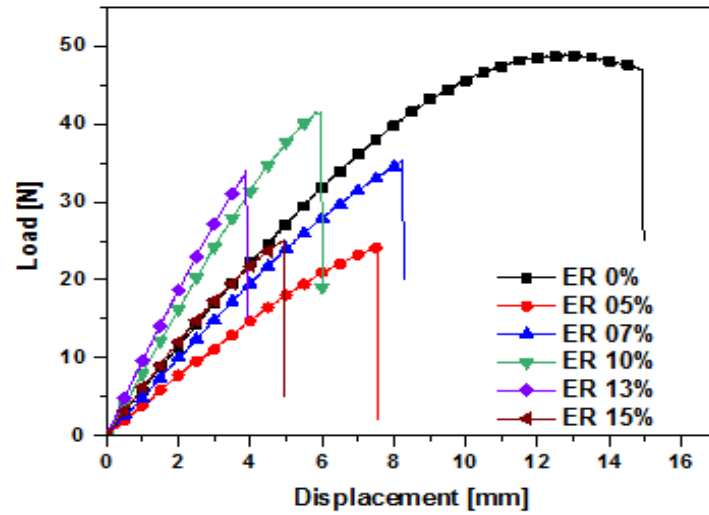


Fig IV. 8 Load-displacement curves of different bio-composites (ER) in three-point bending tests

The curves exhibit a linear increase, followed by a non-linear progression, culminating in eventual breakage. Flexural modulus and Flexural strength can be calculated during the linear segment using formulas (1) and (2). Table VI.1 and Figure IV.9, present the values of these mechanical behaviour for different types of bio-composites (ER0, ER05, ER07, ER10, ER13 and ER15).

Table IV. 1 Mechanical proprieties of different types of bio-composite (ER)

ER types	Mechanical properties	
	E(MPa)	σ (MPa)
ER0	2588±16.72	34.32±7.68
ER05	2706±145.19	35.47±3.91
ER07	2927±79.11	44.51±3.54
ER10	3385±89.16	46.46±2.59
ER13	3131±60.55	31.98±0.96
ER 15	1894±153.58	26.59±0.55

The increase in flexural modulus is evident with the rise in fiber percentage across the initial specimens (ER0, ER5, ER7, ER10), peaking at 3.385 GPa in the case of ER10 (Fig.VI. 9). Subsequently, a decline is noted in the flexural modulus for specimens (ER13, ER15), with the value at ER15 dropping below that of ER0. This reduction can be attributed to a decrease in resin-

fiber bonding as the fiber content increases. Similar trends are observed in the flexural strength (Fig. IV.10), where it ascends to 46.46 MPa at ER10%, only to decrease to 26.59 MPa at ER15%.

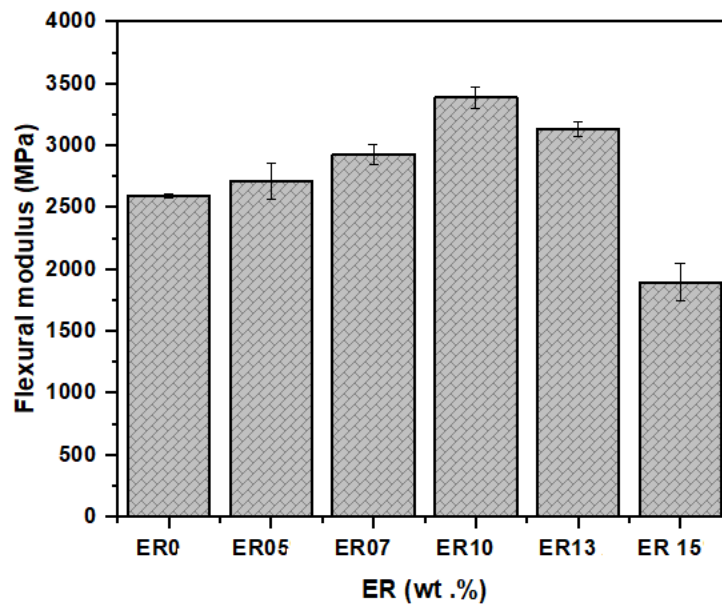


Fig IV. 9 Flexural modulus of different bio-composites ER

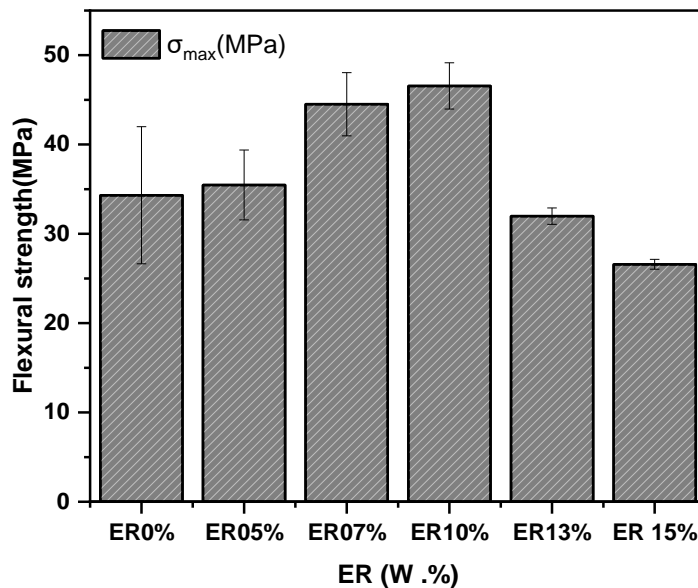


Fig IV. 10 Flexural strength of different bio-composite ER

The ER10 composite material exhibits superior mechanical properties compared to those reported in previous studies. For instance, when compared to the flexural modulus of 3.11 GPa achieved by the rachis/epoxy compound in the study of R.Benzidane [76], the flexural modulus of

the ER10 composite stands out. Additionally, the ER10 composite surpasses the tensile strength modulus reported for EFR10 (0.52 GPa) and PFR10 (0.90 GPa) in Tarek's study [4]. Furthermore, in contrast to the tensile strength modulus of 537.9 MPa reported for EPL10% (Lif-epoxy) composites in Djabloun's study [77], the ER10% composite exhibits superior mechanical properties. Similarly, the ER10% composite demonstrates favorable mechanical properties.

IV.2.1.2. Hardness behavior of bio-composite ER (Brinell hardness)

The provided statement delves into the Brinell hardness (HBN) values of bio-composite ER across various fiber contents, offering insightful interpretation and analysis. Within the context of material characterization, the Brinell hardness values serve as a crucial metric indicating the resistance of materials to indentation or deformation. In this case, the analysis begins by presenting the Brinell hardness values obtained for the bio-reinforced fiber composites, showcasing a range between 14.31 and 6.98 HB. Notably, these values collectively suggest that the bio-reinforced fiber composites are inherently soft materials, displaying lower resistance to deformation compared to harder materials. Furthermore, the interpretation scrutinizes the relationship between fiber content and composite hardness. It discerns a consistent trend wherein an increase in the fiber weight ratio corresponds to a decrease in composite hardness. This trend is exemplified by the progressive decrease in hardness observed across the varying fiber content compositions, labeled as ER5, ER7, ER10, ER13, and ER15, representing fiber weight ratios of 5%, 7%, 10%, 13%, and 15%, respectively. Figure .IV.11. Moreover, the analysis draws parallels with previous findings in bamboo [129] fiber composites, reinforcing the observed trend across different fiber-reinforced materials. Importantly, the interpretation provides a plausible explanation for this observed trend, attributing it to the inherent softness of the fibers relative to the pure epoxy resin matrix. This implies that the incorporation of a higher proportion of softer fibers into the composite matrix dilutes its overall hardness, resulting in the observed decrease. In essence, this comprehensive interpretation elucidates the relationship between fiber content and composite hardness while offering insights into the underlying material properties influencing this behavior.

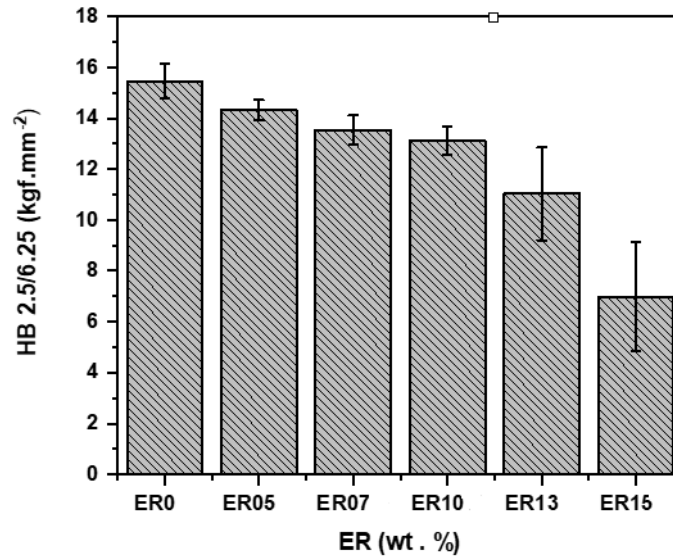


Fig IV. 11 Hardness properties of different types of bio-composite ER

IV.2.2. Thermal-physical properties of bio-composite ER

IV.2.2.1. Thermal conductivity of ER

Insulation materials are critically evaluated based on their thermal performance, which is primarily measured by thermal conductivity or thermal resistance [14], [15]. The selection of ideal insulation materials is based on these factors, as demonstrated in previous studies [16]. Table VI.2 shows the thermal behavior values for different types of bio-composite ER.

Table IV. 2 Thermal properties of different types of a bio-composite ER

(ER) types	Thermal conductivity [W/m.°K]	Thermal Diffusivity [mm/s ²]	Specific heat [Mj/m ³ .°K]
ER0	0.2676 ± 10^{-3}	0.199 ± 10^{-3}	0.096 ± 10^{-3}
ER5	0.2534 ± 10^{-3}	0.186 ± 10^{-3}	1.145 ± 10^{-3}
ER7	0.2252 ± 10^{-3}	0.177 ± 10^{-3}	1.332 ± 10^{-3}
ER10	0.2110 ± 10^{-3}	0.144 ± 10^{-3}	1.468 ± 10^{-3}
ER13	0.2103 ± 10^{-3}	0.142 ± 10^{-3}	1.475 ± 10^{-3}
ER15	0.2101 ± 10^{-3}	0.138 ± 10^{-3}	1.512 ± 10^{-3}

Each measurement's thermal conductivity value was determined only after achieving measurement stabilization, a crucial step illustrated by the lambda-versus-time curve in Figure.IV.14.

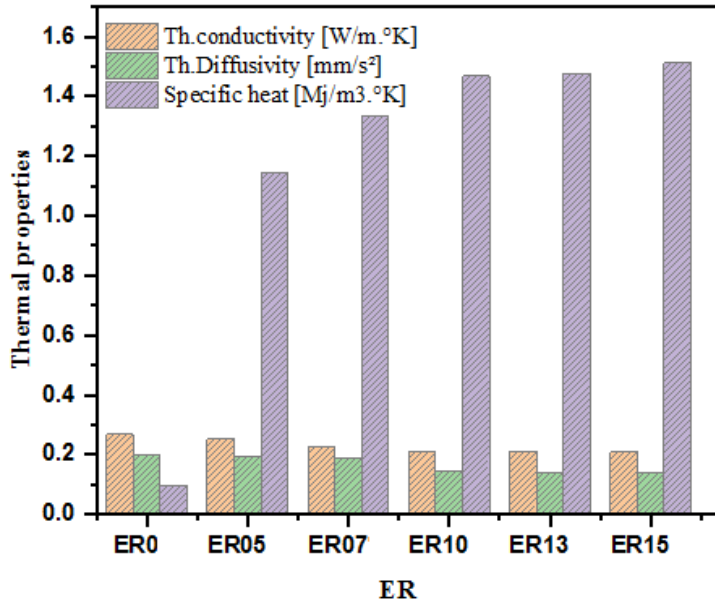


Fig IV. 12 Thermal behaviour of different types of bio-composite ER

The bio-composite ER emerges as a standout contender due to its commendable thermal properties, positioning it as a promising choice across diverse thermal insulation applications. Noteworthy is its ability to either match or surpass the thermal conductivity values of existing materials, affirming its potential as a highly efficient and dependable thermal insulator. Comparatively, rubber mortar compounds, as cited in [130], demonstrated thermal conductivity ranging from 0.255 to 0.443 W/(m·K), while Asyraf's pure PF uterus [131] reached 0.348 W/(m·K), and date palm fibers [132] spanned from 0.075 to 0.6 W/(m·K), all indicating values higher than those observed in the current study, as delineated. This underscores the significance of the bio-composite ER thermal performance and its potential to outperform conventional insulation materials.

IV.2.2.2. TGA and DSC analysis of bio-composite ER

The TGA and DSC analysis of the rachis fiber/epoxy resin composite provides valuable insights into its thermal behavior shown in fig IV.13.

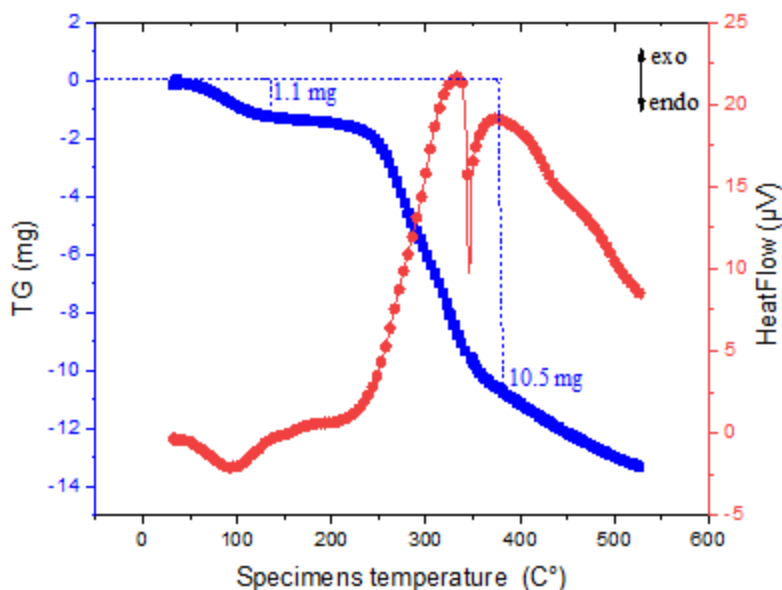


Fig IV. 13 TGA and DSC of bio-composite ER

The TGA curve shows an initial slight weight loss below 150°C, which can be attributed to moisture evaporation. The main degradation occurs between 200°C and 400°C, with a significant weight loss of around 11 mg, corresponding to the thermal decomposition of the epoxy matrix and the lignocellulosic components of the rachis fibers, such as hemicellulose and cellulose. Beyond 400°C, a slower degradation phase occurs, leaving a residue of approximately 10.5 mg, likely representing the inorganic ash content. The DSC curve shows an initial exothermic peak between 50°C and 150°C, associated with moisture evaporation. A broader exothermic event occurs between 200°C and 400°C, indicating energy release during the decomposition of the fibers and epoxy resin. A final exothermic peak around 450°C marks the final stages of degradation. This thermal profile highlights the composite's decomposition stages and offers insights into its thermal stability, which is crucial for high-temperature applications.

IV.2.2.3. Water absorption of bio- composite ER

The water absorption percentages observed in the bio-composite ER, as depicted in Fig. IV.14 exhibits a clear and consistent trend in the data.

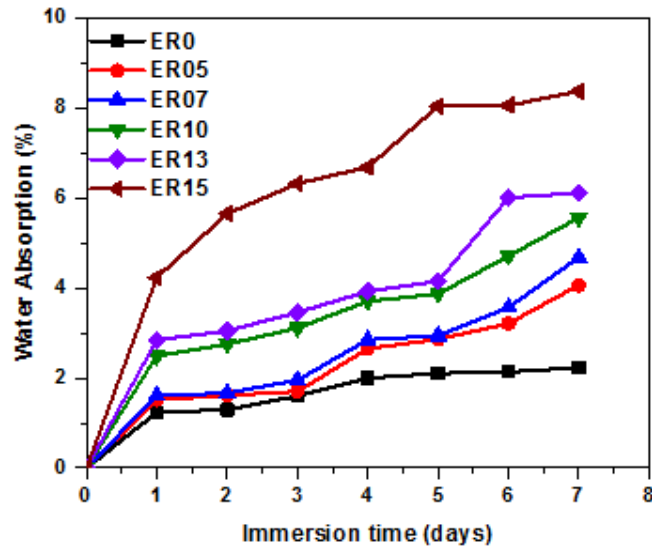


Fig IV. 14 Water absorption tendencies of bio-composite ER

There is a noticeable increase in water absorption values as the percentage of Rachis fibers in the epoxy matrix rises, particularly evident with longer soaking times. It is noteworthy that the specimens reach a saturation point at approximately seven days of soaking. This observed behavior can be attributed to the inherently hydrophilic nature of Rachis fibers, which stems from the presence of polar groups. These polar groups facilitate robust hydrogen bonding between water molecules and the cellulose molecules within the Rachis fibers. This phenomenon is effectively represented schematically in Figure (IV.15) providing a visual understanding of the interactions driving the water absorption behavior in the Rachis/Epoxy composites.

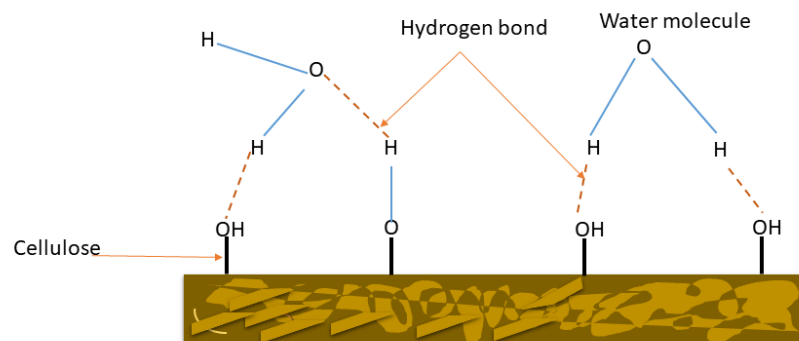


Fig IV. 15 Enhancing Water-Molecule and Cellulose Interaction: A Schematic Diagram of Hydrogen Bonding [79, 110].

In the realm of fiber-reinforced epoxy composites, the water absorption percentage serves as a critical indicator of material performance and longevity. A low water absorption percentage is highly desirable, as it signifies enhanced resistance to moisture-related issues such as swelling, weakening, or delamination. This characteristic indicates effective collaboration between the epoxy resin and fibers in fortifying the composite against water ingress, thereby imparting robustness and resilience against environmental stressors. In applications where top-notch quality, extended durability, and minimal maintenance are paramount, maintaining a low water absorption rate becomes imperative.

This study underscores a significant observation regarding the water absorption of Rachis/epoxy ER (wt. %) composites, which exhibit values lower than those reported in prior literature. These comparisons encompass a wide range of materials, including natural fiber-based composites [133], flax/bio epoxy composites [134], mineral wool, sisal-reinforced building blocks [135], starch/Poly lactide composites [136], and focus on oil Palm empty fruit Bunch/Sugarcane bagasse fiber-Based Composites [137]. The outcomes of this research reveal exceptional results, demonstrating the manufactured material's remarkably low water absorption capacity. Consequently, it positions itself as a promising candidate for applications requiring excellent water resistance, particularly as an effective insulator.

IV.2.2.4. Bulk Density of bio- composite ER

The experimentally recorded values of different types of bio-composite ER densities are illustrated in Figure.IV.16.

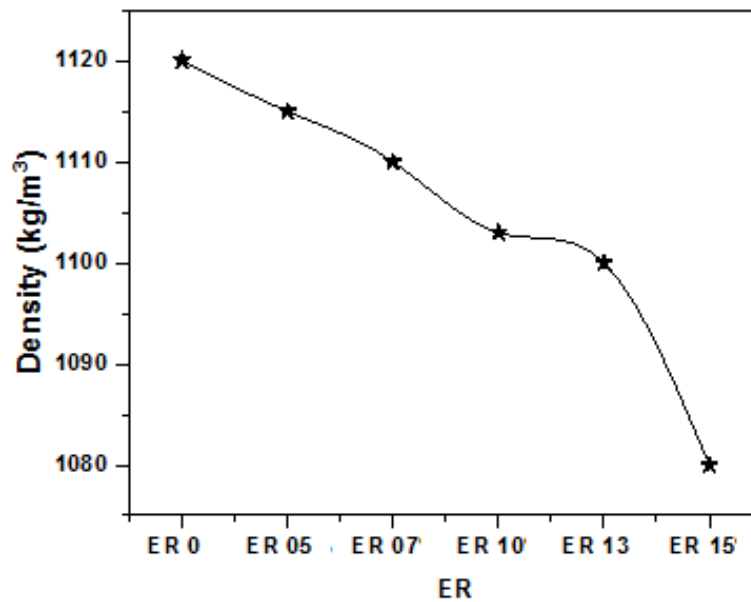


Fig IV. 16 Density values of different types of bio-composite ER

The density of the ER0 specimens is measured at 1120 kg/m³. As the proportion of fibers increases, there is a consistent decrease in composite density, with values ranging from 1115 kg/m³ for the 5% ER specimens to 1080 kg/m³ for the 15% ER specimens. Other studies focusing on date palm waste-based compounds have reported relatively higher densities. For instance, date kernel compounds exhibited densities ranging from 1205 to 1225 kg/m³ [138], while polylactic acid/date palm wood powder composites ranged from 1220 to 1187 kg/m³ [139]. Additionally, other natural compounds such as banana (1350 kg/m³) and sisal (1450 kg/m³) [132], as well as kenaf core fibers/butylene succinate composites (ranging from 1260 to 1430 kg/m³) [109], have demonstrated higher density values compared to the Rachis/Epoxy composites studied herein.

The notable decrease in density observed with increasing component fiber contents can be attributed to the lower densities of ER5, ER7, ER10, ER13, and ER15 compared to pure ER0%. Conversely, the slight decrease in experimental density observed when using fillers in this work can be attributed to the presence of voids in the produced composites.

IV.2.3. Structural properties of the bio-composite ER

IV.2.3.1. Scanning electron microscopy (SEM) of ER

The investigation into composite materials delves deeply into the critical aspect of adhesion between the filler and matrix, recognizing its pivotal role in determining material properties.

Surface morphology studies were meticulously conducted, with a particular focus on tensile properties, and the results are vividly depicted in Figure. IV.17.

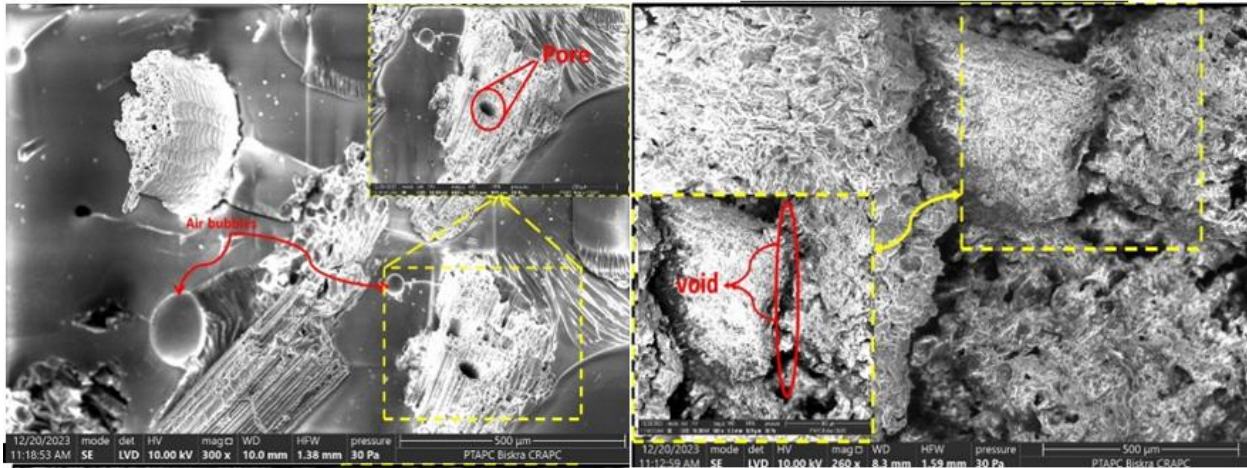


Fig IV. 17 SEM micrographs for the Rachis/Epoxy (ER) composites with 10 wt. % of the rachis

These images intricately showcase composites with varying filler loadings (ranging from 0% to 15%), unveiling a compelling correlation between filler content and void formations. Notably, lower voids are discernible at lower filler loadings, whereas an increase in filler loading corresponds to a marked escalation in void content. These compelling results strongly suggest that insufficient wetting of the hydrophobic Epoxy Resin with the hydrophilic Rachis fibers might be chiefly responsible for these observed voids. Importantly, this inadequacy in wetting is anticipated to profoundly impact the ductile nature of the material, rendering it more susceptible to crack propagation during subsequent flexural analysis. Such findings underscore the paramount importance of optimizing wetting interactions to achieve enhanced adhesion and, consequently, bolstered mechanical properties of the composite materials.

IV.2.3.2.X-ray diffraction (DRX) of bio-composite ER

The prepared of bio-composite ER specimens were analyzed using X-ray diffraction (XRD) techniques, with the diffraction patterns shown in Fig (IV.18).

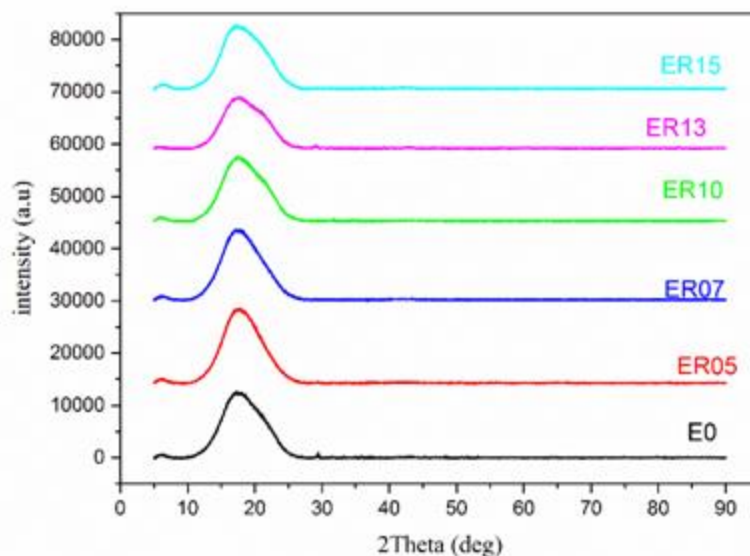


Fig IV. 18 DRX spectra of the bio-composite ER

The XRD results reveal broad amorphous peaks in the 2θ range of 10° – 30° , which indicate the mainly amorphous structure of the epoxy composites [140]. This amorphous nature indicates the absence of long-range crystalline order within the material. In addition, it is important to note that the addition of graphene sheets to the bio-composite ER had no significant effect on the crystallinity of the epoxy. The XRD patterns of all samples were consistent, showing no significant changes or differences, further confirming that the incorporation of fibers does not affect the crystalline properties of the composite.

IV.2.3.3. Fourier-Transform Infrared Spectroscopy (FTIR) of bio-composite ER

The FTIR spectra for the bio-composite ER presented with varying fiber weight ratios in Figure (IV.19). Offer a detailed analysis of the distinctive peaks found in the filler material. In the ER% composite, a broad peak at 3338 cm^{-1} is identified, corresponding to the stretching vibrations of hydroxy groups present in cellulose, hemicellulose, and lignin. Additionally, the peaks at 2919 cm^{-1} and 2852 cm^{-1} are attributed to the asymmetric and symmetric C-H stretching vibrations within cellulose and hemicellulose, respectively. The peak at 1745 cm^{-1} is linked to the C=O stretching of acetyl groups in hemicellulose. Changes in the FTIR spectra of date palm residual material are also noted, including the shift of a major peak from 1748 cm^{-1} to 1745 cm^{-1} , and a shift from 1211 cm^{-1} to 1220 cm^{-1} [141]. These shifts suggest that hydrogen bonding influences the stretching and bending behavior of C-O groups. Furthermore, the spectra highlight

characteristic lignin bands, such as the peak around 1520 cm^{-1} , and hemicellulose presence is indicated by the band near 1720 cm^{-1} , corresponding to C-O elongation in xylene [142]. During the drying process of ER%, intra-chain hydrogen bonding, similar to the observed spectral shifts, occurs due to structural changes during crystallization. This is supported by several peaks within the $1211\text{--}1042\text{ cm}^{-1}$ range, which are linked to C-O groups [143] from carboxyl groups and C-O-C stretching vibrations [144]. A peak at 957 cm^{-1} is associated with the rocking motion of the CH₃ group [145], while another peak at 870 cm^{-1} relates to C=C bond stretching [146]. Additionally, a peak at 756 cm^{-1} corresponds to C-O bond bending [147]. These observations enhance the understanding of the molecular interactions and structural transformations during the drying of ER%, aligning with existing literature. The FTIR analysis underscores the chemical differences between fibers from date palm waste and epoxy resin, emphasizing the hydrophilic nature of the fibers in contrast to the hydrophobic

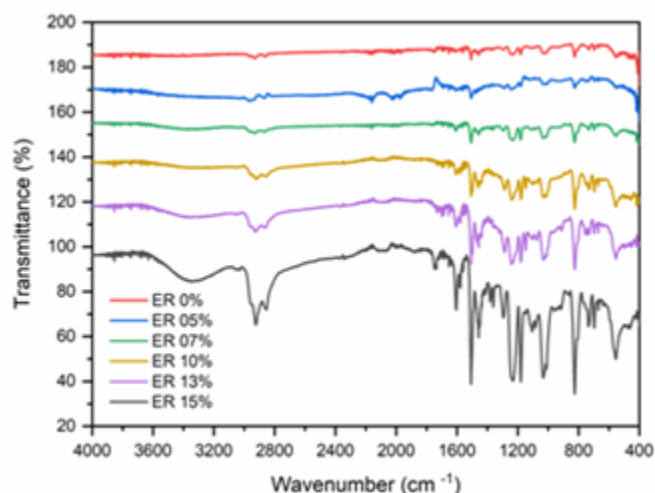


Fig IV. 19 FTIR spectra of the bio-composite ER

Offer a detailed analysis of the distinctive peaks found in the filler material. In the ER% composite, a broad peak at 3338 cm^{-1} is identified, corresponding to the stretching vibrations of hydroxy groups present in cellulose, hemicellulose, and lignin. Additionally, the peaks at 2919 cm^{-1} and 2852 cm^{-1} are attributed to the asymmetric and symmetric C-H stretching vibrations within cellulose and hemicellulose, respectively. The peak at 1745 cm^{-1} is linked to the C=O stretching of acetyl groups in hemicellulose. Changes in the FTIR spectra of date palm residual material are also noted, including the shift of a major peak from 1748 cm^{-1} to 1745 cm^{-1} , and a shift from 1211 cm^{-1} to 1220 cm^{-1} [141]. These shifts suggest that hydrogen bonding influences

the stretching and bending behavior of C-O groups. Furthermore, the spectra highlight characteristic lignin bands, such as the peak around 1520 cm^{-1} , and hemicellulose presence is indicated by the band near 1720 cm^{-1} , corresponding to C-O elongation in xylene [142]. During the drying process of ER%, intra-chain hydrogen bonding, similar to the observed spectral shifts, occurs due to structural changes during crystallization. This is supported by several peaks within the $1211\text{-}1042\text{ cm}^{-1}$ range, which are linked to C-O groups [143] from carboxyl groups and C-O-C stretching vibrations [144]. A peak at 957 cm^{-1} is associated with the rocking motion of the CH₃ group [145], while another peak at 870 cm^{-1} relates to C=C bond stretching [146]. Additionally, a peak at 756 cm^{-1} corresponds to C-O bond bending [147]. These observations enhance the understanding of the molecular interactions and structural transformations during the drying of ER%, aligning with existing literature. The FTIR analysis underscores the chemical differences between fibers from date palm waste and epoxy resin, emphasizing the hydrophilic nature of the fibers in contrast to the hydrophobic

IV.2.4. Mechanical properties of petiole agglomerate Pt (petiole particles/white glue)

IV.2.4.1. Three points bending test of petiole agglomerate Pt

Findings derived from three-point bending tests conducted on specimens comprising various petiole agglomerate compositions (designated as Pt15, Pt17, Pt20, Pt23, and Pt26) offer substantial scientific insights into the mechanical behavior and strength characteristics of the material. The load-displacement curves as illustrated in Figure (IV.20).

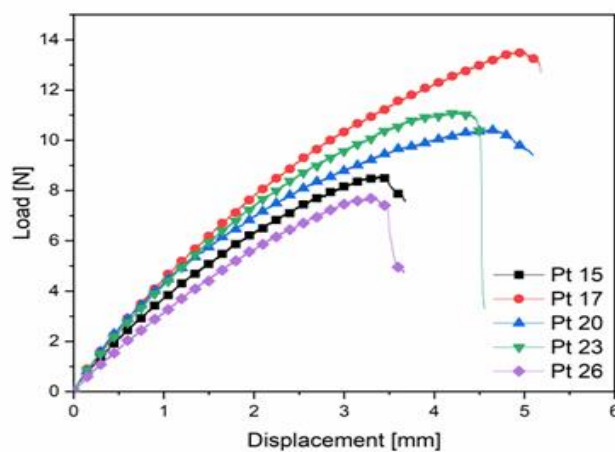


Fig IV. 20 Load -. Displacement curve for different types of Pt in three points bending test

This curve offers a comprehensive representation of the correlation between applied load and displacement, unveiling distinctive patterns of deformation and failure. By employing prescribed equations (1), (2), and (3), the flexural modulus and flexural strength can be precisely calculated from the linear segment of these curves to provide quantifiable assessments of the material's rigidity and resistance to deformation. The numerical data presented in Table 3 further bolster these findings to delineate the mechanical attributes of each petiole agglomeration configuration to facilitate direct comparisons.

Table IV. 3Mechanical property values of different types of petiole agglomerate Pt

Specimens	Mechanical properties	
	E(MPa)	σ (MPa)
Pt15	347.13±3.75	1.72±0.29
Pt17	429.30 ±4.04	2.01±0.09
Pt20	368.14±14.81	1.95±0.23
Pt23	334.05±2.8	1.56±0.14
Pt26	255.51±15.44	1.24±0.06

The results of three-point bending tests on various petiole agglomerate compositions reveal crucial insights into their mechanical behavior. Load-displacement curves exhibit distinct patterns of deformation and failure allowing for a precise determination of Flexural modulus and Flexural strength. Notably, Pt17 demonstrates superior mechanical properties compared to other compositions highlighting its enhanced structural performance. These findings, in line with established principles of materials science, underscore the importance of composition and interfacial adhesion in determining mechanical characteristics.

IV.2.4.2. Compression tests of Petiole agglomerate

Stress-strain curves shown in Figure (IV.21) show the results of compression tests conducted in the longitudinal (CL) and transverse (CT) directions on the platinum type which has the best elastic modulus (Pt17) among the other types.

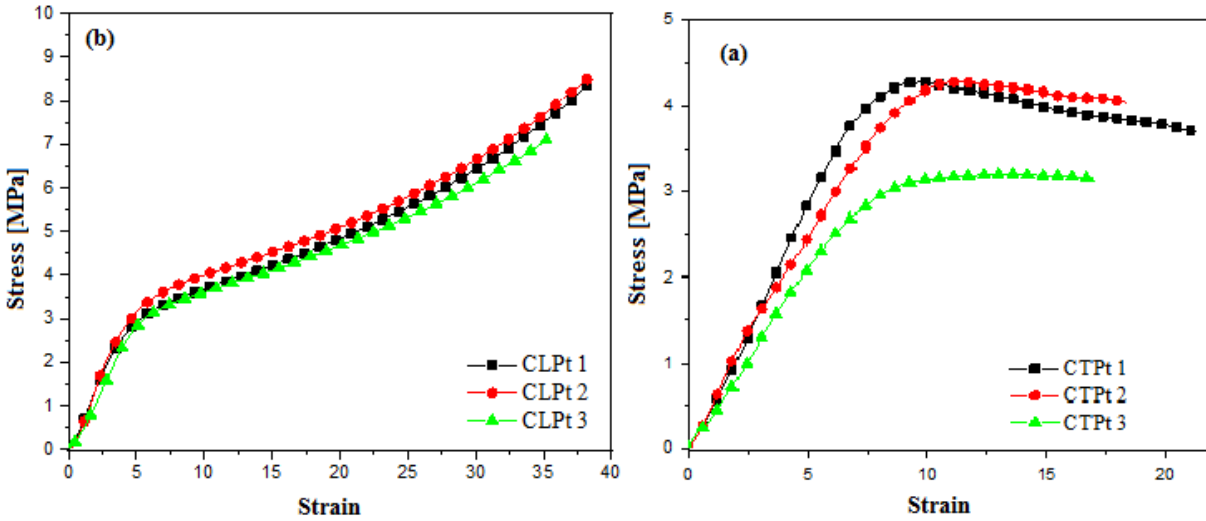


Fig IV. 21 Stress-strain curve of Pt17 by compression tests (a): in the transverse directions, (b): in the longitudinal directions

Figure IV.21 gives the evolution of the applied stress as a function of the deformation, for different types of specimens (longitudinal and transverse) in the petiole agglomerate (Pt17) stressed by compression. The behavior of the specimens is similar and can be divided into 3 main phases. The first phase is the elastic part corresponding to a linear increase in the applied stress with the deformation. The modulus of elasticity is determined by the equation of Hook's law (III.3). The second phase is the plastic part which corresponds to a non-linear increase in the stress of the deformation. The third phase is a resumption of a linear increase in the stress as a function of the deformation. Indeed, from this deformation, the cells are crushed which stiffens the petiole agglomerate.

Table IV.4 represents the values the longitudinal and transverse elasticity modulus of petiole agglomerate (Pt17) subjected to compression tests.

Table IV. 4Elasticity modulus longitudinal and Transverse of petiole agglomerate (Pt17)

N°: Specimens	longitudinal direction (CL) $E_{CT}(\text{MPa})$	Transverse direction (CT) $E_{CL}(\text{MPa})$
1	0.645	0.518
2	0.654	0.566
3	0.649	0.451
E average	$0,649\pm 0,005$	$0,512\pm 0,040$

The results obtained from the analysis indicate that there is a change in the elastic modulus across the longitudinal and transverse directions of Pt17. After taking three samples for each direction, we notice that the elastic modulus values are similar for each direction. We also notice that the longitudinal elastic modulus is greater than the transverse elastic modulus for Pt17.

The bio-composite Pt17 material is considered orthotropic to transverse isotropic. In the direction of the orthotropic axis, the elastic modulus is estimated at 0.512 Mpa while in the isotropic plane, it is estimated at 0.649 Mpa.

IV.2.5. Thermal-physical properties results of petiole agglomerate (Pt)

IV.2.5.1. Thermal conductivity results of petiole agglomerate (Pt)

The thermal properties measured for the petiole agglomerate (Pt) reveal its excellent insulation capabilities, establishing it as a strong candidate for thermal insulation applications. Notably, the selected specimen (Pt) demonstrates superior thermal performance when compared to other composite materials. The low thermal conductivity (λ) values, particularly when $\lambda \leq 0.9$, indicate enhanced insulation properties as detailed in Table (IV.5). Further confirms that among the tested specimens, the bio-composite petiole agglomerate (Pt) exhibited the best thermal conductivity, ranging between 0.11 and 0.12 W/(m.K). This is a significant finding, as the thermal conductivity of the petiole composite is not only comparable to but often superior to widely recognized materials such as wood fiber/Ecovio (0.119 W/m.K) [38], banana/PP (0.157 W/m.K) [39], bamboo/bone (0.118 W/m.K) [40], raw wood of palm date (0.123 W/m.K) [41], hemp (0.115 W/m.K) [42], and wheat straw (0.56 W/m.K) [43]. Table (IV.5) present the different values of thermal proprieties of different types of petiole agglomerate (Pt).

Table IV. 5 Thermal properties of bio-composite material

Specimens	Thermal properties		
	Th. Conductivity (W/m.K)	Th. Diffusivity (mm ² /s)	Spec. Heat (MJ/m ³ .K)
Pt15	0,1134342 ±10 ⁻⁴	0,1641180±10 ⁻⁴	0,704002±10 ⁻⁴
Pt17	0,1136350 ±10 ⁻⁴	0,1644110±10 ⁻⁴	0,704028±10 ⁻⁴
Pt20	0,1138700±10 ⁻⁴	0,1643681±10 ⁻⁴	0,704135±10 ⁻⁴
Pt23	0,1138842 ±10 ⁻⁴	0,1645643±10 ⁻⁴	0,704145±10 ⁻⁴
Pt26	0,1138984 ±10 ⁻⁴	0,1648740±10 ⁻⁴	0,704608±10 ⁻⁴

These comparisons underscore the superior thermal insulation potential of the petiole composite material, positioning it as a viable alternative to conventional insulation materials. Its low thermal conductivity suggests that it could provide improved energy efficiency in various applications, particularly in sustainable construction and industrial insulation. Moreover, the petiole composite's favorable insulation properties, combined with its potential for eco-friendly sourcing and production, present a compelling case for its broader adoption in thermal management systems. As the global demand for sustainable materials grows, the petiole composite offers a promising solution, outperforming traditional materials in key thermal metrics while contributing to sustainability efforts in the materials science and engineering fields.

IV.3.5.2. Thermogravimetric (TGA) and differential scanning calorimetry (DSC) results of petiole agglomerate (Pt).

The thermogravimetric (TGA) and differential scanning calorimetry (DSC) analysis of the petiole agglomerate (Pt) offers key insights into its thermal behavior and decomposition patterns shown in Fig (IV.22).

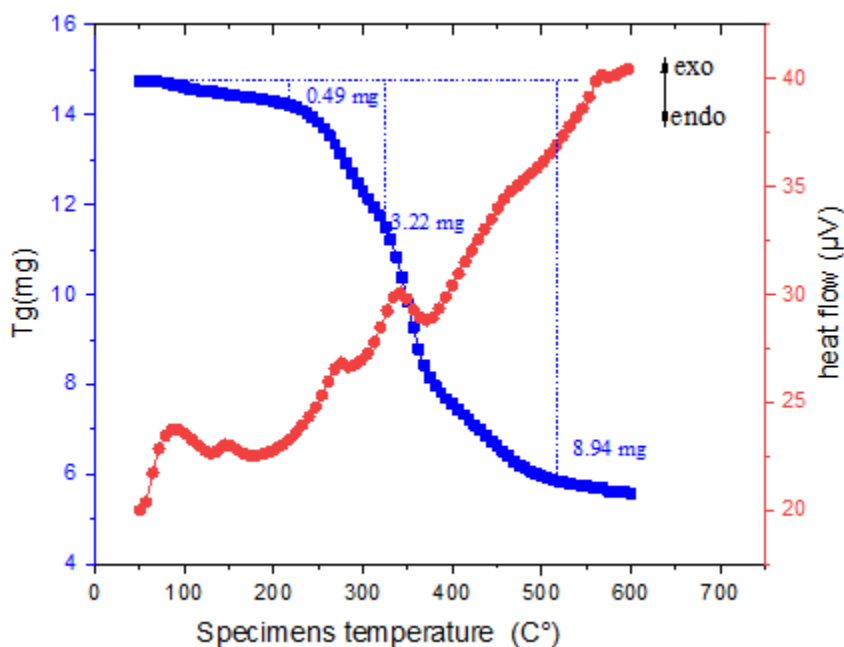


Fig IV. 22 TGA and DSC curve of bio-composite petiole agglomerate (PT17)

Initially, a slight weight loss is observed below 150°C, corresponding to the evaporation of absorbed moisture, a common characteristic of natural fiber composites. The main thermal degradation occurs between 200°C and 400°C, with a significant mass loss of around 22 mg, attributed to the breakdown of hemicellulose, cellulose from the petiole fibers, and the PVA matrix. Beyond 400°C, the degradation process slows down, leaving a residual ash content of 8.54 mg by 600°C, representing the inorganic materials. The DSC analysis reveals an initial exothermic peak between 50°C and 150°C due to moisture evaporation, followed by a broader exothermic event from 200°C to 400°C, reflecting the energy released during the decomposition of the organic components. A final exothermic rise beyond 400°C is associated with the degradation of remaining materials and the formation of carbonaceous residues. This thermal profile is crucial for understanding the composite's thermal stability and performance in high-temperature applications.

IV.2.5.3. Water absorption tests of petiole agglomerate (Pt)

The investigation focused on analyzing the water absorption behavior of various biomaterials denoted as Pt15, Pt17, Pt20, Pt23, and Pt26 Wt. %. The experimental setup involved immersing these biomaterial specimens in distilled water for around ten hours with measurements taken at two-hour intervals until signs of damage and decomposition began to manifest. Notably, all specimens demonstrated a consistent trend: they reached a state of saturation approximately eight hours after immersion commenced after which further absorption plateaued. Beyond the saturation point degradation processes characterized by visible structural changes and the formation of voids are initiated around the tenth hour. Figure (IV.23) illustrates the distinct water absorption percentages for each biomaterial specimen highlighting Pt17 as having a notably lower absorption rate compared to Pt20, Pt23, and Pt26.

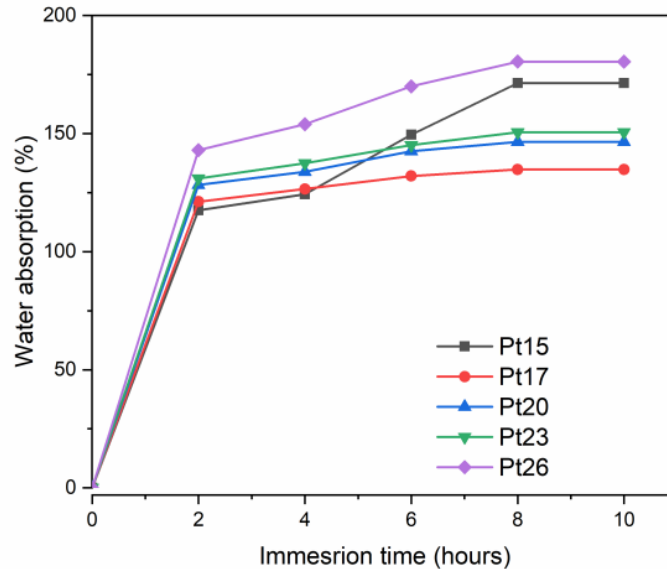


Fig IV. 23 Percentage of water absorption for different types of petiole agglomerate (Pt)

The mechanism behind water absorption in the bio-material (petiole agglomerate) can be attributed to the presence of inherent porosity, voids and minor cracks within the interfacial adhesion between petiole particles and the epoxy resin matrix. These microstructural features act as reservoirs for water molecules to allow the biomaterials to absorb moisture until reaching a saturation point where further absorption becomes limited. This saturation phase is critical as it marks the beginning of irreversible changes in the composite's physical properties that lead to potential mechanical weaknesses over time due to the formation of voids and the loss of structural integrity.

Furthermore, the comparative analysis revealed that Pt17 exhibited water absorption rates comparable to or lower than those reported for other biomaterials such as petiole (146%) [81] and Sisal (230%) [148]. This finding underscores the variability in water absorption characteristics among different biomaterial compositions which is influenced by factors such as the density of interfacial defects and the efficiency of water uptake pathways within the composite structure.

while the observed high water absorption in the bio-material (petiole agglomerate) is indicative of its porous nature The presence of weak interfacial adhesion sites that facilitate water storage, the saturation and subsequent formation of voids underscore potential challenges in maintaining long-term durability and performance of biomaterial-based composites in various applications from construction materials to biomedical implants.

IV.2.5.4. Bulk Density tests of petiole agglomerate (Pt)

The density results of the composite materials are depicted in Figure IV. 24 and Table IV.6, reveal a clear trend: increasing the petiole particle ratio results in higher material density. The lowest density value approximately 0.28 g/cm³, is observed in the specimens labeled "Pt 15." Interestingly, the specimens labeled "Pt 17" exhibit a density very close to Pt 15 with a 0.3 g/cm³ value. This suggests that small variations in the petiole particle ratio can significantly impact the density of the composite material.

Comparing these results with existing literature underscores the competitive nature of our composite material. [81] reported a density of $\rho=0.88$ g/cm³, [149] documented a density of $\rho=0.73$ g/cm³, and [83] recorded a density of 0.53 g/cm³. Our material demonstrates a notably lower density positioning it as a promising candidate for applications where minimizing weight and density is critical. Furthermore, the similarity in density between our specimens (Pt 17) and Pt 15 indicates that it is possible to achieve an optimal balance between density and performance to enhance the material's versatility and utility.

This analysis indicates that our composite material has a lower density than other materials documented in the literature and can be fine-tuned to meet specific density and performance requirements. This makes it suitable for a wide range of applications where lightness and material performance are crucial. Table (IV.6) presents different values of Bulk density on petiole agglomerate (Pt).

Table IV. 6 Bulk density values of different types of petiole agglomerate

Specimens	Density [g/cm ³]
Pt 15	0.28
Pt 17	0.30
Pt 20	0.40
Pt 23	0.42
Pt 26	0.43

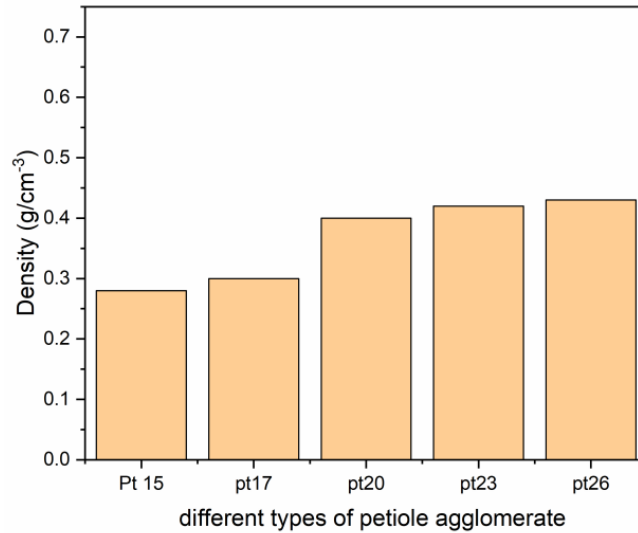


Fig IV. 24 Density of tested bio-composite materials

IV.2.6.Structural properties of petiole agglomerate (Pt)

IV.2.6.1.Scanning Electron Microscope (SEM) of petiole agglomerate (Pt)

The SEM image of the specimen surface shown in Figure (IV.25) provides crucial insights of the microstructure of petiole agglomerate (Pt17).

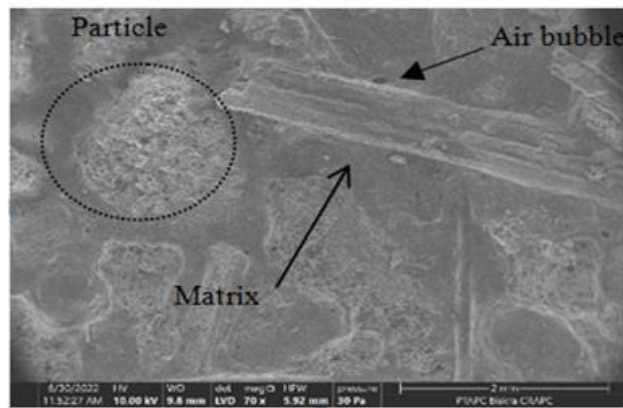


Fig IV. 25 SEM image of the Petiole agglomerate (Pt17)

It clearly shows the presence of numerous large dominant composites and voids which are indicative of the material's internal composition and structural integrity. The observation of these large dominant granules suggests the existence of substantial particles or aggregates dispersed throughout the specimens highlighting the heterogeneous nature of the composite material. In addition, the SEM image reveals an irregular surface characterized by filaments, impurities, cells and pores. These surface features create contact points that enhance adhesion between the fibers

and the PVA matrix to contribute significantly to the overall strength and performance of the composite material. This intricate network of surface irregularities plays a crucial role in promoting mechanical interlocking and bonding between the reinforcing fibers and the matrix material. Such enhanced bonding mechanisms are well-documented in material science and engineering literature to improve mechanical properties and resistance to deformation. Furthermore, the roughened surface topography created by these irregularities further reinforces the structural integrity of the composite material. The SEM image provides valuable insights to the morphology and distribution of the (Pt17), within the specimen and confirms its structural integrity and potential suitability for applications requiring robust and durable materials. Further comprehensive analysis and interpretation of the SEM image alongside complementary characterization techniques will continue to enrich our understanding of the material's microstructural properties and pave the way for future research advancements.

The results obtained from the chemical composition of our specimens are recorded in the table.IV7. The primary composition of date palm stems consists of carbon (42.2%), oxygen (47.7%) and a small amount of hydrogen (2.20%) which is a characteristic of organic matter. The rest of the composition includes trace amounts of various minerals such as silicon, calcium, potassium, magnesium, phosphorus, sodium and iron. These results are similar to the study of A.kinza [81]. When comparing these values with those reported in the literature for similar types of wood K. Riahi [150] and B. Agoujil [74] our specimens show much lower concentrations of these elements. This discrepancy is mainly attributed to the chemical composition of the soil and the specific environmental conditions where the palm trees were grown. Soil pH, nutrient availability, water quality and environmental pollutants play crucial roles in the uptake of elements by plants, thus influencing the overall chemical composition of the wood. Variations in these factors lead to differences in the mineral content and element distribution within the wood specimens. Table 7 presents the chemical composition of petiole agglomerate.

Table IV. 7Chemical composition of petiole agglomerate (Pt17)

Chemical Composition	C	O	H	Cu	Mg	Zn	Fe	Na	Ca	K	P
Percentage %	42.2	47.7	2.90	0.73	1.89	0.79	1.99	0.13	0.78	0.18	0.98

IV.2.6.2.X-ray diffraction (XRD) of petiole agglomerate

Figure (IV.26) Presents the X-ray diffraction (XRD) patterns of petiole agglomerate (Pt) to elucidate the key crystalline characteristics.

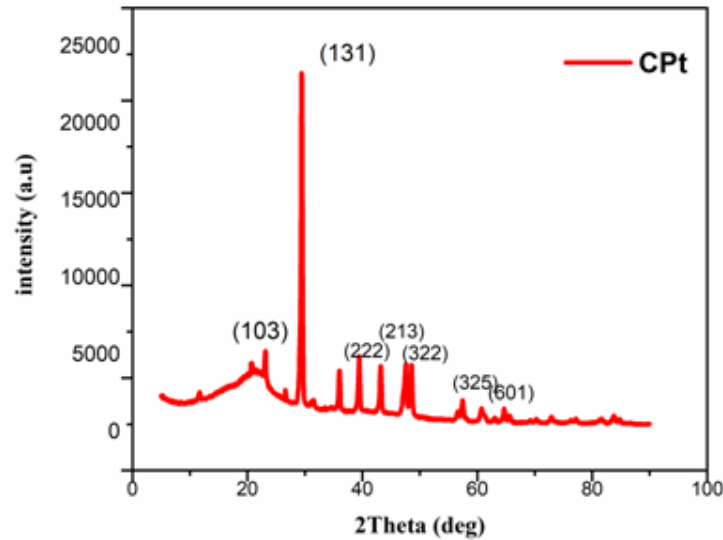


Fig IV. 26 XRD spectra of petiole agglomerate

The diffraction spectrum exhibits several notable peaks: a sharp peak at $2\theta = 29.47^\circ$, a broad peak at 23.13° and less defined peaks at 36.03° , 39.46° and 47.56° . These peaks correspond to the (131), (103), (222), (213) and (322) crystal planes, respectively. The presence of these distinct peaks in the XRD spectrum indicates that the fibers possess crystalline regions. These crystalline features are crucial as they contribute to the structural integrity and mechanical properties of the fibers. Sharp peaks typically signify well-ordered crystalline regions while broad peaks may indicate areas with a more amorphous nature. The crystalline regions within the fibers can impact their performance in various applications, particularly in composite materials where crystallinity can affect factors such as tensile strength, thermal stability and overall durability. Thus, understanding the crystalline structure through XRD analysis provides valuable insights into the material properties of the untreated petiole fibers.

Conclusion

This chapter presents an in-depth analysis of the mechanical, physical, and thermal characteristics of various date palm fiber and particle composites. Composites with short date palm fibers in an

epoxy matrix demonstrated a significant improvement in flexural modulus compared to the unreinforced matrix, with an optimal 10% ER fiber content yielding the highest elastic modulus, an increase of 31%. While fiber contents of 5% and 7% also enhanced the elastic modulus, they caused a slight decrease in maximum stress. Beyond 10% ER, however, both the elastic modulus and maximum stress decreased due to the added rigidity from high fiber content, which, while increasing resistance to deformation, also introduced weak points that could lower fracture strength. Therefore, fiber content selection should be tailored to each application's specific requirements, as these composites also show advantageous thermal conductivity. For instance, the 10% ER composite exhibits notable stiffness, strong interlayer adhesion, and impressive thermal insulation at 0.2 W/m K. Likewise, PVA composites with short date palm fibers showed improved flexural modulus compared to the unreinforced matrix; however, fiber contents exceeding 17% Pt resulted in reduced elastic modulus and maximum stress. High Pt fiber content, though beneficial for certain applications, can make the material somewhat brittle, with decreased fracture toughness due to added weak points. Despite this, the 17% Pt core provides exceptional thermal insulation, with a thermal conductivity of 0.11-0.12 W/(m K), a thermal diffusivity of 0.096-0.109 mm²/s, and a low density of 0.3002 g/cm³, highlighting its suitability for applications prioritizing thermal performance.

Chapter V Experimental investigation of Sandwich Structures for thermal insulation purpose

Chapter V: Experimental investigation of sandwich structure for thermal insulation purpose

Introduction

The implementation of sandwich panels is a well-established technique that has been utilized across various industries for a significant period. These structures are renowned for their lightweight nature and advantageous properties, such as thermal and acoustic insulation, impact resistance, and fatigue resistance. These properties are closely linked to the selection of materials for the skins and core, as well as the quality of their interfaces. Incorporating plant materials in the production of these sandwich panels presents considerable environmental benefits.

This chapter of the thesis is dedicated to the preparation of sandwich structures using the materials discussed in the previous chapters. Specifically, it focuses on the development and characterization of sandwich structures featuring a petiole agglomerate, type (Pt17) in the core and the skins made from a bio-composite, type (ER10).

In this chapter we present the materials and experimental techniques considered in our work, which consists of studying sandwiches, developed at the Department of Mechanical Engineering at Biskra University.

This chapter aims to explore the feasibility of creating a sandwich composite using date palm materials that exhibit desirable mechanical and thermal properties. Various types of sandwich plates have been developed, incorporating petiole agglomerate and rachis fibers from the date palm. The mechanical characteristics of these composites will be assessed through three-point bending tests. Additionally, the fracture surfaces resulting from these tests will be analyzed to understand the nature of the damage. The thermal conductivity of these composites will also be evaluated to determine their effectiveness in thermal insulation applications.

V.1. Sandwich components

These sandwich panels are composed of the petiole agglomerate type (Pt17) in the core and the bio-composite type (ER10) in the skins.

V.1.1 Skin (Bio-composite ER10)

The skins used in the preparation of the sandwich structures are meticulously crafted from bio-composite based on an epoxy resin reinforced with rachis fibers. Specifically, the composition includes an epoxy resin combined with rachis fibers at a mass fraction of 10% dense fibers (referred to as ER10). This composition was selected based on its demonstrated mechanical properties and compatibility with the core materials, as discussed in Chapter III. The inclusion of rachis fibers within the epoxy matrix provides enhanced stiffness and strength to the skins, making them suitable for the intended application in sandwich structures. To provide a visual representation, Figure 1 showcases a composite mat plate labeled ER10, which illustrates the distribution and integration of rachis fibers within the epoxy matrix. This careful selection and preparation of the skins are crucial for ensuring the overall performance and durability of the sandwich composite structures being developed in this study.

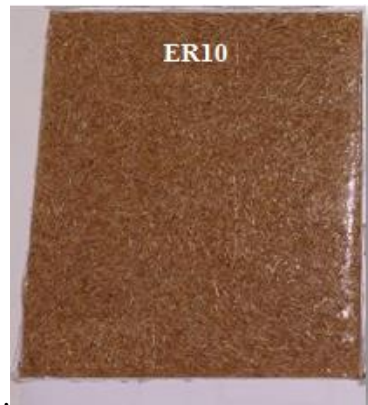


Fig V. 1 Bio-composite ER10 used as a skin in the sandwich

Table (V.1) presents the proprieties of bio-composite ER10 obtained in the chapter III.

Table V. 1 proprieties of bio-composite ER10

Bio-composite	E_f (MPa)	σ_{max} (Mpa)	λ (W/m.°K)	HB (kgf.mm ⁻²)	Density(Kg/m ³)
ER10	3385±89.16	46.46±2.59	0.2110 ± 10 ⁻³	13	1105

V.1.2 Core (Petiole agglomerate Pt17)

The core used in the preparation of the sandwich structures is meticulously crafted from bio-composite based on a resin epoxy (white glue (PVA)) reinforced with a petiole particle of (0-1)mm in the size. Specifically, this bio-composite includes a PVA matrix combined with petiole particle at a mass fraction of 17%, referred to as Pt17. The process of developing and studying the composites with petiole particles (Pt17) is thoroughly described in Chapter III. Figure 2 presents the various materials utilized as cores in the sandwich structures, showcasing the different configurations and compositions employed.

The mechanical characteristics of these core materials, including their stiffness, strength, and overall performance, are detailed to provide a comprehensive understanding of their suitability for use in sandwich composites. The selection of petiole particles as core materials is based on their lightweight nature and favorable mechanical properties, essential for enhancing the performance and efficiency of the developed sandwich structures. The combination of the PVA matrix with petiole agglomerate aims to optimize the core's mechanical properties, ensuring that the final sandwich structure can withstand various stresses and maintain structural integrity in its intended applications.



Fig V. 2 Petiole agglomerate Pt17 used as a cores in the sandwich

Table V. 2 Properties of bio-composite ER10

Petiole agglomerate	E_f (MPa)	σ_{max} (Mpa)	λ (W/m.°K)	E_{CT} (MPa)	E_{CL} (MPa)
Pt17	429.30 ±4.04	2.01±0.09	0.113 ±10 ⁻⁴	0.649±0.005	0.512±0.040

V.1.3. Sandwich preparation [petiole agglomerate (Pt17)/Rachis fibers -epoxy resin (ER10)]

After the preparation of the core of the petiole agglomerate. The implementation of the sandwiches is carried out at the technical hall of the mechanical engineering department at the University of Biskra by the gluing method. This study is carried out a sandwich defined by two skins ER10 with 3mm thickness and a core in Pt17 with 20 mm thickness.

To prepare this type of sandwich (SP/R), we can follow these steps:

- Weigh 10g of the rachis fibers and 90g of epoxy resin and mixed the two components together. Fill the mold (150x130x3) mm³ with this resulting mixture to obtain the bio-composite ER10.
- Place the specimen of the Pt17 on this bio-composite ER10 to obtain the first skin, and then leave at room temperature for 24 hours just to dry, and then unmold the semi sandwich (sandwich with a single skin).
- Prepare another plate of the bio-composite ER10 to use as the second skin of the sandwich.
- Place the semi sandwich (the face without skin) on the previous plate to obtain the second skin and also leave it to dry.
- Finally unmold and cut the specimens to obtain the sandwich (S_{PR}).

These steps can be summarized in a protocol following in Figure (V.3).



Fig V. 3 Sandwich preparation protocol (SP/R)

Two types of sandwiches used in this work to perform three-point bending tests and thermal properties. They are presented in figure (V.4).

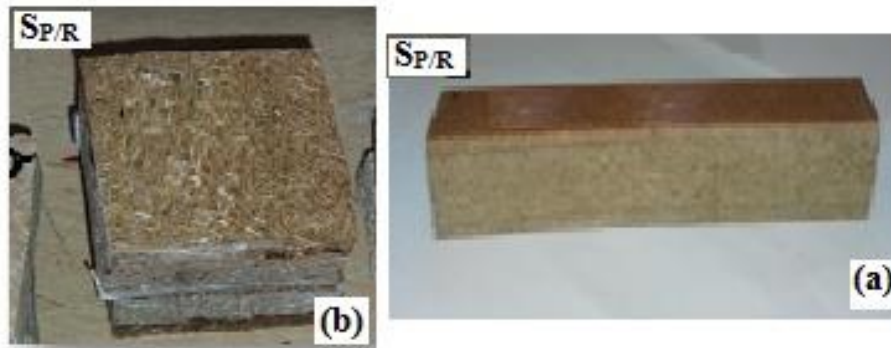


Fig V. 4 Sandwich specimen's types (a): SP/R to three points bending tests, (b): SP/R to Thermal properties tests

V.2. Experimental technique of sandwich structure (SP/R)

The tests performed in this part are mechanical and thermal properties; three-point bending tests to obtain the overall stiffness and thermal tests to obtain the thermal conductivity and thermal diffusivity.

V.2.1. Mechanical properties of sandwich (SP/R)

These tests determine the overall stiffness (D_G) in the sandwich (SP/R). We consider a sandwich with (B) in width, (L) in length, two identical skins with (t_f) in thickness and a core with (t_c) in thickness (Figure V.5).

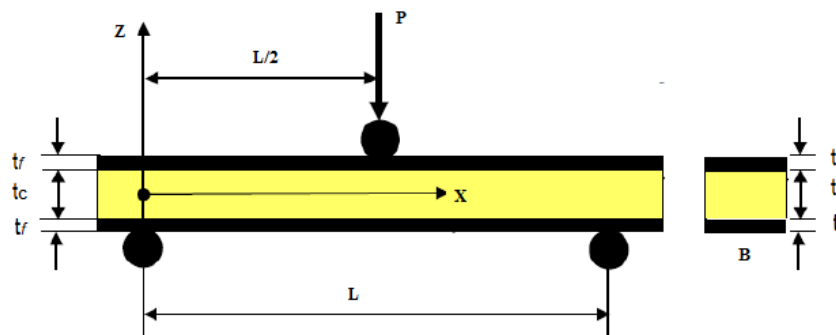


Fig V. 5 Geometric dimensions of a sandwich by three point bending

These tests were carried out on specimens according to standards ASTM C393- 62.1988 [6]. They were performed by applying the load (P) in perpendicular direction in the middle of the upper skin of the specimen. It was placed on two supports with 80 mm of distance Figure (V.6).

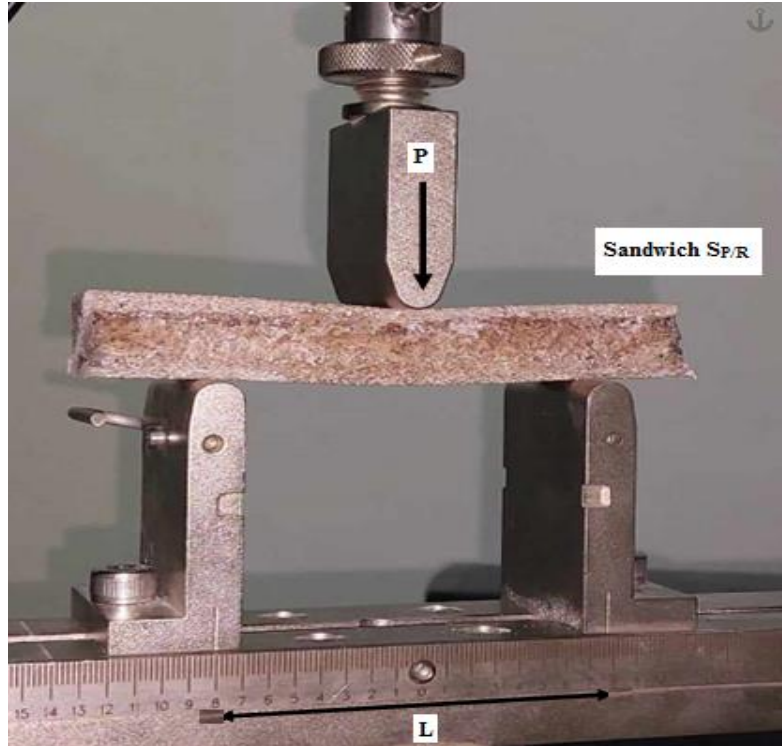


Fig V. 6 Three-point bending test of Sandwich SP/R

Overall stiffness is calculated from a linear part of a curve load (P) – deflection (δ). Elastic deflection can be expressed by the following:

$$\delta = \delta_f + \delta_s \quad (\text{V.1})$$

$$\delta = \frac{PL^3}{48D} + \frac{PL}{4S} \quad (\text{V.2})$$

$$\delta = \left[\frac{L^3}{48D} + \frac{L}{4S} \right] \cdot P \quad (\text{V.3})$$

$$\delta = [F_G] \cdot P \text{ or } P = [D_G] \cdot \delta \quad (\text{V.4})$$

$$D_G = \frac{1}{F_G} \quad (\text{V.5})$$

Where **D** is the flexural stiffness, **S** is the shear stiffness.

With D_G (Overall stiffness) is a slope of the linear part of the curve. This formula is valid only for the beginning of bending tests when the deflection is relatively small. Three specimens of sandwich ($S_{P/R}$) used to determine the overall stiffness (D_G).

V.2.2. Thermal properties of sandwich ($S_{P/R}$)

The thermal properties of sandwich samples, each with dimensions of (40x40x20) mm³, were systematically measured using the HOT Disk TPS 500 shown in Figure (V.7), a specialized thermal characterization device.

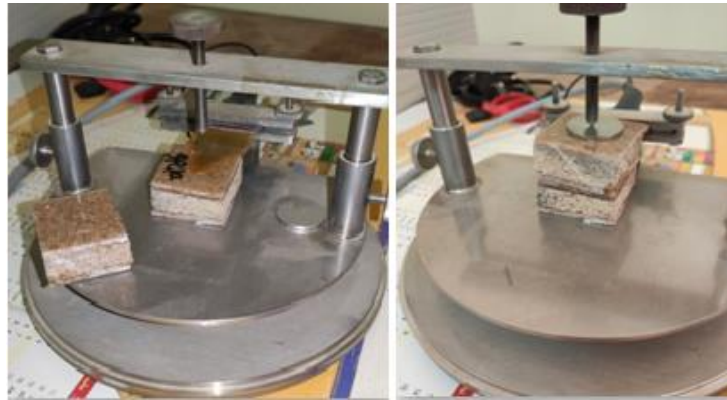


Fig V. 7 Experimental Analysis of Thermal Properties Sandwich $S_{P/R}$

This device, equipped with a temperature probe capable of reaching a maximum of 60°C, enabled precise assessment of the samples under controlled conditions. The measurements were conducted in an environment maintained at 28°C with 20% relative humidity, ensuring consistent conditions for reliable data collection. The study focused on three key thermal properties:

Thermal conductivity, thermal diffusivity, and specific heat. These properties were observed to vary depending on the molding method applied to the samples, highlighting the influence of manufacturing techniques on the thermal performance of the material. By analyzing how these properties change with different molding processes, the research provided valuable insights into optimizing thermal behavior in engineered sandwich structure.

V.3. Results and discussion

V.3.1. Results of Mechanical properties of sandwich ($S_{P/R}$)

The results of the three-point bending tests on three sandwiches $S_{P/R}$ (1) beams made from are illustrated through load-deflection curves (Figure.V.8).

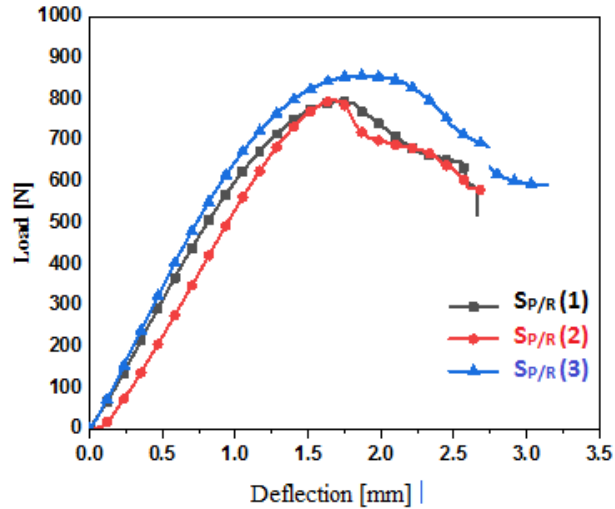


Fig V. 8 Load-deflection curves of Sandwiches SP/R during three-point bending test

These curves depict the relationship between the applied load and the deflection. Across of three sandwich (SP/R) tested, the three-point bending behavior consistently exhibits three main phases: an initial linear increase in applied load with deflection, followed by a nonlinear phase leading up to the maximum load, and finally, a sharp decline in load until the specimen fails. In the linear part of the curve, the overall stiffness (DG) is determined by calculating the slope of the load-deflection curve (as defined by Formula V.4).

The experimental values of overall stiffness (DG) in N/mm and the maximum load for each sandwich structure are summarized in Table (V.1), derived from the load-deflection data.

The load-displacement graph shows the rigidity performance of three specimens (SP1, SP2, and SP3) tested under similar conditions. SP3 demonstrates the highest rigidity, with a peak load between 850-900 N and a displacement of about 2.5 mm at failure, indicating that it can bear the greatest load before breaking. SP1 follows closely, with a peak load around 800 N and a similar displacement at failure, suggesting it also has strong rigidity but slightly less load-bearing capacity compared to SP3. On the other hand, SP2 shows the lowest performance, with a peak load of approximately 750 N and a higher displacement at failure (around 2.7 mm), implying that it has a lower stiffness and greater flexibility. This suggests that SP3 has the best structural integrity, while SP2 is softer and more prone to deformation under load.

Table V. 3 Overall stiffness values of sandwich SP/R by three point bending test

Sandwich SP/R	Width B [mm]	Thickness (tc+2tf) [mm]	Length L [mm]	Overall stiffness D_G [MPa]
SP/R (1)	20,65	20,7	80	794.37
SP/R (2)	19,63	20,56	80	797.91
SP/R (3)	20,3	19.34	80	857.38
D_G (average)				816,56 ±27,21

It is observed that the overall stiffness of SP/R (petiole agglomerate Pt17 in the core and bio-composite ER10 in the skins) is 816,56 MPa, which is higher than the toughness of another sandwich (cork agglomerate/glass fiber - polyester resin) (290.70 MPa) which has been studied in other studies [151].

Djemai et al. 2022[88] also studied the D_G of several types of sandwiches (SP₀₁, S_{CA} and S_{RP}).

Comparing the D_G value obtained in our work with the results obtained by Djemai et al. 2022[88], we note

Almost the same value of the manufactured material S_{P01} with: 818.90 MPa and its value was greater than the value of the S_{CA} material with: 106.73 MPa and the value of the S_{RP} material with: 569.11 MPa.

Thus, we can say that the S_{P/R} biomaterial has a specific hardness and can be used in several fields, taking into account its thermal aspect.

V.3.2. Thermal properties

The thermal properties of date palm core sandwich structures demonstrate their effectiveness as insulators; this low thermal conductivity makes date palm-based sandwiches particularly well-suited for insulation applications. This table Table V. 4 shows the thermal properties of three sandwich samples selected for this study. These materials significantly outperform traditional natural insulators such as coconut, flax, wood fiber, and cork, whose conductivities typically range between 0.42 and 0.87 W/m³K. Overall, these results confirm the

effectiveness of date palm waste as high insulators, comparable to or superior to other natural materials commonly used for thermal insulation.

Table V. 5 Thermal properties of new sandwich-structured composite

Sandwich	Thermal conductivity [W/m.°K]	Thermal Diffusivity [mm/s ²]
SP/R 1	0,15	0,128
SP/R 2	0,15	0,115
SP/R 3	0,149	0,114
Average	0,1497±5,77E-04	0,119±7,81E-03

Fig V. 9 Thermal properties of sandwich structure beam specimens bio-composite

V.4. Thermal Evaluation, Application in Solar Flat collector

In this part, we compared the thermal resistivity of the different sandwich materials with that of the new material we developed. The thermal characteristics of this new material were then used to calculate the thermal performance of solar collectors for drying applications. We initiated with a comparative analysis between two different types of solar Flat plate collectors FPCs, differentiated by their rear insulation materials

For the calculation of the thermal performances of FPCs, we used the calculation code developed by Labeled [154].

V.4.1. Theoretical analysis

V.4.1.1. Thermal resistance of sandwiches

Sandwich panels are primarily composed of two main parts: the skins and the core. The structure and components of these panels are illustrated in the following figure. For sandwich panels made of three similar or different materials, the equivalent thermal conductivity is determined by considering the thermal resistance of each material. This resistance is defined by two key properties: the thickness of the material e (mm) measured in millimeters and its thermal conductivity λ (W/m K).

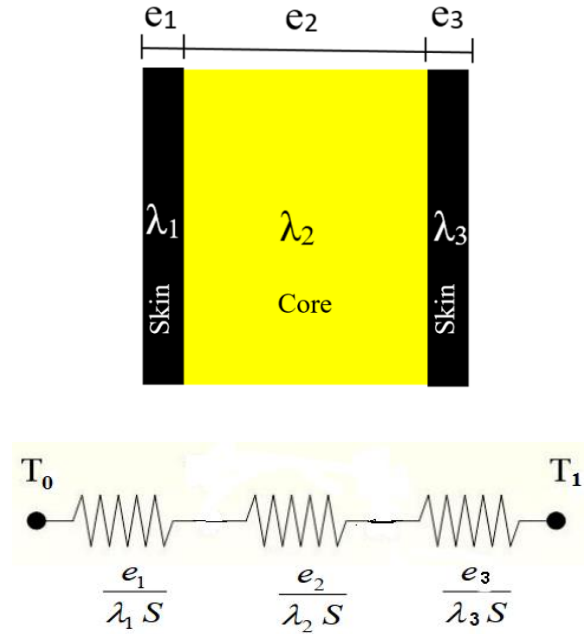


Fig V. 10 Equivalent Electrical Model of Thermal Resistance in Composite Walls

With

$$R_{tot} = \frac{e_1}{\lambda_1} + \frac{e_2}{\lambda_2} + \frac{e_3}{\lambda_3} = R_{Core} + 2R_{skin} \quad (V.1)$$

$\frac{e_1}{\lambda_1}$ The resistance belonging to the first skin material (e_1, λ_1)

$\frac{e_2}{\lambda_2}$ The resistance belonging to the core material (e_2, λ_2)

$\frac{e_3}{\lambda_3}$ The resistance belonging to the second skin material (e_3, λ_3)

V. 4.1.2 Comparison of Thermal Resistance of different Sandwiches

In order to compare our best-developed sandwich composite material with different industrial materials, we presented in Figure V.11 the calculated values of thermal resistivity of different sandwich materials in Table V.5. These sandwiches are presented and numbered in Table V.6.

Table V. 6 Materials Composing the Sandwiches and Their Thermal Conductivity

Skin	Conductivity $\lambda(\text{W/mK})$	Core	Conductivity $\lambda(\text{W/mK})$
Plywood	0.11	Petiole Pt17	0.113
Epoxy Resin	0.196	Raw wood of palm date (Djouidi)	0.123
Recycled Paper	0.021	Wood fiber/ ecovio	0.119
ER10	0.21	Polysterene	0.038

The materials used in the sandwiches include those forming the skins and those creating the cores, as shown in the following table.

Table V. 6 Different material combinations used for comparison

Sandwich	Sandwich 1	Sandwich 2	Sandwich 3	Sandwich 4	Sandwich 5	Sandwich 6	Sandwich7 Calculated SP3	Sandwich7 Measured SP3
Core	Raw wood of palm date Djouidi	Pt17	Wood fibre	Polystyrene	Pt17	Pt 17	Pt17	Pt17
Skin	Epoxy Resin	Epoxy resin	Plywood	Plywood	Plywood	Recycled paper	ER10	ER10

It seems from Fig.10, that the composite material Pt17 present presents a good choice for thermal insulation when sandwiched between recycled papers. It is also seen that the calculated resistivity of our new sandwich (S7C) is higher than that of the measured resistivity S7M. Anyway, we can say that the values of the thermal resistance of our new sandwich are very acceptable to be used as insulating materials; on the other hand the core made of petiole can be

sandwiched between other materials such as recycled paper to give a better thermal resistivity if the application does not involve humidity.

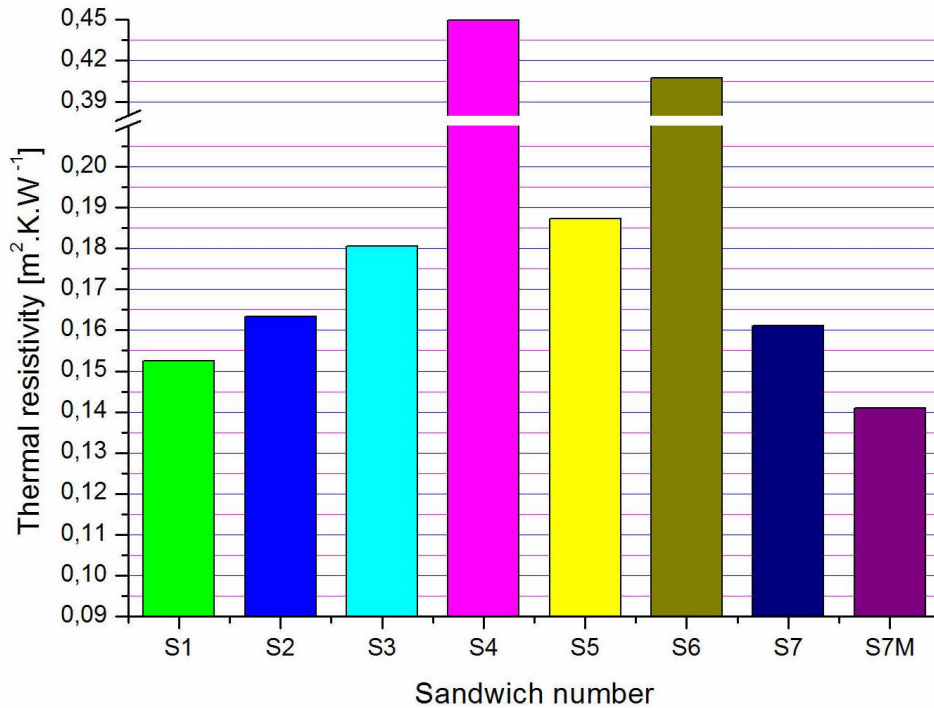


Fig V. 11 Comparison between the Thermal Resistance of our new sandwich with different Sandwich materials

V.4.2. Application in Solar Flat plate collectors (FPCs)

To evaluate the thermal performances of our new composite, we integrated this composite material in FPC as rear insulation and compared it to conventional FPC equipped with a polystyrene sheet in the rear insulation. Both studied collectors are equipped with diverging channel ducts for the air outlet and inlet cross sections, allowing the airflow to be adjusted.

V.4.2.1. Presentation of FPCs Models

The dimensions of the collector components are as follows: a single glass cover with a thickness of 5 mm, an air gap of 25 mm between the cover and the absorber plate, and an air duct

height of 25 mm. The absorber measures 1.96 m × 0.9 m with a thickness of 0.4 mm, while the rear insulation has a thickness of 30 mm.

Both solar air heaters are constructed using identical materials, except for the insulation. The absorbers are made from galvanized steel coated with a non-selective black finish to enhance heat absorption. Heated air flows between the inner surface of the absorber plate and the back plate. The rear insulation consists of a 20 mm thick polystyrene or bio-composite sheet, sandwiched between two plywood sheets, each 5 mm thick.

As shown in Figure 12, the FPC with polystyrene insulation and plywood sheets (model A) features an absorber plate positioned behind the transparent glass cover, separated by a static air layer to improve thermal efficiency.

In the second flat plate FPC (model B), the rear and lateral insulation is provided by composite material (Pt 17).

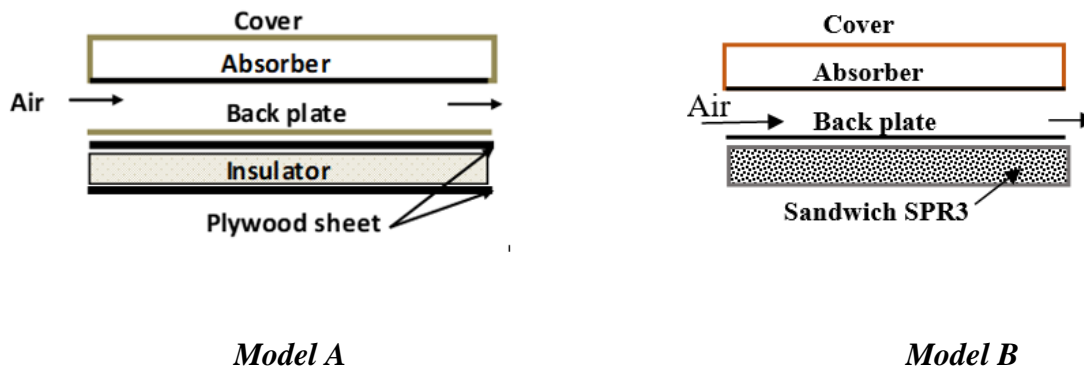


Fig V. 12 Schematic view of FPC models

V.4.4.2. Theoretical analysis

Before the presentation of the proposed configurations in the previous section, we present the expressions used for the calculation of global heat loss, useful energy and efficiency of the solar collectors:

The useful energy gain had been established [155] as below:

$$Q_u = mc_p(T_{fo} - T_{fi}) \quad (V.2)$$

And the following heat balance expresses the thermal performance of a collector under steady-state condition

$$Q_u = A_C F_R [I_G (\tau_v \alpha_{abs}) - U_L (T_{fi} - T_a)] \quad (V.3)$$

A measure of collector performance is the collector efficiency, defined as the ratio of useful heat gain over any time period to the incident solar radiation over the same period, we can define efficiency as,

$$\eta = \frac{Q_u}{I_G A_C} \quad (V.4)$$

Solving Eqs. (2) - (4), and η can be obtained as:

$$\eta = \frac{mc_p(T_{fo} - T_{fi})}{I_G A_C} \quad (V.5)$$

The collector efficiency can also be related to the inlet fluid temperature using Eq. (6).

$$\eta = F_R \left[(\tau_v \alpha_{abs}) - U_L \frac{(T_{fi} - T_a)}{I_G} \right] \quad (V.6)$$

Here, $F_R (\tau_v \alpha_{abs})$ and $F_R U_L$ are two major parameters that constitute the simplest practical collector model. $F_R (\tau_v \alpha_{abs})$ is an indication of how energy is absorbed and $F_R U_L$ is an indication of how energy is lost. Besides, U_L is the collector overall heat loss coefficient. The thermal energy lost from the collector to the surroundings by conduction, convection and infrared radiation. U_L is equal to the sum of energy loss through the top (U_t), bottom (U_b) and edge (U_e) of the collectors given below [156].

$$U_L = U_t + U_b + U_e \quad (7)$$

To make a simple, direct and very clear comparison, a standard test procedure ASHRAE 93-2003 has been adopted. The general test procedure is to operate the collector in the test facility under nearly study conditions, measure I_G , T_i and T_o which are needed for the analysis method, this means outdoor tests are done in midday hours on clear days when the beam radiation nearly normal to the collector. Thus the transmittance-absorptance product for this test conditions is approximately the normal incidence value and is written as $\tau_v \alpha_{abs}$ [155].

V.4.2.3. Thermal Performances Evaluation of FPCs

The outlet air temperature of the flat plate collector (FPC) is a key indicator for assessing the collector's performance and predicting its efficiency. This parameter also significantly influences the effectiveness of the drying process. In this study, calculations were performed to estimate the outlet temperatures of two FPC models, as shown in Figure 13. The results indicate that the FPC with polystyrene insulation (model A) achieves the highest outlet temperature. However, the difference between the temperatures produced by both solar FPCs is minimal. Notably, the outlet temperature provided by the FPC using composite materials (model B) across a wide range of air flow rates (40–55°C) is sufficient to meet the energy requirements for drying applications.

The efficiency (η) of the FPCs was also analyzed as a function of air flow rate, as depicted in Figure V.14. The thermal performance improvements are significant for both models. For the FPC with polystyrene and plywood (model A), the efficiency reaches 50% at a mass flow rate of 80 m³/h. Similarly, the FPC with composite material (model B) achieves an efficiency of 45% at the same flow rate.

The analysis reveals that the efficiency of both models increases with higher air mass flow rates. While model A exhibits slightly better efficiency compared to model B, the difference is marginal, particularly for applications like drying and heating that do not demand high-performance specifications.

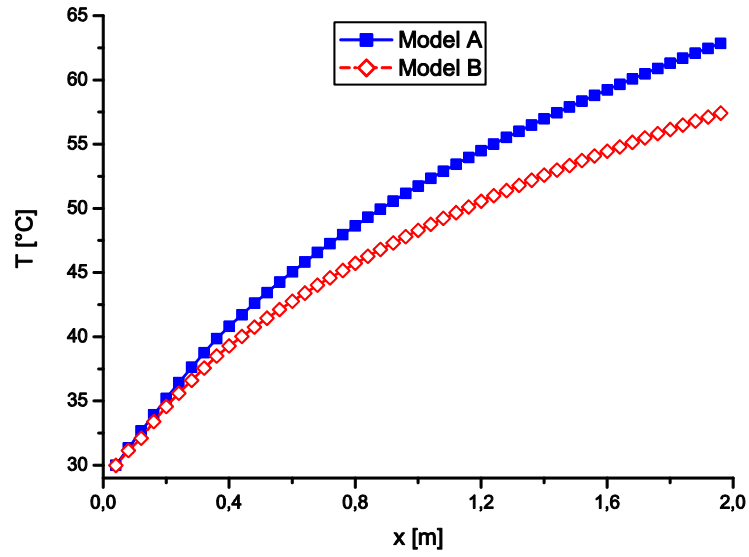


Fig V. 13 Variation of the air outlet Températures Vs. FPCs length

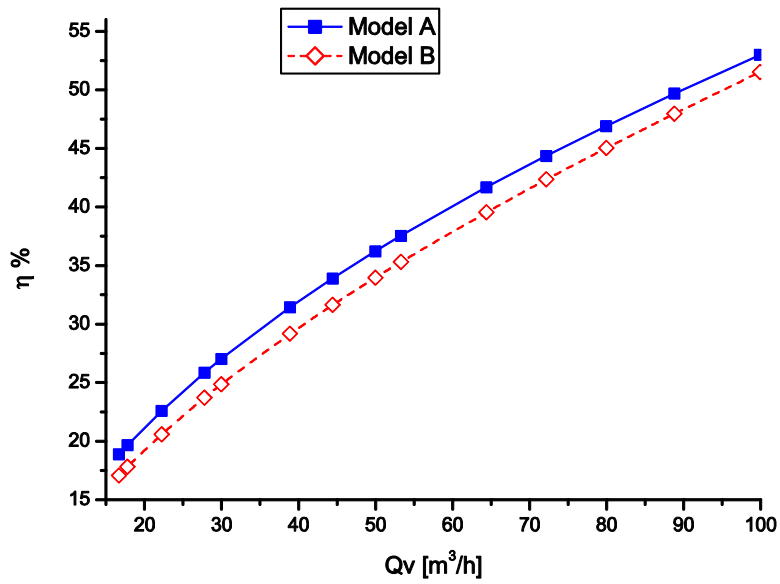


Fig V. 14 Variation of the FPCs efficiencies Vs. the air flow rate, Q_v

Conclusion

In this chapter, a mechanical characterization was carried out using a three-point bending test on sandwich structures, along with an analysis of their thermal conductivity. This process required the development of specific fabrication methods for these sandwich structures, which were based on materials derived from date palm fronds.

The various types of sandwich structures were prepared using the same skins (EFR10) and cores (Pt 17) but with different manufacturing techniques. The load-displacement curves obtained from the three-point bending tests allowed for the calculation of the global stiffness (DG) for each sandwich type. The sandwich structure with the core (SP3) exhibited the highest global stiffness compared to the others. The structures produced using a direct bonding method without adhesive demonstrated higher overall stiffness compared to those manufactured through direct molding.

In terms of thermal conductivity, we can say that the values of the thermal resistance of our new sandwich are very acceptable to be used as insulating materials; on the other hand the core made of petiole can be sandwiched between other materials such as recycled paper to give a better thermal resistivity if the application does not involve humidity.

General Conclusion

General Conclusion

In conclusion,

In this work, we have focused on one of the largest deposits of abandoned wood in the Middle East and North Africa, and Algeria in particular; it is the waste of date palms.

Date palm groves produce vast quantities of dry fronds annually, which are typically discarded. The ability to repurpose this biomass without the need for replanting makes it a highly sustainable and ecologically sound choice. Since this product is renewed annually and does not need to be replanted. This gives the ability to repurpose this biomass without the need for replanting makes it a highly sustainable and ecologically sound choice.

In this doctoral thesis, we demonstrated the significant potential of date palm waste, particularly fibers from mature palms, as a renewable and sustainable resource for bio-composite materials, offering a compelling alternative to conventional wood-based products.

Experimental investigations carried out in the first phase of this research, focused on the characterization of the physical and chemical properties of date palm fibers, specifically petiole and rachis. This included analyses of fiber volume, lignin content, chemical composition, thermal behavior and density, providing a comprehensive understanding of the raw materials. This initial assessment revealed considerable variability in the properties of date palm fibers, a factor attributed to species diversity and variations within the same palm.

Two types of composites were developed and analyzed in the 2nd phase: epoxy/rachis fiber (ER%) composites for the skin and petiole/PVA fiber (Pt%) composites for the core. The mechanical and morphological properties were examined across different fiber sizes and mass fractions, revealing that higher fiber content increased rigidity and modulus, although with a slight decrease in fracture resistance. These findings underscore the importance of balancing fiber content to optimize mechanical performance. Furthermore, the exploitation of these bio-composites in sandwich structures, with composite skins made of rachis fiber/epoxy and a petiole/PVA as core, is presented. Three-point bending tests demonstrated the mechanical viability of these sandwich structures, showing that the Pt17% composite core with ER10% skins offered substantial stiffness, strong interlayer adhesion, and excellent thermal insulation properties (0.2 W/m·K).

General Conclusion

Comprehensive testing showed that the Pt17% core exhibited outstanding insulation (thermal conductivity of 0.11–0.12 W/(m·K), thermal diffusivity of 0.096–0.109 mm²/s) and low density (0.3002 g/cm³), making it ideal for lightweight applications. Moreover, the ER10% composite skin achieved a flexural modulus of 3.21 GPa, bending strength of 9.28 MPa, and thermal conductivity of 0.21 W/(m·K), with a thermal diffusivity of 0.17 mm²/s, confirming its effectiveness as a thermally insulating, ductile, and durable surface material.

As application, a comparative investigation between the thermal performances of two solar flat plate collectors (FPCs), distinguished by their rear insulation material, with the aim of valorizing our novel local date waste bio-material is presented for solar drying tests. The first FPC (Model A) utilized conventional insulation materials which are a polystyrene sheet sandwiched between two plywood sheets, and the second FPC is equipped with our new bio-composite sandwich material. It's noteworthy that the efficiencies of the conventional FPC (Model A) exhibit a slight superiority when compared to the new FPC featuring bio-composite insulation material (Model B). However, it should be noted that, the values of the thermal resistance of our new sandwich are very acceptable to be used as insulating materials; on the other hand the core made of petiole can be sandwiched between other materials such as recycled paper to give a better thermal resistivity if the application does not involve humidity. These findings underscore the importance of carefully considering the impact of various parameters, such as mass flow rate and insulation material, in optimizing the performance of solar air heaters for efficient and successful energy conversion.

Overall, these results highlight the feasibility of using date palm fibers in the bio-composites industry, supporting the development of innovative, low-cost, eco-friendly materials with minimal environmental impact. By converting agricultural waste into high-performance composite structures, this study provides a valuable foundation for future research and industrial applications in fields requiring sustainable, thermally efficient materials.

References

1. Barreca, F., Cardinali, G., Barbaresi, A., Bovo, M.: Bio-based building components: A newly sustainable solution for traditional walls made of *Arundo donax* and gypsum. *Heat Transfer*. 52, 5166–5183 (2023). <https://doi.org/10.1002/htj.22921>
2. Raja, P., Murugan, V., Ravichandran, S., Behera, L., Mensah, R.A., Mani, S., Kasi, A.K., Balasubramanian, K.B.N., Sas, G., Vahabi, H., Das, O.: A Review of Sustainable Bio-Based Insulation Materials for Energy-Efficient Buildings. *Macromolecular Materials and Engineering*. 308, 1–11 (2023). <https://doi.org/10.1002/mame.202300086>
3. DJEBLOUN, Y.: Contribution à la caractérisation des matériaux composites renforcés de fibres végétales, PhD Thesis', university of biskra. (2018)
4. Djoudi, T.: Elaboration et caractérisation de composites bio-sourcés à base de fibres de palmier dattier ,PhD Thesis', university of biskra, <http://archives.univ-biskra.dz:80/handle/123456789/24690>, (2019)
5. Djemai, H.: Génie Mécanique Contribution à l' étude de l' endommagement dans les matériaux composites sandwiches .PhD Thesis', university of biskra. (2017)
6. Harb, N., Dilmi, H., Bezzazi, B., Hamitouche, K.: Effect of Alternating Hybridisation of Fibres on the Physico - Mechanical Behaviour of Composite Materials. *Civil and Environmental Engineering*. 19, 406–413 (2023). <https://doi.org/10.2478/cee-2023-0036>
7. Kumar, K.M., Naik, V., Kaup, V., Waddar, S., Santhosh, N., Harish, H. V: Review Article Nontraditional Natural Filler-Based Biocomposites for Sustainable Structures. (2023). <https://doi.org/10.1155/2023/8838766>
8. Kurniawati Dwi, Aprilian Pratama, J.I.K.G.: *Ac Ac Ac Ac*. *Power*. 1, 2012 (2014)
9. Zhang, Z., Mu, Z., Wang, Y., Song, W., Yu, H., Zhang, S., Li, Y., Niu, S., Han, Z., Ren, L.: Lightweight Structural Biomaterials with Excellent Mechanical Performance: A Review. *Biomimetics*. 8, (2023). <https://doi.org/10.3390/biomimetics8020153>
10. Nagavally, R.R.: Composite Materials - History, Types, Fabrication Techniques, Advantages, and Applications. *Proceedings of 29th IRF International Conference*. 25–30 (2016)
11. Boudjma, H.L.: Elaboration de matériaux composites biodégradables issus de ressources renouvelables. *Université d'Oran 2 (Algérie)*. 163 (2016)
12. Paul, R., Dai, L.: Interfacial aspects of carbon composites. *Composite Interfaces*. 25, 539–605 (2018). <https://doi.org/10.1080/09276440.2018.1439632>
13. Yu, W., Jiang, L.: Application of Carbon Fiber Reinforced Aluminum Matrix Composites in Automotive Industry. *International Journal of Automotive Manufacturing and Materials*. 3 (2024). <https://doi.org/10.53941/ijamm.2024.100009>

14. Walkowiak, M., Reinicke, U., Anders, D.: Numerical Investigation of Different Core Topologies in Sandwich-Structured Composites Subjected to Air-Blast Impact. *Applied Sciences (Switzerland)*. 12, (2022). <https://doi.org/10.3390/app12189012>
15. Khoshgoftar, M.J., Barkhordari, A., Limuti, M., Buccino, F., Vergani, L., Mirzaali, M.J.: Bending analysis of sandwich panel composite with a re-entrant lattice core using zig-zag theory. *Scientific Reports*. 12, 1–12 (2022). <https://doi.org/10.1038/s41598-022-19930-x>
16. Mukherjee, G.S., Jain, A., Banerjee, M.: Engineering Matrix Materials for Composites: Their Variety, Scope and Applications. *Fine Chemical Engineering*. 4, 13–45 (2023). <https://doi.org/10.37256/fce.4120232128>
17. Drahansky, M., Paridah, M., Moradbak, A., Mohamed, A., Owolabi, F., Abdulwahab taiwo, Asniza, M., Abdul Khalid, S.H.: We are IntechOpen , the world ' s leading publisher of Open Access books Built by scientists , for scientists TOP 1 %. *Intech. i*, 13 (2016). <https://doi.org/http://dx.doi.org/10.5772/57353>
18. Majewski, M.: Micromechanical and numerical analysis of shape and packing effects in elastic-plastic particulate composites. (2022)
19. Kassim, M.T.E., Karash, E.T., Sultan, J.N.: A Mathematical Model for Non-Linear Structural Analysis Reinforced Beams of Composite Materials. *Mathematical Modelling of Engineering Problems*. 10, 311–333 (2023). <https://doi.org/10.18280/MMEP.100137>
20. Bhaskar, J., Kumar Sharma, A., Bhattacharya, B., Adhikari, S.: A review on shape memory alloy reinforced polymer composite materials and structures. *Smart Materials and Structures*. 29, 073001 (2020). <https://doi.org/10.1088/1361-665X/AB8836>
21. Hommel, P., Roth, D., Binz, H., Kreimeyer, M.: Implementation of a Design Guideline for Aluminum Foam Sandwich Based on Industrial Demands. *Proceedings of the Design Society*. 3, 2235–2244 (2023). <https://doi.org/10.1017/pds.2023.224>
22. Raad, H., Njim, E.K., Jweeg, M.J., Al-Waily, M.: Sandwiched Plate Vibration Analysis with Open and Closed Lattice. *Physics and Chemistry of Solid State*. 24, 312–322 (2023). <https://doi.org/10.15330/pcss.24.2.312-322>
23. Ferjan, Š., Jovičić, M., Lardiés Miazza, N., Ligthart, T., Harvey, C., Fita, S., Mehta, R., Samani, P.: Sustainability Assessment of the End-of-Life Technologies for Biocomposite Waste in the Aviation Industry. *Polymers*. 15, (2023). <https://doi.org/10.3390/polym15122689>
24. Hegazi, H.A., Mokhtar, A.H.: Optimum Design of Hexagonal Cellular Structures Under Thermal and Mechanical Loads. *International Journal of Engineering Research & Technology*. 9, 1151–1159 (2020)
25. Morgan, A.B., Toubia, E.: Cone calorimeter and room corner fire testing of balsa wood core/phenolic composite skin sandwich panels. *Journal of Fire Sciences*. 32, 328–345 (2014). <https://doi.org/10.1177/0734904113514944>
26. Kermani, N.N., Simacek, P., Advani, S.G.: Porosity predictions during co-cure of honeycomb core prepreg sandwich structures. *Composites Part A: Applied Science and Manufacturing*. 132, 105824 (2020).

- <https://doi.org/10.1016/J.COMPOSITESA.2020.105824>
27. Chemami, A.: *Etude de la Performance des Matériaux Composites Sandwichs - Application en Fatigue*, PhD Thesis', university of Annaba, (2012)
 28. Zeggai, F. Z., Touahra, F., Labied, R., Lerari, D., Chebout, R., & Bachari, K.: *Biopolymers-Clay Nanocomposites: Synthesis Pathways, Properties, and Applications*. *Intech*. 8, 13 (2017)
 29. Abanto, S.: *D éveloppement d ' un matériau composite à base de bois laminé avec alliage d ' aluminium* Développement d ' un matériau composite à base de bois laminé avec alliage d ' aluminium, PhD Thesis', university of Canada. (2018)
 30. Access, O., Url, P., Boukhili, R.: *Titre: Comportement sous choc des composites sandwichs et influence*. (2010)
 31. Samy, M., Bekbayeva, L., Mohammed, A.M., Irmukhametova, G., Zhetpisbay, D., Majeed, N.M., Yermukhambetova, B.B., Mun, G.A.: *Overview of biodegradable polymers: synthesis, modification and application*. *Kompleksnoe Ispolzovanie Mineralnogo Syra = Complex Use of Mineral Resources*. 332, 19–31 (2025). <https://doi.org/10.31643/2025/6445.02>
 32. Yashas, Y.G., Ballupete Nagaraju, S., Puttegowda, M., Verma, A., Rangappa, S.M., Siengchin, S.: *Biopolymer-Based Composites: An Eco-Friendly Alternative from Agricultural Waste Biomass*. *Journal of Composites Science*. 7, (2023). <https://doi.org/10.3390/jcs7060242>
 33. Sreevidya, S., Yadav, S., Katre, Y., Singh, A.K., Rahdar, A.: *Chapter 3 Nanocomposites and their Applications*. (2023)
 34. Zorah, M., Mudhafar, M., Naser, H.A., Mustapa, I.R.: *the Promises of the Potential Uses of Polymer Biomaterials in Biomedical Applications and Their Challenges*. *International Journal of Applied Pharmaceutics*. 15, 27–36 (2023). <https://doi.org/10.22159/ijap.2023v15i4.48119>
 35. Chaouki, B., Abdelkader, K., Mouloud, A.: *Recent Advancement via Experimental Investigation of the Mechanical Characteristics of Sisal and Juncus Fibre-Reinforced Bio-Composites*. *Strojniski Vestnik/Journal of Mechanical Engineering*. 69, 339–351 (2023). <https://doi.org/10.5545/sv-jme.2022.456>
 36. Zamora-Mendoza, L., Gushque, F., Yanez, S., Jara, N., Álvarez-Barreto, J.F., Zamora-Ledezma, C., Dahoumane, S.A., Alexis, F.: *Plant Fibers as Composite Reinforcements for Biomedical Applications*. *Bioengineering*. 10, 1–23 (2023). <https://doi.org/10.3390/bioengineering10070804>
 37. Udhayakumar, A., Mayandi, K., Rajini, N., Devi, R.K., Muthukannan, M., Murali, M.: *Extraction and Characterization of Novel Natural Fiber from Cryptostegia Grandiflora as a Potential Reinforcement in Biocomposites*. *Journal of Natural Fibers*. 20, (2023). <https://doi.org/10.1080/15440478.2022.2159607>
 38. de M. de Lima, T.A., de Lima, G.G., Nugent, M.J.D.: *Natural Fibre-Reinforced Polymer Composites: Manufacturing and Biomedical Applications*. 25–63 (2022).

- https://doi.org/10.1007/978-3-030-70266-3_2
39. Parker, R.M., Parton, T.G., Chan, C.L.C., Bay, M.M., Frka-Petesic, B., Vignolini, S.: Bioinspired Photonic Materials from Cellulose: Fabrication, Optical Analysis, and Applications. *Accounts of Materials Research*. 4, 522–535 (2023). <https://doi.org/10.1021/accountsmr.3c00019>
 40. Kaushik, Y., Sooriyaperakasam, N., Rathee, U., Naik, N.: A Mini Review of Natural Cellulosic Fibers: Extraction, Treatment and Characterization Methods. *Journal of Computers, Mechanical and Management*. 2, 32–47 (2023). <https://doi.org/10.57159/gadl.jcmm.2.2.23057>
 41. Quelhas, A.R., Trindade, A.C.: Mimicking Natural-Colored Photonic Structures with Cellulose-Based Materials. *Crystals*. 13, 1–26 (2023). <https://doi.org/10.3390/cryst13071010>
 42. Teng, C. P., Tan, M. Y., Toh, J. P. W., Lim, Q. F., Wang, X., Ponsford, D., ... & Tee, S. Y. (2023). Advances in cellulose-based composites for energy applications. *Materials*, 16(10), 3856.: Energy Applications. (2023)
 43. Börcsök, Z., Pásztor, Z.: The role of lignin in wood working processes using elevated temperatures: an abbreviated literature survey. *European Journal of Wood and Wood Products*. 79, 511–526 (2021). <https://doi.org/10.1007/s00107-020-01637-3>
 44. Pesic, D.B.: Cellulose in Nature – Versatile Sources for Novel Applications: A Literature Review. *Undergraduate Research in Natural and Clinical Sciences and Technology Journal*. 5, (2021). <https://doi.org/10.26685/urncst.200>
 45. PAN, Huaizhi, ZHENG, Biao, YANG, Hui, et al. Effect of loblolly pine (pinus taeda l.) hemicellulose structure on the properties of hemicellulose-polyvinyl alcohol composite film. *Molecules*, 2022, vol. 28, no 1, p. 46.: Effect of Loblolly Pine (Pinus taeda L .) Hemicellulose Structure. (2023)
 46. Selig, M.J., Thygesen, L.G., Felby, C.: Correlating the ability of lignocellulosic polymers to constrain water with the potential to inhibit cellulose saccharification. *Biotechnology for Biofuels*. 7, 1–10 (2014). <https://doi.org/10.1186/s13068-014-0159-x>
 47. Riaz, M.W., Yousaf, M.I., Hussain, Q., Yasir, M., Sajjad, M., Shah, L.: Role of Lignin in Wheat Plant for the Enhancement of Resistance against Lodging and Biotic and Abiotic Stresses. *Stresses*. 3, 434–453 (2023). <https://doi.org/10.3390/stresses3020032>
 48. Towle, Z., Cruickshank, F., Mackay, C.L., Clarke, D.J., Horsfall, L.E.: Tracking the Chemical Diversity of Enzymatically Oxidised Lignin. 1–3 (2023)
 49. Ruwoldt, J., Blindheim, F.H., Chinga-Carrasco, G.: Functional surfaces, films, and coatings with lignin - a critical review. *RSC Advances*. 13, 12529–12553 (2023). <https://doi.org/10.1039/d2ra08179b>
 50. Lourenço, A., & Gominho, J.: Lignin as Feedstock for Nanoparticles Production. *Intech*. 11, 13 (2016)
 51. Fan, Z., Cheng, P., Chu, L., Han, J.: Exploring the Rheological and Structural

- Characteristics of Novel Pectin-Salecan Gels. *Polymers*. 14, 1–7 (2022).
<https://doi.org/10.3390/polym14214619>
52. McCarthy, T.W., Der, J.P., Honaas, L.A., dePamphilis, C.W., Anderson, C.T.: Phylogenetic analysis of pectin-related gene families in *Physcomitrella patens* and nine other plant species yields evolutionary insights into cell walls. *BMC Plant Biology*. 14, (2014). <https://doi.org/10.1186/1471-2229-14-79>
 53. Emran, T. Bin, Islam, F., Mitra, S., Paul, S., Nath, N., Khan, Z., Das, R., Chandran, D., Sharma, R., Lima, C.M.G., Awadh, A.A. Al, Almazni, I.A., Alhasaniah, A.H., Guiné, R.P.F.: Pectin: A Bioactive Food Polysaccharide with Cancer Preventive Potential. *Molecules*. 27, 1–21 (2022). <https://doi.org/10.3390/molecules27217405>
 54. Martínez-Sabando, J., Coin, F., Melillo, J.H., Goyanes, S., Cerveny, S.: A Review of Pectin-Based Material for Applications in Water Treatment. *Materials*. 16, (2023). <https://doi.org/10.3390/ma16062207>
 55. Cosentino, L., Fernandes, J., Mateus, R.: A Review of Natural Bio-Based Insulation Materials. *Energies*. 16, (2023). <https://doi.org/10.3390/en16124676>
 56. A. Shalwan, Talal Alajmi, Naser Alajmi: Study on sisal fibres as insulator in building materials: Review. *Global Journal of Engineering and Technology Advances*. 15, 124–140 (2023). <https://doi.org/10.30574/gjeta.2023.15.2.0101>
 57. Almusaed, A., Almssad, A., Alasadi, A., Yitmen, I., Al-Samaraee, S.: Assessing the Role and Efficiency of Thermal Insulation by the “BIO-GREEN PANEL” in Enhancing Sustainability in a Built Environment. *Sustainability (Switzerland)*. 15, (2023). <https://doi.org/10.3390/su151310418>
 58. Muñoz-Tebar, N., Viuda-Martos, M., Lorenzo, J.M., Fernandez-Lopez, J., Perez-Alvarez, J.A.: Strategies for the Valorization of Date Fruit and Its Co-Products: A New Ingredient in the Development of Value-Added Foods. *Foods*. 12, 1–19 (2023). <https://doi.org/10.3390/foods12071456>
 59. Jorjandi, F.K.: Evaluation of diversity in selected populations of Iranian date palm (*Phoenix dactylifera* L.) using ISSR markers. 1–17 (2023)
 60. DEBABECHE, K., BOUAFIA, A., BENCHEIKH, A.: Phenotypic diversity of date palm varieties (*Phoenix dactylifera* L.) from southwest Algeria estimated by fruit characteristics. *Acta agriculturae Slovenica*. 119, 1–10 (2023). <https://doi.org/10.14720/aas.2023.119.1.2611>
 61. Mehdi Shah, S.M., Abbas Naqvi, S., Jafar Jaskani, M., Mehdi Shah, I.: a Review on Phytochemicals and Pharmacological Chemicals of Date Palm (*Phoenix Dactylifera*). *Journal of Advance Research in Food, Agriculture and Environmental Science (ISSN: 2208-2417)*. 9, 8–25 (2023). <https://doi.org/10.53555/nnfaes.v9i8.1811>
 62. Boukhelouf, W., Si Bachir, A., Mezerdi, F., Ghazi, C., Saouache, Y.: Sap beetles (Nitidulidae) of date palms of the Deglet Nour variety in the Ziban region (Algeria): distribution patterns and effectiveness of date bunch bagging. *Agricultura Tropica et Subtropica*. 57, 12–22 (2024). <https://doi.org/10.2478/ats-2024-0002>

63. Faiad, A., Alsmari, M., Ahmed, M.M.Z., Bouazizi, M.L., Alzahrani, B., Alrobei, H.: Date Palm Tree Waste Recycling: Treatment and Processing for Potential Engineering Applications. *Sustainability (Switzerland)*. 14, (2022). <https://doi.org/10.3390/su14031134>
64. Vidal, J., Ponce, D., Mija, A., Rymarczyk, M., Castell, P.: Sustainable Composites from Nature to Construction: Hemp and Linseed Reinforced Biocomposites Based on Bio-Based Epoxy Resins. *Materials*. 16, (2023). <https://doi.org/10.3390/ma16031283>
65. Alsuwait, R.B., Souiyah, M., Momohjimoh, I., Ganiyu, S.A., Bakare, A.O.: Recent Development in the Processing, Properties, and Applications of Epoxy-Based Natural Fiber Polymer Biocomposites. *Polymers*. 15, (2023). <https://doi.org/10.3390/polym15010145>
66. Barde, M., Auad, M., Jones, J., Yan, Y., Lu, N., Pillay, S., Ning, H.: Natural Fiber Composite with α -Resorcylic Acid Based Bio-Epoxy Matrix. *Universal Journal of Materials Science*. 10, 9–20 (2022). <https://doi.org/10.13189/ujms.2022.100201>
67. Bojković, J., Marašević, M., Stojić, N., Bulatović, V., Radičević, B.: Thermal and Sound Characterization of a New Biocomposite Material. *Materials*. 16, (2023). <https://doi.org/10.3390/ma16124209>
68. Fatra, W., Anuar, K., Oktriyono, F.D., Fernando, R., Helwani, Z., Rusyana, A., Zul Amraini, S.: Biocomposite Innovation: Assessing Tensile and Flexural Performance with Maleated Natural Rubber Additives. *Leuser Journal of Environmental Studies*. 1, 69–80 (2023). <https://doi.org/10.60084/ljes.v1i2.98>
69. Gurupranes, S. V., Rajendran, I., Gokulkumar, S., Aravindh, M., Sathish, S., Elias Uddin, M.: Preparation, Characteristics, and Application of Biopolymer Materials Reinforced with Lignocellulosic Fibres. *International Journal of Polymer Science*. 2023, (2023). <https://doi.org/10.1155/2023/1738967>
70. Almi, K., Benchabane, A., Lakel, S., Kriker, A.: Potential utilization of date palm wood as composite reinforcement. *Journal of Reinforced Plastics and Composites*. 34, 1231–1240 (2015). <https://doi.org/10.1177/0731684415588356>
71. Abdal-Hay, A., Suardana, N.P.G., Jung, D.Y., Choi, K.S., Lim, J.K.: Effect of diameters and alkali treatment on the tensile properties of date palm fiber reinforced epoxy composites. *International Journal of Precision Engineering and Manufacturing*. 13, 1199–1206 (2012). <https://doi.org/10.1007/s12541-012-0159-3>
72. Elseify, L. A., & Midani, M.: Characterization of date palm fiber. *Date palm fiber composites: processing, properties and applications*, p. 227-255. (2020)
73. Mahdavi, S., Kermanian, H., Varshoei, A.: Comparison of mechanical properties of date palm fiber- polyethylene composite. *BioResources*. 5, 2391–2403 (2010). <https://doi.org/10.15376/biores.5.4.2391-2403>
74. Agoudjil, B., Benchabane, A., Boudenne, A., Ibos, L., Fois, M.: Renewable materials to reduce building heat loss: Characterization of date palm wood. *Energy and Buildings*. 43, 491–497 (2011). <https://doi.org/10.1016/J.ENBUILD.2010.10.014>
75. Bezazi, A., Boumediri, H., Garcia del Pino, G., Bezzazi, B., Scarpa, F., Reis, P.N.B.,

- Dufresne, A.: Alkali Treatment Effect on Physicochemical and Tensile Properties of Date Palm Rachis Fibers. *Journal of Natural Fibers*. 19, 3770–3787 (2022).
<https://doi.org/10.1080/15440478.2020.1848726>
76. Benzidan, R.: Intitulé Étude du comportement en fatigue des plaques sandwichs à base de bois de palmier, PhD Thesis, (2019)
77. youcef, D.: Contribution à la caractérisation des matériaux composites renforcés de fibres végétales, PhD Thesis', university of biskra, (2018)
78. Supian, A.B.M., Jawaid, M., Rashid, B., Fouad, H., Saba, N., Dhakal, H.N., Khiari, R.: Mechanical and physical performance of date palm/bamboo fibre reinforced epoxy hybrid composites. *Journal of Materials Research and Technology*. 15, 1330–1341 (2021).
<https://doi.org/10.1016/j.jmrt.2021.08.115>
79. Alshammari, B.A.: Evaluation of mechanical, physical, and morphological properties of epoxy composites reinforced with different date palm fillers. *Materials*. 12, (2019).
<https://doi.org/10.3390/ma12132145>
80. Abu-Jdayil, B.: Green Thermal Insulation Material Based on Date Palm Wastes. In: 18th International Conference on Renewable Energies and Power Quality (ICREPQ'20) Granada (Spain), 1st to 2nd April 2020, Icrepq.Com
81. ALMI, k: Développement et caractérisation de matériaux à base du bois de palmier dattier adaptés aux applications de développement durable en Algérie, PhD Thesis', university of biskra, (2018)
82. Mohanty, J.R., Das, S.N., Das, H.C., Mahanta, T.K., Ghadei, S.B.: Solid particle erosion of date palm leaf fiber reinforced polyvinyl alcohol composites. *Advances in Tribology*. 2014, (2014). <https://doi.org/10.1155/2014/293953>
83. Djoudi, T., Djemai, H., Hecini, M., Ferhat, A.: Physical, Thermal and Mechanical Characterization of a New Material Composite Based on Fibrous Wood Particles of Date Palm Tree. *Revue des Composites et des Matériaux Avances*. 32, 45–52 (2022).
<https://doi.org/10.18280/rcma.320107>
84. Masri, T., Ounis, H., Sedira, L., Kaci, A., Benchabane, A.: Characterization of new composite material based on date palm leaflets and expanded polystyrene wastes. *Construction and Building Materials*. 164, 410–418 (2018).
<https://doi.org/10.1016/J.CONBUILDMAT.2017.12.197>
85. Boukhattem, L., Boumhaout, M., Hamdi, H., Benhamou, B.: Moisture content influence on the thermal conductivity of insulating building materials made from date palm fibers mesh. *Construction and Building Materials*. 148, 811–823 (2017).
<https://doi.org/10.1016/j.conbuildmat.2017.05.020>
86. Benmansour, N., Agoudjil, B., Gherabli, A., Kareche, A., Boudenne, A.: Thermal and mechanical performance of natural mortar reinforced with date palm fibers for use as insulating materials in building. *Energy and Buildings*. 81, 98–104 (2014).
<https://doi.org/10.1016/j.enbuild.2014.05.032>
87. Oushabi, A., Sair, S., Abboud, Y., Tanane, O., Bouari, A. El: An experimental

- investigation on morphological, mechanical and thermal properties of date palm particles reinforced polyurethane composites as new ecological insulating materials in building. *Case Studies in Construction Materials*. 7, 128–137 (2017). <https://doi.org/10.1016/j.cscm.2017.06.002>
88. Djemai, H., Djoudi, T., Labed, A.: Experimental Investigation of Mechanical Behaviour and Damage of Bio-Sourced Sandwich Structures Based on Date Palm Tree Waste and Cork Materials. *Revue des Composites et des Materiaux Avances*. 32, 215–222 (2022). <https://doi.org/10.18280/rcma.320501>
 89. Djoudi, T., Djemai, H., Hecini, M.: Investigating the Impact of Core Type on the Properties of Novel Bio-Composites with a Sandwich Structure Derived from Date Palm Waste. *Revue des Composites et des Materiaux Avances*. 34, 169–176 (2024). <https://doi.org/10.18280/rcma.340206>
 90. Khalili, P., Skrifvars, M., Dhakal, H.N., Dashatan, S.H., Danielsson, M., Gràcia, A.F.: Mechanical Properties of Bio-Based Sandwich Composites Containing Recycled Polymer Textiles. *Polymers*. 15, 1–14 (2023). <https://doi.org/10.3390/polym15183815>
 91. Djemai, H., Labed, A., Hecini, M., Djoudi, T.: Delamination analysis of composite sandwich plate of cork agglomerate/glass fiber-polyester: An experimental investigation. *Revue des Composites et des Materiaux Avances*. 31, 193 (2021). <https://doi.org/10.18280/RCMA.310402>
 92. Benzidane, M.A., Benzidane, R., Hamamousse, K., Adjal, Y., Sereir, Z., Poilâne, C.: Valorization of date palm wastes as sandwich panels using short rachis fibers in skin and petiole ‘wood’ as core. *Industrial Crops and Products*. 177, (2022). <https://doi.org/10.1016/j.indcrop.2021.114436>
 93. Nft, A., Supports, M., Ac, M.P., Str, M., Stratification, A., Str, M., Str, M., Str, L.M., Str, L.M., Hors, H.R., Smar, O., Smar, O.: *Medapoxy str*. 81, 65–66 (2017)
 94. Bouhemame, N., Aiadi, K.E., Bezazi, A., Boumediri, H., Reis, P.N.B., Imad, A., Scarpa, F.: Tensile Properties Optimization of Date Palm Leaflets Using Taguchi Method. *Journal of Natural Fibers*. 19, 6348–6364 (2022). <https://doi.org/10.1080/15440478.2021.1916674>
 95. Zakrzewska, A., Zargarian, S.S., Rinoldi, C., Gradys, A., Jarzabek, D., Zanoni, M., Gualandi, C., Lanzi, M., Pierini, F.: Electrospun Poly(vinyl alcohol)-Based Conductive Semi-interpenetrating Polymer Network Fibrous Hydrogel: A Toolbox for Optimal Cross-Linking. *ACS Materials Au*. 3, 464–482 (2023). <https://doi.org/10.1021/acsmaterialsau.3c00025>
 96. Kim, J., Ishikawa, S., Naito, M., Li, X., Chung, U. il, Sakai, T.: Miscibility and ternary diagram of aqueous polyvinyl alcohols with different degrees of saponification. *Scientific Reports*. 13, 1–10 (2023). <https://doi.org/10.1038/s41598-023-35575-w>
 97. Bledzki, A.K., Reihmane, S., Gassan, J.: Properties and modification methods for vegetable fibers for natural fiber composites. *Journal of Applied Polymer Science*. 59, 1329–1336 (1996). [https://doi.org/10.1002/\(sici\)1097-4628\(19960222\)59:8<1329::aid-app17>3.3.co;2-5](https://doi.org/10.1002/(sici)1097-4628(19960222)59:8<1329::aid-app17>3.3.co;2-5)

98. D790, A.: D790 Standard Test Methods for Flexural Properties of Unreinforced and Reinforced Plastics and Electrical Insulating Materials, <https://www.astm.org/d0790-17.html>
99. Instron ISO 14125 Flexural Properties of Fiber-Reinforced Plastic Composites | Instron, <https://www.instron.com/fr-fr/testing-solutions/iso-standards/iso-14125>
100. ASTM D790 - 81 Standard Test Methods for Flexural Properties of Unreinforced and Reinforced Plastics and Electrical Insulating Materials (supersedes ASTM D790 - 81) | Building CodeHub, <https://codehub.building.govt.nz/resources/astm-d790-81>
101. D-, A.: Standard Test Method for iTeh Standards iTeh Standards Document Preview. i, 5–7 (2010). <https://doi.org/10.1520/D0790-10.2>
102. Aslam, M., Shafigh, P., Jumaat, M.Z., Bhosale, A., Zade, N.P., Sarkar, P., Davis, R., Dimov, D., Amit, I., Gorrie, O., Barnes, M.D., Townsend, N.J., Neves, A.I.S., Withers, F., Russo, S., Craciun, M.F., Gahete, J.A., Benítez, A., Otero, R., Esquivel, D., Sanchidrián, C.J., Morales, J., Caballero, Á., Salguero, F.R., Method, S.T., Wei et al.: iTeh Standards iTeh Standards Document Preview. *Nanomaterials*. 126, 13–15 (2022). <https://doi.org/10.1520/D0198-21A.10.1520/D0198-22.Copyright>
103. Methods, S.T.: Standard Test Methods for Structural Panels in Tension 1. *Methods*. 90, 1–6 (2010)
104. Sulfate, M.: iTeh Standards iTeh Standards. Designation: E 778 – 87 (Reapproved 2004). i, 3–5 (2018)
105. Yi, S., Oh, N., Min, K.E., Shin, J.S., Kim, C.: Thermo-Viscoelastic Characterization of 3D Printing Polymers. *Applied Sciences (Switzerland)*. 13, 1–15 (2023). <https://doi.org/10.3390/app13052876>
106. Rojek, B., Wesolowski, M.: A combined differential scanning calorimetry and thermogravimetry approach for the effective assessment of drug substance–excipient compatibility. *Journal of Thermal Analysis and Calorimetry*. 148, 845–858 (2023). <https://doi.org/10.1007/s10973-022-11849-9>
107. Kelly, C.A., Hay, J.N., Turner, R.P., Jenkins, M.J.: The effect of a secondary process on the analysis of isothermal crystallisation kinetics by differential scanning calorimetry. *Polymers*. 12, (2020). <https://doi.org/10.3390/polym12010019>
108. ASTM, 1895_17: iTeh Standards iTeh Standards Document. 10, 1–5 (2021). <https://doi.org/10.1520/D1895-17.This>
109. Saffian, H.A., Yamaguchi, M., Ariffin, H., Abdan, K., Kassim, N.K., Lee, S.H., Lee, C.H., Shafi, A.R., Alias, A.H.: Thermal, physical and mechanical properties of poly(Butylene succinate)/kenaf core fibers composites reinforced with esterified lignin. *Polymers*. 13, (2021). <https://doi.org/10.3390/polym13142359>
110. Alodan, H.A., Alsuhybani, M.S., Alshammari, B.A., Alkhuraiji, T.S.: Effect of Fiber Loading on Physical, Mechanical, and Thermal Properties of Low Density Polyethylene/Palm Tree Waste Fiber Composites. *Science of Advanced Materials*. 10, 1341–1350 (2018). <https://doi.org/10.1166/sam.2018.3320>

111. Singh, Y.: X-Ray Diffraction in Mineralogical Research. *Journal of ISAS*. 1, 1–11 (2023). <https://doi.org/10.59143/isas.jisas.1.4.wcjb9374>
112. Fewster, P.F.: The Limits of X-ray Diffraction Theory. *Crystals*. 13, (2023). <https://doi.org/10.3390/cryst13030521>
113. Yanxon, H., Weng, J., Parraga, H., Xu, W., Ruett, U., Schwarz, N., Kelly, S.D.: Artifact identification in X-ray diffraction data using machine learning methods. *Journal of Synchrotron Radiation*. 30, 137–146 (2023). <https://doi.org/10.1107/S1600577522011274>
114. ASTM: Standard Practice for Obtaining JK Inclusion Ratings Using Automatic Image Analysis. *Image (Rochester, N.Y.)*. 03, 1–9 (2002)
115. Cheng, Y.-L., Lee, C.-Y., Huang, Y.-L., Buckner, C.A., Lafrenie, R.M., Dénomée, J.A., Caswell, J.M., Want, D.A., Gan, G.G., Leong, Y.C., Bee, P.C., Chin, E., Teh, A.K.H., Picco, S., Villegas, L., Tonelli, F., Merlo, M., Rigau, J., Diaz, D., Masuelli, M., Korrapati, S., Kurra, P., Puttugunta, S., Picco, S., Villegas, L., Tonelli, F., Merlo, M., Rigau, J., Diaz, D., Masuelli, M., Tascilar, M., de Jong, F.A., Verweij, J., Mathijssen, R.H.J.: We are IntechOpen , the world ' s leading publisher of Open Access books Built by scientists , for scientists TOP 1 % . *Intech*. 11, 13 (2016)
116. Johnson, J.B., Walsh, K.B., Naiker, M., Ameer, K.: The Use of Infrared Spectroscopy for the Quantification of Bioactive Compounds in Food: A Review. *Molecules*. 28, (2023). <https://doi.org/10.3390/molecules28073215>
117. Alberts, M., Laino, T., Vaucher, A.C.: Leveraging Infrared Spectroscopy for Automated Structure Elucidation. *ChemRxiv*. 1–25 (2023)
118. Jung, G., Jung, S.G., Cole, J.M.: Automatic materials characterization from infrared spectra using convolutional neural networks. *Chemical Science*. 14, 3600–3609 (2023). <https://doi.org/10.1039/d2sc05892h>
119. Houthuijs, K.J., Berden, G., Engelke, U.F.H., Gautam, V., Wishart, D.S., Wevers, R.A., Martens, J., Oomens, J.: An In Silico Infrared Spectral Library of Molecular Ions for Metabolite Identification. *Analytical Chemistry*. 95, 8998–9005 (2023). <https://doi.org/10.1021/acs.analchem.3c01078>
120. Maroua, F., Adnane, L., Hocine, D.: Use of Date Palm Waste to Produce Bio-Composite Material. *Proceedings of the Second International Conference of Innovative Textiles and Developed Materials-ITDM'2; 05-06 May 2023; Tunisia*. 147–152 (2024). https://doi.org/10.1007/978-981-99-7950-9_14
121. Debabeche, N.: Synthesis and characterization of composites : thermoplastic / lignocellulosic fibers from the Biskra region, (2023)
122. By-nc-nd, C.C.: Saaidia , A ., Bezazi , A ., Belbah , A ., Bouchelaghem , H ., Scarpa , F ., & Amirouche , S . (2017). Mechano-physical properties and statistical design of Jute Yarns . *Measurement* , 111 , 284-294 . 284–294 (2017)
123. Fiore, V., Scalici, T., Valenza, A.: Characterization of a new natural fiber from *Arundo donax* L. as potential reinforcement of polymer composites. *Carbohydrate Polymers*. 106, 77–83 (2014). <https://doi.org/10.1016/j.carbpol.2014.02.016>

124. Puglia, D., Monti, M., Santulli, C., Sarasini, F., De Rosa, I.M., Kenny, J.M.: Effect of alkali and silane treatments on mechanical and thermal behavior of Phormium tenax fibers. *Fibers and Polymers*. 14, 423–427 (2013). <https://doi.org/10.1007/S12221-013-0423-X>
125. De Rosa, I.M., Kenny, J.M., Puglia, D., Santulli, C., Sarasini, F.: Morphological, thermal and mechanical characterization of okra (*Abelmoschus esculentus*) fibres as potential reinforcement in polymer composites. *Composites Science and Technology*. 70, 116–122 (2010). <https://doi.org/10.1016/j.compscitech.2009.09.013>
126. Benchouia, H.E., Guerira, B., Chikhi, M., Boussehel, H., Tedeschi, C.: An experimental evaluation of a new eco-friendly insulating material based on date palm fibers and polystyrene. *Journal of Building Engineering*. 65, (2023). <https://doi.org/10.1016/j.jobe.2022.105751>
127. Boubou Cisse, Stephane Luchini, J.P.M.: To cite this version : *Revue Teledetection*. 8, 17–34 (2006)
128. Scarpa, F., Amroune, S., Bezazi, A.: Analyse Statistique et Effet des Traitements Chimique sur le Comportement Physico - Mécanique des Fibres des Bras de Grappe des Palmiers Dattier = Statistical Analysis and Effect of Chemical Treatment on the Physicomechanical Behavior of Fibres from Date-Pa. *Synthèse : Revue des Sciences et de la Technologie*. 108–120 (2015). <https://doi.org/10.12816/0027867>
129. Banga, H., Singh, V.K., Choudhary, S.K.: Fabrication and Study of Mechanical Properties of Bamboo Fibre Reinforced Bio-Composites. *Innovative Systems Design and Engineering*. 6, 84–99 (2015)
130. Eiras, J.N., Segovia, F., Borrachero, M. V., Monzó, J., Bonilla, M., Payá, J.: Physical and mechanical properties of foamed Portland cement composite containing crumb rubber from worn tires. *Materials & Design*. 59, 550–557 (2014). <https://doi.org/10.1016/J.MATDES.2014.03.021>
131. Asyraf, M.R.M.: Mechanical properties of oil palm fibre-reinforced polymer composites: a review. *Journal of Materials Research and Technology*. 17, 33–65 (2022). <https://doi.org/10.1016/j.jmrt.2021.12.122>
132. Abu-Jdayil, B.: Unsaturated Polyester Microcomposites. *Unsaturated Polyester Resins: Fundamentals, Design, Fabrication, and Applications*. 67–100 (2019). <https://doi.org/10.1016/B978-0-12-816129-6.00003-X>
133. Ameli, A., Jahani, D., Nofar, M., Jung, P.U., Park, C.B.: Development of high void fraction polylactide composite foams using injection molding: Mechanical and thermal insulation properties. *Composites Science and Technology*. 90, 88–95 (2014). <https://doi.org/10.1016/j.compscitech.2013.10.019>
134. Muñoz, E., García-Manrique, J.A.: Water absorption behaviour and its effect on the mechanical properties of flax fibre reinforced bioepoxy composites. *International Journal of Polymer Science*. 2015, 16–18 (2015). <https://doi.org/10.1155/2015/390275>
135. Gutiérrez-Orrego, D.A.: Mechanical and Physical Properties of Soil-Cement Blocks

- Reinforced with Mineral Wool and Sisal Fiber. *Journal of Materials in Civil Engineering*. 29, 04016225 (2017). [https://doi.org/10.1061/\(ASCE\)MT.1943-5533.0001753](https://doi.org/10.1061/(ASCE)MT.1943-5533.0001753)
136. Yang, X.: Improved dispersion of grafted starch granules leads to lower water resistance for starch-g-PLA/PLA composites. *Composites Science and Technology*. 86, 149–156 (2013). <https://doi.org/10.1016/j.compscitech.2013.07.013>
137. Ramlee, N.A.: Tensile, physical and morphological properties of oil palm empty fruit bunch/sugarcane bagasse fibre reinforced phenolic hybrid composites. *Journal of Materials Research and Technology*. 8, 3466–3474 (2019). <https://doi.org/10.1016/j.jmrt.2019.06.016>
138. Barkhad, M.S., Abu-Jdayil, B., Iqbal, M.Z., Mourad, A.H.I.: Thermal insulation using biodegradable poly(lactic acid)/date pit composites. *Construction and Building Materials*. 261, 120533 (2020). <https://doi.org/10.1016/J.CONBUILDMAT.2020.120533>
139. Abu-Jdayil, B., Barkhad, M.S., Mourad, A.H.I., Iqbal, M.Z.: Date palm wood waste-based composites for green thermal insulation boards. *Journal of Building Engineering*. 43, 103224 (2021). <https://doi.org/10.1016/J.JOBE.2021.103224>
140. Alhumade, H., Rezk, H., Nassef, A.M., Al-Dhaifallah, M.: Fuzzy Logic Based-Modeling and Parameter Optimization for Improving the Corrosion Protection of Stainless Steel 304 by Epoxy-Graphene Composite. *IEEE Access*. 7, 100899–100909 (2019). <https://doi.org/10.1109/ACCESS.2019.2930902>
141. Arunan, E.: Defining the hydrogen bond: An account (IUPAC Technical Report). *Pure and Applied Chemistry*. 83, 1619–1636 (2011). <https://doi.org/10.1351/PAC-REP-10-01-01>
142. Belgacem, C., Serra-Parareda, F., Tarrés, Q., Mutjé, P., Delgado-Aguilar, M., Boufi, S.: The integral utilization of date palm waste to produce plastic composites. *Polymers*. 13, (2021). <https://doi.org/10.3390/polym13142335>
143. Vasile, C., Pamfil, D., Râpă, M., Darie-Niță, R.N., Mitelut, A.C., Popa, E.E., Popescu, P.A., Draghici, M.C., Popa, M.E.: Study of the soil burial degradation of some PLA/CS biocomposites. *Composites Part B: Engineering*. 142, 251–262 (2018). <https://doi.org/10.1016/J.COMPOSITESB.2018.01.026>
144. Akindoyo, J.O.: Effects of surface modification on dispersion, mechanical, thermal and dynamic mechanical properties of injection molded PLA-hydroxyapatite composites. *Composites Part A: Applied Science and Manufacturing*. 103, 96–105 (2017). <https://doi.org/10.1016/J.COMPOSITESA.2017.09.013>
145. Kassouf, A.: Attenuated total reflectance-mid infrared spectroscopy (ATR-MIR) coupled with independent components analysis (ICA): A fast method to determine plasticizers in polylactide (PLA). *Talanta*. 147, 569–580 (2016). <https://doi.org/10.1016/J.TALANTA.2015.10.021>
146. Torres-Huerta, A.M.: Comparative assessment of miscibility and degradability on PET/PLA and PET/chitosan blends. *European Polymer Journal*. 61, 285–299 (2014). <https://doi.org/10.1016/J.EURPOLYMJ.2014.10.016>

147. Abu-Jdayil, B., Mourad, A.H.I., Hussain, A., Al Abdallah, H.: Thermal insulation and mechanical characteristics of polyester filled with date seed wastes. *Construction and Building Materials*. 315, 125805 (2022).
<https://doi.org/10.1016/j.conbuildmat.2021.125805>
148. Tolêdo Filho, R.D., Scrivener, K., England, G.L., Ghavami, K.: Durability of alkali-sensitive sisal and coconut fibres in cement mortar composites. *Cement and Concrete Composites*. 22, 127–143 (2000). [https://doi.org/10.1016/S0958-9465\(99\)00039-6](https://doi.org/10.1016/S0958-9465(99)00039-6)
149. Braiek, A., Karkri, M., Adili, A., Ibos, L., Ben Nasrallah, S.: Estimation of the thermophysical properties of date palm fibers/gypsum composite for use as insulating materials in building. *Energy and Buildings*. 140, 268–279 (2017).
<https://doi.org/10.1016/J.ENBUILD.2017.02.001>
150. Riahi, K., Thayer, B. Ben, Mammou, A. Ben, Ammar, A. Ben, Jaafoura, M.H.: Biosorption characteristics of phosphates from aqueous solution onto *Phoenix dactylifera* L. date palm fibers. *Journal of Hazardous Materials*. 170, 511–519 (2009).
<https://doi.org/10.1016/J.JHAZMAT.2009.05.004>
151. Hocine, D., Mabrouk, H., Labed, A.: On the characterization of sandwich panels for solar flat plate collectors' applications: theoretical and experimental investigation. (2016)
152. Aghahadi, M.: Etude expérimentale et modélisation physique des transferts couplés chaleur-humidité dans un isolant Mohammad Aghahadi To cite this version : HAL Id : tel-02192796. (2019)
153. Nabil, M., Khodadadi, J.M.: Computational/analytical study of the transient hot wire-based thermal conductivity measurements near phase transition. *International Journal of Heat and Mass Transfer*. 111, 895–907 (2017).
<https://doi.org/10.1016/j.ijheatmasstransfer.2017.04.043>
154. LABED, Adnane. Contribution à l'étude des échanges convectifs en régime transitoire dans les Capteurs Solaires Plans à air; Application au Séchage des produits agro-alimentaires. Diss. UNIVERSITE MOHAMED KHIDER BISKRA, 2012.
155. Duffie J. A., Beckman D., *Solar engineering of thermal processes*, Jhon & Wiley & Sons, Inc., Hoboken, New Jersey, USA ed. 908 pp (2006).
156. Labed, Adnane, Noureddine Moumami, and Adel Benchabane. "Experimental investigation of various designs of solar flat plate collectors: Application for the drying of green chili." *Journal of Renewable and Sustainable Energy* 4.4 (2012).

